

2013

Robust Control Methods for Nonlinear Systems with Uncertain Dynamics and Unknown Control Direction

Chau T. Ton
Embry-Riddle Aeronautical University

Follow this and additional works at: <https://commons.erau.edu/edt>



Part of the [Aerospace Engineering Commons](#), and the [Engineering Physics Commons](#)

Scholarly Commons Citation

Ton, Chau T., "Robust Control Methods for Nonlinear Systems with Uncertain Dynamics and Unknown Control Direction" (2013). *Doctoral Dissertations and Master's Theses*. 153.
<https://commons.erau.edu/edt/153>

This Dissertation - Open Access is brought to you for free and open access by Scholarly Commons. It has been accepted for inclusion in Doctoral Dissertations and Master's Theses by an authorized administrator of Scholarly Commons. For more information, please contact commons@erau.edu.

**ROBUST CONTROL METHODS FOR NONLINEAR
SYSTEMS WITH UNCERTAIN DYNAMICS AND
UNKNOWN CONTROL DIRECTION**

By

Chau T. Ton

A Dissertation Submitted in Partial Fulfillment of the
Requirements for the Degree of

DOCTOR OF PHILOSOPHY

(Engineering Physics)

Embry-Riddle Aeronautical University

2013

Copyright by Chau Ton 2013

All Rights Reserved

ROBUST CONTROL METHODS FOR NONLINEAR SYSTEMS WITH UNCERTAIN DYNAMICS AND UNKNOWN CONTROL DIRECTION

By Chau Ton

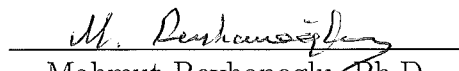
This dissertation was prepared under the direction of the candidate's dissertation committee chair, Dr. William MacKunis, Department of Physical Sciences, and has been approved by the members of his dissertation committee. It was submitted to the Department of Physical Sciences and was accepted in partial fulfillment of the requirements for the

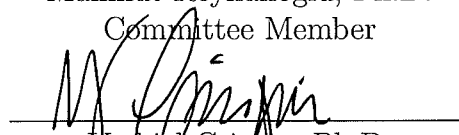
Degree of
Doctor of Philosophy in Engineering Physics

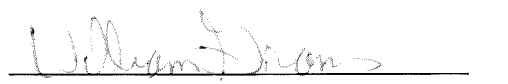
DISSERTATION COMMITTEE:

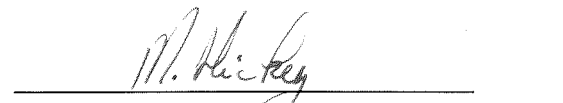

William MacKunis, Ph.D.
Committee Chair


Sergey V. Drakunov, Ph.D.
Committee Member


Mahmut Reyhanoglu, Ph.D.
Committee Member


Nediel Crispin, Ph.D.
Committee Member


William Grams, Ph.D.
Dean of College of Arts and Sciences


Michael Hickey, Ph.D.
Dean of Research and Graduate Studies

November 6th, 2013

Date

Acknowledgments

I would like to express my very great appreciation to Dr. William MacKunis for his guidance, support of my research, and enthusiastic encouragement. He played an instrumental role in the completion of this dissertation, and his willingness to give his time so generously is greatly appreciated. I also wish to express my sincere gratitude to Dr. Sergey Drakunov for his valuable and constructive suggestions during the development of this research. His insights were invaluable in inspiring the research direction and in completing the research project. I want to also thank Dr. Mahmut Reyhanoglu, Dr. Yechiel Crispin, and the committee for their suggested improvements on the dissertation. I would like to express my sincere gratitude to the Department of Physical Sciences at Embry-Riddle Aeronautical University for their moral and financial support. I also want to thank my friends for their stimulating discussions and for all the fun we had during the last few years.

Last but not least, I would like to thank my parents, who risked everything so their children could have a bright future and a better life.

Abstract

Robust nonlinear control design strategies using sliding mode control (SMC) and integral SMC (ISMC) are developed, which are capable of achieving reliable and accurate tracking control for systems containing dynamic uncertainty, unmodeled disturbances, and actuator anomalies that result in an unknown and time-varying control direction. In order to ease readability of this dissertation, detailed explanations of the relevant mathematical tools is provided, including stability definitions, Lyapunov-based stability analysis methods, SMC and ISMC fundamentals, and other basic nonlinear control tools. The contributions of the dissertation are three novel control algorithms for three different classes of nonlinear systems: single-input multiple-output (SIMO) systems, systems with model uncertainty and bounded disturbances, and systems with unknown control direction. Control design for SIMO systems is challenging due to the fact that such systems have fewer actuators than degrees of freedom to control (i.e., they are underactuated systems). While traditional nonlinear control methods can be utilized to design controllers for certain classes of cascaded underactuated systems, more advanced methods are required to develop controllers for parallel systems, which are not in a cascade structure. A novel control technique is proposed in this dissertation, which is shown to achieve asymptotic tracking for dual parallel systems, where a single scalar control input directly affects two subsystems. The result is achieved through an innovative sequential control design algorithm, whereby one of the subsystems is indirectly stabilized via the desired state trajectory that is commanded to the other subsystem. The SIMO system under consideration

does not contain uncertainty or disturbances. In dealing with systems containing uncertainty in the dynamic model, a particularly challenging situation occurs when uncertainty exists in the input-multiplicative gain matrix. Moreover, special consideration is required in control design for systems that also include unknown bounded disturbances. To cope with these challenges, a robust continuous controller is developed using an ISMC technique, which achieves asymptotic trajectory tracking for systems with unknown bounded disturbances, while simultaneously compensating for parametric uncertainty in the input gain matrix. The ISMC design is rigorously proven to achieve asymptotic trajectory tracking for a quadrotor system and a synthetic jet actuator (SJA)-based aircraft system. In the ISMC designs, it is assumed that the signs in the uncertain input-multiplicative gain matrix (i.e., the actuator control directions) are known. A much more challenging scenario is encountered in designing controllers for classes of systems, where the uncertainty in the input gain matrix is extreme enough to result in an a priori-unknown control direction. Such a scenario can result when dealing with highly inaccurate dynamic models, unmodeled parameter variations, actuator anomalies, unknown external or internal disturbances, and/or other adversarial operating conditions. To address this challenge, a SMC-based self-reconfigurable control algorithm is presented, which automatically adjusts for unknown control direction via periodic switching between sliding manifolds that ultimately forces the state to a converging manifold. Rigorous mathematical analyses are presented to prove the theoretical results, and simulation results are provided to demonstrate the effectiveness of the three proposed control algorithms.

Contents

Acknowledgments	iv
Abstract	i
1 Introduction	2
1.1 Contributions	8
2 Math Background	9
2.1 Lyapunov Stability	10
2.1.1 Linear Systems	12
2.1.2 Stability Definitions	14
2.1.3 Stabilization of Linear and Nonlinear Systems	15
2.2 Nonlinear Control Design	19
2.2.1 Integrator Backstepping	20
2.2.2 Adaptive Control	26
2.2.3 Variable Structure Control (VSC)	31
2.2.4 Sliding Mode Control (SMC)	35
2.2.5 Integral Sliding Mode	43

2.2.6	Method of Equivalent Control	51
3	Dual Parallel Systems with Single Input	54
3.1	Introduction	54
3.2	Problem Formulation	59
3.3	Control Design	60
3.3.1	Stability Proof	63
3.4	Simulation Results	66
3.4.1	Discussion of Results	74
3.5	Conclusion	75
4	Robust Attitude Tracking Control of a Quadrotor Helicopter in the Presence of Uncertainty	77
4.1	Introduction	77
4.2	Quadrotor Model and Properties	82
4.3	Control Development	84
4.3.1	Control Objective	84
4.3.2	Error System Development	85
4.3.3	Controller Formulation	86
4.4	Stability Analysis	88
4.5	Simulation Results	92
4.5.1	Simulation Model	92
4.5.2	Simulation Results	95
4.5.3	Discussion of Results	95
4.6	Conclusion	96

5	Robust Nonlinear Aircraft Tracking Control Using Synthetic Jet	98
	Actuators	98
5.1	Introduction	98
5.2	Dynamic Model and Properties	102
5.2.1	Robust Nonlinearity Inverse	103
5.2.2	Control Development	105
5.2.3	Closed-loop Error System	107
5.3	Stability Analysis	112
5.4	Simulation Results	114
5.5	Conclusion	116
6	Self-Reconfigurable Control	119
6.1	Introduction	119
6.1.1	Multi-Manifold Sliding Mode Control	122
6.2	Example	130
6.3	Conclusion	132
7	Conclusions	133
A	Quadrotor	135
A.0.1	Proof of Lemma 1	135
B	Synthetic Jets Actuator	137
B.0.2	Proof of Lemma 2	137
	Bibliography	140

Chapter 1

Introduction

Control of nonlinear dynamic systems is complicated due to the fact that the corresponding dynamic equations (i.e., nonlinear differential equations) cannot be solved analytically. To cope with this challenge, Lyapunov-based control design methods are popularly utilized. Lyapunov-based analysis is a well-established method for analyzing the stability and convergence properties of nonlinear systems without explicitly solving the dynamic equations. Additional complications arise in control design for dynamic systems containing parametric uncertainty and unknown nonlinear disturbances. To cope with these challenges, robust and adaptive nonlinear control methods can be amalgamated with Lyapunov-based techniques to achieve reliable and accurate control of nonlinear systems subjected to underactuation, dynamic uncertainty, and disturbances. Active research in robust control has produced a number of novel techniques for systems containing dynamic uncertainty and disturbances. Some examples include H-infinity loop-shaping, quantitative feedback theory, gain scheduling, loop transfer recovery, and others. The primary methods utilized in this dissertation

are sliding mode control (SMC) and integral of SMC, which falls in the general class of control methods called variable structure control (VSC) (DeCarlo, Zak, & Matthews, 1988).

Detailed studies of sliding mode control (SMC) systems as subset of variable structure systems (VSS) appeared in the 1950s and 1960s at the Institute of Control Sciences in Moscow and Moscow University, USSR, see references in (DeCarlo, Drakunov, & Li, 2000). The first development of SMC was by Irmgard Flugge-Lotz, S.V Emelianov, and V.I Utkin. Continuing research shows that SMC are capable of compensating for model uncertainty, unknown disturbances, and nonlinearities without the need for parameter adaptation, estimation, or linearization. This robustness has resulted in SMC being successfully utilized in various applications, such as automotive systems, spacecraft systems, power systems, process control, and others. The challenges associated with VSC involve defining so-called switching surfaces, at which the system instantaneously changes its structure to enable new state trajectories that might not be inherent in the original system structure. These new trajectories are called sliding modes. By exploiting the robustness of VSS, SMC can be used to address the challenges involved in designing controllers for underactuated systems, parallel systems with a single input, systems containing dynamic uncertainty and bounded disturbances, and systems with unknown control direction. SMC can also be applied to distributed parameter, systems with delay and more general described by semigroups (Drakunov & Utkin, 1992).

While SMC can compensate for systems with model uncertainty and disturbances, underactuated parallel systems, or SIMO (single-input multiple-output) systems, present particular control design challenges, because multiple states are directly cou-

pled through a single control input. An example of a SIMO system is the inverted pendulum on a cart; there is only one input to control the acceleration of the cart, and that input simultaneously affects both the translation of the cart and the angle of the pendulum. One of the contributions of this dissertation is a novel control law that can stabilize a class of underactuated parallel systems using a SMC technique. This novel control law can stabilize all system states via a single (scalar) control input by designing an innovative sliding surface that allows the states to converge in a sequential manner. This novel technique can be applied to spacecraft dynamics, photovoltaic power generation systems, unmanned aerial vehicles (UAV), and others.

The robust integral of the signum of the error (RISE) control technique is a feedback control strategy that contains an integral signum control term that can compensate for smooth bounded disturbances. The technique was originally developed by Zhihua Qu in 1998 (Qu, 1998). The RISE control method is capable of achieving asymptotic convergence in the presence of bounded nonlinear disturbances disturbances. Moreover, the structure of the RISE controller is continuous, which means that it does not require infinite bandwidth as standard SMC does. By exploiting the RISE control structure, new robust algorithms are proposed in this dissertation for an unmanned quadrotor systems and synthetic jet actuator-(SJA) based systems.

Versatile unmanned aerial vehicles such as the quadrotor have garnered traction as a reliable and practical vehicle for reconnaissance, search and rescue, scouting, mapping, and more. The quadrotor is an underactuated system, because it has six degrees of freedom and only four control inputs. Fortunately, the four control inputs can be used in unison to control both attitude and translation, allowing the quadrotor to be fully controllable. Recently developed methods for quadrotor control include

PID control, adaptive control, robust control, differential flatness, dynamic inversion, backstepping, neural network, and SMC (Salih, Moghavvemi, Mohamed, & Gaeid, 2010; Huang, Hoffmann, Waslander, & Tomlin, 2009; J. Wang et al., 2011; Das, Subbarao, & Lewis, 2009; Al-Younes, Al-Jarrah, & Jhemi, 2010; Vries & Subbarao, 2010; Mian & Daobo, 2008; Dydek, Annaswamy, Company, & Beach, 2010; Gillula, Huang, Vitus, & Tomlin, 2010; Zhu & Huo, 2010; Tayebi & McGilvray, 2006; Waslander & Wang, 2009; Madani & Benallegue, 2007; Achtelik, Bierling, Wang, & Holzapfel, 2011; Chamseddine, Zhang, Rabbath, Fulford, & Apkarian, 2011; Chamseddine & Zhang, 2010; D. Lee et al., 2009; Dierks & Jagannathan, 2010; Besnard, Shtessel, & Landrum, 2007). For quadrotor control in the presence of parametric uncertainty and unknown disturbances, adaptive and SMC methods are popular (Chamseddine et al., 2011; D. Lee et al., 2009; Dierks & Jagannathan, 2010). Adaptive control methods can require observers and online parameter adaptation schemes that can be computationally expensive, while robust control methods are designed to compensate for a worst-case scenario, without the need for online adaptation. Another contribution of the research in this dissertation is the design of a continuous robust control method using RISE to compensate for the model uncertainty and norm-bounded disturbances inherent in real-world quadrotor systems. The control technique can compensate for significant parametric uncertainty in the control input dynamics in addition to rejecting bounded, non-vanishing disturbances.

After a non-trivial reworking of the controller design, the RISE control technique can also be used to controlling synthetic jet actuator (SJA)-based systems, where the dynamic model contains actuator nonlinearities in addition to model uncertainty and disturbances. Synthetic jet actuators are small in size, easy to operate, and in-

expensive, making them a promising tool in aircraft tracking control applications. Aircraft tracking control objectives are traditionally achieved using mechanical deflection surfaces (i.e., elevators, ailerons, and rudders). However, mechanical limits in the actuators along with limitations on the operational range of angle of attack can hinder control performance. Active flow control methods using SJAs could reduce flow separation near aircraft wings, thereby improving aerodynamic performance and expanding the operational envelope (Deb, Tao, Burkholder, & Smith, 2005a). SJAs work via the periodic ejection and suction of fluid (i.e., air) through an orifice, which is produced from a vibrating diaphragm. Resulting trains of air vortices (or jets) achieve the transfer of momentum to the system with zero net mass injection across the boundary. Thus, there is no need for an external fuel supply. Nonlinear control algorithms using neural networks and adaptive control methods are often applied to SJA-based systems (Tchieu, Kutay, Muse, Calise, & Leonard, 2008; Mondschein, Tao, & Burkholder, 2011; Deb et al., 2005a; Deb, Tao, Burkholder, & Smith, 2005b, 2006, 2007, 2008; Liu et al., 2006; Liu, 2008; Singhal, Tao, & Burkholder, 2009; Tao, 2003, 1996; Jee et al., 2009; Shageer, Tao, & Burkholder, 2008). Although these intelligent and adaptive control methods can achieve good performance, one of the contributions in this dissertation is the design of a computationally minimal robust feedback control strategy that can achieve tracking control performance that is comparable to adaptive or neural network-based methods. Although this technique is robust with respect to parametric uncertainty in the control input matrix, heavier uncertainty, such as unknown sign of the control input direction, requires more advanced control design methods.

While SMC methods can be used to compensate for uncertainty and bounded

disturbances in a dynamic model, unmodeled variations in the commanded control direction represent further complications to be addressed in the control design. In 1983, Morse's famous conjecture states that systems with unknown control signs cannot be asymptotically stabilized (Mudgett & Morse, 1984). Nussbaum, however, showed that systems with unknown control direction can be stabilized through a class of smooth functions, called *Nussbaum* functions, using adaptive control (Nussbaum, 1983). Challenges in this control design include the requirement for infinite control gain. In (Drakunov, 1993), Drakunov showed that a purely robust SMC can compensate for unknown control direction. This method is based on self-reconfiguration, where the sliding surface σ is extended in sliding space, and the control automatically adjusts itself to the unknown changing control sign. Partial knowledge of the input matrix for this method is required. The third contribution of this dissertation research is the development of a self-reconfigurable control law similar to (Drakunov, 1993), which can compensate for unknown control direction without partial knowledge of the input matrix. The control algorithm is purely robust, requiring no online adaptation, observers, or function approximators. Additional research has developed novel methods to deal with the unknown control direction problem using robust control, adaptive control, and SMC with monitoring functions (Lozano & Brogliato, 1992; Xudong & Jingping, 1998; Kaloust & Qu, 1997; Yan & Xu, 2004; Hsu, Oliveira, & Peixoto, 2006; Yan, Hsu, Costa, & Lizarralde, 2008; Yang, Yam, Li, & Wang, 2009; Bartolini & Pisano, 2008; Bartolini, Ferrara, & Giacomini, 2003; Ferrara, Giacomini, & Vecchio, 2009; Bartolini, Punta, & Zolezzi, 2010, 2011).

1.1 Contributions

The contributions of this dissertation are

- design a novel technique to stabilize a class of underactuated parallel systems
- develop a robust control algorithm to compensate for systems with norm-bounded disturbances and parametric uncertainty
- use sliding mode control to stabilize a class of systems with unknown control direction

The chapters are organized as follows: Chapter 2 introduces the mathematical background of Lyapunov stability for linear and nonlinear systems. Nonlinear control tools such as backstepping, adaptive control law, and RISE are also discussed, along with properties of SMC. Chapter 3 deals with underactuated parallel systems. A novel control technique is presented, and simulation results are provided to demonstrate its effectiveness. Chapter 4 introduces the second-order dynamic system of the quadrotor. A continuous robust controller is designed, and simulation results are provided to show the performance of the control law. Chapter 5 deals with SJA-based control, where the dynamic model contains actuator nonlinearities in addition to parametric uncertainty and unknown nonlinear disturbances. The approach uses RISE to compensate for the uncertainty, and simulation results are presented to demonstrate the effectiveness of the proposed control algorithm. Chapter 6 deals with a general class of dynamic systems with unknown control direction. The approach used is an extension of the method in (Drakunov, 1993), in which sign of input matrix is uncertain. Chapter 7 summarizes the results and discusses future work.

Chapter 2

Math Background

This chapter covers the mathematical background involved in the subsequent developments presented in this research. Lyapunov-based stability theorems for linear and nonlinear systems are analyzed. Then, nonlinear control design methods, such as integrator backstepping, adaptive control, and RISE, are presented for different classes of systems. The mathematical background for variable structure control (VSC) is explained and two relevant functions, the *sat* and *sign*, are compared to show their advantages and disadvantages in real-world implementation. Sliding mode control (SMC), a form of VSC, is presented to demonstrate its robustness to disturbances and model uncertainty. A Lyapunov-based analysis is used to show that SMC achieves finite-time convergence to a stable sliding manifold. A brief discussion of the existence of solutions for systems with discontinuous right-hand sides is presented. The method of equivalent control is then presented to show how real sliding motion occurs when a system is near the vicinity of the discontinuous surface. Finally, an application of VSC for a system with unknown control direction is presented.

2.1 Lyapunov Stability

Stability is an indispensable aspect of any discussion involving systems theory and control system design. There are many different definitions of stability in dynamical systems, but the focus in this section is on the stability of equilibrium points. The mathematical development of stability of equilibrium points was originally developed by the Russian mathematician Aleksandr Lyapunov in the late 19th century (Liapunov, 1992). Equilibrium points can generally be categorized into two groups: stable and unstable. An equilibrium point is said to be stable if solutions starting at nearby points remain within a neighborhood of the equilibrium points throughout the time-evolution of the system state. An equilibrium point is unstable if it is not stable. An equilibrium point is asymptotically stable if all solutions starting within a neighborhood of an equilibrium point converge to the equilibrium point as time approaches infinity. An illustration of a stable equilibrium is in Figure 2.1. Even if there is a small perturbation imposed on the ball in the figure, it would oscillate at the bottom of the bowl; and in the presence of friction, the ball would converge to the bottom of the bowl (asymptotic stability). An unstable equilibrium point is illustrated in Figure 2.2. If there is a small perturbation on the ball, it would fall off the bowl and would never return to its original position.

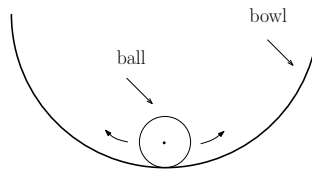


Figure 2.1: Stable Equilibrium Point

The mathematical theorems developed by Lyapunov can be applied to analyze the

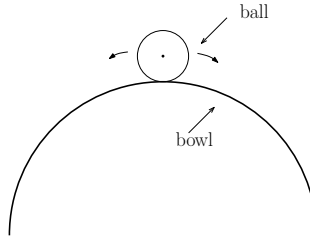


Figure 2.2: Unstable Equilibrium Point

stability properties of dynamic systems without having to explicitly solve the equations for an analytical solution. This is especially important for nonlinear systems or systems containing unmodeled disturbances, where explicit solutions can be difficult or impossible to obtain. Lyapunov's original work proposes two stability theorems to analyze stability: **Lyapunov's First Stability Theorem**, or the indirect method of Lyapunov, uses system linearization to analyze nonlinear system stability near an equilibrium point; **Lyapunov's Second Stability Theorem**, or the direct method of Lyapunov, uses a so-called Lyapunov function, which is analogous to an energy function, to analyze system stability without the need for linearizing the system dynamics.

Before the Lyapunov theorems are described, an introduction to the Lipschitz condition will be provided. A function $f : \mathbb{R}^n \times \mathbb{R} \rightarrow \mathbb{R}^n$ is considered Lipschitz if it satisfies the inequality

$$\|f(x, t) - f(y, t)\| \leq L \|x - y\| \quad (2.1)$$

for all (x, t) and (y, t) in some neighborhood of (x_0, t_0) , where L is a positive constant called the *Lipschitz constant*. The function $f(x, t)$ is *globally Lipschitz* if it is Lipschitz $\forall x \in \mathbb{R}^n$. Moreover, the function $f(x, t)$ is locally Lipschitz on a domain $D \subset \mathbb{R}^n$

if each point in D has a neighborhood D_0 such that $f(x, t)$ satisfies the Lipschitz condition for all points in D_0 with some Lipschitz constant L_0 (Khalil, 2002).

For the scalar case where $f(x) : \mathbb{R} \rightarrow \mathbb{R}$ is autonomous, the Lipschitz condition can be expressed as

$$\frac{|f(x) - f(y)|}{|x - y|} \leq L. \quad (2.2)$$

The inequality in (2.2) implies that the Lipschitz condition is that the slope of $f(x)$ be finite. Any function that has an infinite slope at a point is not going to be Lipschitz at that point, and any discontinuous function is not Lipschitz at the discontinuity.

In the following, Lyapunov's first and second stability theorems will be described.

2.1.1 Linear Systems

Linear systems have been studied extensively by Pierre-Simon Laplace, Harry Nyquist, Edward John Routh, Adolf Hurwitz and others (Ogata, 2002). At first, feedforward or open-loop control was sufficient for certain control systems, but there are limitations to the design. To overcome the limitations of open-loop control, feedback control was introduced, and pole placement techniques were invented to achieve desirable tracking objectives for linear systems. Feedback control system outputs information measured from sensors (feedback) to continuously update the commands delivered by the control system. This control structure can be visualized as a feedback signal that connects the output measurement back to the control input; hence, the system now contains a feedback loop, and is referred to a closed-loop system. Closed-loop systems can be employed to reject disturbances, stabilize unstable processes, reduce sensitivity to variations in the system parameters, improve tracking performance, and

guarantee convergence in the presence of model uncertainty.

The following derivation presents a simple control design method for linear systems and shows how the stability of a linearized system can be used to analyze the local stability properties of the corresponding nonlinear system.

Consider the linear time-invariant (LTI) system

$$\dot{x} = Ax + Bu, \quad (2.3)$$

where $x(t) \in \mathbb{R}^n$, $A \in \mathbb{R}^{n \times n}$, $B \in \mathbb{R}^{n \times n}$, $u(t) \in \mathbb{R}^n$. Let the control input $u(t)$ be designed as the full-state feedback law

$$u = -Kx, \quad (2.4)$$

where $K \in \mathbb{R}^{n \times n}$ is a user-defined (usually diagonal) control gain matrix. Substituting (2.4) into (2.3), the closed loop system can be obtained as

$$\dot{x} = (A - BK)x. \quad (2.5)$$

Based on (2.5), stability of the origin of the system in (2.3) is completely determined by the eigenvalues of $A - BK$, and for a controllable system, the gain matrix K can be designed to assign arbitrary values for the eigenvalues of $A - BK$. The linear differential equation in (2.5), can be solved as

$$x(t) = e^{(A-BK)t}x(0). \quad (2.6)$$

Thus, provided the real parts of the eigenvalues of $A - BK$ are negative, the state $x(t) \rightarrow 0$ as $t \rightarrow \infty$.

The system (2.3) is controllable if $\text{rank} \begin{bmatrix} B & AB & A^2B & \dots & A^{n-1}B \end{bmatrix} = n$.

2.1.2 Stability Definitions

Consider the nonlinear system in (2.10). Assume that there exists an equilibrium point x^* in (2.10) such that (Wie, 2008)

$$f(t, x^*) = 0 \quad \forall t \geq 0. \quad (2.7)$$

The equilibrium x^* of (2.10) is

- Lyapunov stable, if $\forall \varepsilon > 0$, there exists $\delta = \delta(\varepsilon, t_0) > 0$ such that

$$\|x(t_0) - x^*\| < \delta \implies \|x(t) - x^*\| \leq \varepsilon \quad \forall t \geq t_0. \quad (2.8)$$

If δ does not depend on t_0 , then it is uniformly Lyapunov stable.

- locally asymptotically stable (LAS), if it is Lyapunov stable and

$$\|x(t_0) - x^*\| < \delta \implies x(t) \longrightarrow x^* \quad \text{as} \quad t \rightarrow \infty. \quad (2.9)$$

- globally asymptotically stable (GAS), if it is Lyapunov stable and $x(t) \rightarrow x^*$ as $t \rightarrow \infty$ for all $x(t_0)$.
- unstable, if not stable.

A necessary condition for an equilibrium point to be locally asymptotically stable is that it be isolated. A necessary condition for an equilibrium point to be global asymptotically stable is that it be the only equilibrium point.

Conceptually, in (2.8) Lyapunov stable implies that the solution starts within δ distance of the equilibrium point will remain close within distance ε . In (2.9) local asymptotic stability means that the system starts with δ distance away from the equilibrium and eventually converges to the equilibrium. Global asymptotic stability implies that it does not matter where $x(t_0)$ resides, the system (2.10) will converge to the equilibrium point x^* .

2.1.3 Stabilization of Linear and Nonlinear Systems

Consider an nonautonomous system

$$\dot{x} = f(t, x), \quad (2.10)$$

where $x \in D$, $f(x) : [0, \infty] \times D \rightarrow \mathbb{R}^n$ locally Lipschitz and piecewise continuous, and $D \subset \mathbb{R}^n$ is a domain that contains the origin. By introducing the transformation

$$z = x - x^*, \quad (2.11)$$

where x^* is the equilibrium point, and $z(t)$ is a small perturbation from x^* , the following can be obtained:

$$\dot{x} = \dot{z} = f(x^* + z, t). \quad (2.12)$$

After linearization, Equation (2.12) as can be written as

$$\dot{z} = Az, \quad (2.13)$$

where $A \triangleq \left. \frac{\partial f}{\partial x} \right|_{x^*}$ is a Jacobian matrix evaluated at x^* .

The origin $z = 0$ of the linearized system (2.13) is asymptotically stable if all the eigenvalues of A have negative real parts. It is Lyapunov stable if none of the eigenvalues has a positive real part and there are no repeated eigenvalues on the imaginary axis. The stability properties of the origin of the linearized system (2.13) can be utilized to determine the stability properties of the equilibrium point x^* of the nonlinear system in the neighborhood of x^* . **Lyapunov's First Stability Theorem** is used to analyze the stability of equilibrium points of nonlinear systems via the stability of the corresponding linearized system (Wie, 2008).

Theorem 1 *Lyapunov's First Stability Theorem*

- *If the origin $z = 0$ of the linearized system is asymptotically stable, then the equilibrium point x^* of the nonlinear system is locally asymptotically stable.*
- *If the origin $z = 0$ of the linearized system is unstable, then the equilibrium point x^* of the nonlinear system is also unstable*
- *If the origin $z = 0$ of the linearized system is Lyapunov stable, then nothing can be said about the equilibrium point x^* of the nonlinear system based on linear analysis.*

The second Lyapunov's stability theorem uses a positive definite function call

Lyapunov function $V(x)$ to show that the system is stable if the time derivative of $V(x)$ is negative definite.

The following theorem states Lyapunov's Second Stability Theorem (Khalil, 2002).

Theorem 2 *Lyapunov's Second Stability Theorem*

Let $x = 0$ be an equilibrium point for $f(x)$ and $D \subset \mathbb{R}^n$ be a domain containing $x = 0$. Let $V : D \rightarrow \mathbb{R}$ be a continuously differential function such that

$$V(0) = 0 \quad \text{and} \quad V(x) > 0 \quad \text{in} \quad D - \{0\} \quad (2.14)$$

$$\dot{V}(x) \leq 0. \quad (2.15)$$

Then $x = 0$ is stable. Moreover, if

$$\dot{V}(x) < 0 \quad \text{in} \quad D - \{0\} \quad (2.16)$$

then $x = 0$ is asymptotically stable.

The function $V(x)$ is radially unbounded if $\|x\| \rightarrow \infty \Rightarrow V(x) \rightarrow \infty$. Lyapunov's second stability theorem gives *sufficient* conditions for system stability, but they are not *necessary* conditions. Lyapunov's direct method is a conservative analysis: A system cannot be proven unstable using Lyapunov's second method; it is always possible that a different Lyapunov function could be chosen to prove stability for the system.

An illustration of Lyapunov's stability definitions can be seen in Figures 2.3 - 2.5. From Figure 2.3, for an equilibrium point x^* that is Lyapunov stable, state trajectories beginning within a δ -neighborhood of x^* remain within an ϵ -neighborhood

of x^* but do not converge directly to x^* . Figure 2.4 shows that an equilibrium point is asymptotically stable if state trajectories initially in a δ -neighborhood of the equilibrium point x^* will converge directly to x^* . Figure 2.5 shows that a system is not Lyapunov stable if the state trajectory departs the ϵ -neighborhood of x^* .

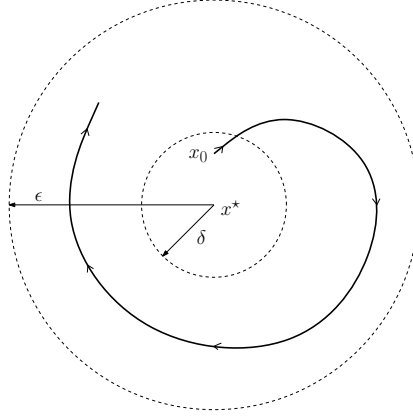


Figure 2.3: Lyapunov Stable

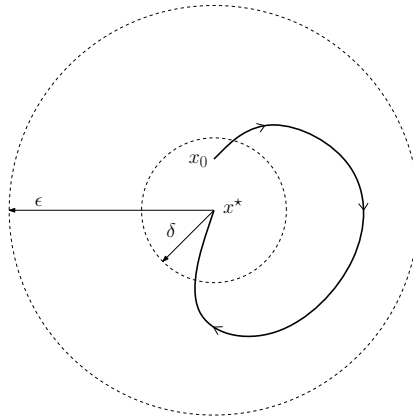


Figure 2.4: Lyapunov Asymptotically Stable

This section considered control design of linear systems and stability analysis methods for nonlinear systems via Lyapunov methods. The next section introduces nonlinear control algorithms such as integrator backstepping, adaptive control, vari-

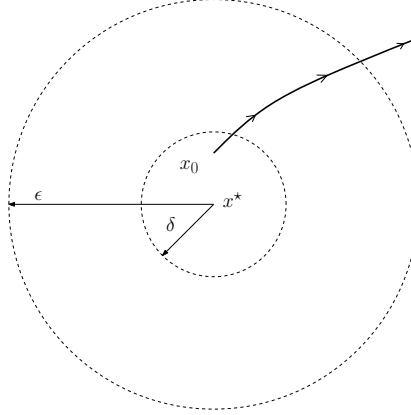


Figure 2.5: Lyapunov unstable

able structure control, and robust control. These nonlinear control tools can be utilized to cope with model uncertainty and disturbances, which are unavoidable in real-world dynamic systems.

2.2 Nonlinear Control Design

This section discusses nonlinear control tool such as adaptive control, robust integral of the signum of the error (RISE), and integrator backstepping. These nonlinear control methods leverage well-accepted mathematical theorems, including LaSalle's invariance principle and Barbalat's lemma. Details of these theorems can be found in (Khalil, 2002) and are summarized in the following.

Theorem 3 *Barbalat's Lemma*

Let $\phi : R \rightarrow R$ be a uniformly continuous function on $[0, \infty]$. Suppose that $\lim_{t \rightarrow \infty} \int_0^t \phi(\tau) d\tau$ exists and is finite. Then,

$$\phi(\tau) \rightarrow 0 \quad \text{as} \quad t \rightarrow \infty. \quad (2.17)$$

Theorem 4 *LaSalle's Theorem*

Let $\Omega \subset D$ be a compact set that is positively invariant with respect to (2.10). Let $V : D \rightarrow \mathbb{R}$ be a continuously differential function such that $\dot{V}(x) \leq 0$ in Ω . Let E be the set of all points in Ω where $\dot{V}(x) = 0$. Let M be the largest invariant set in E . Then every solution starting in Ω approaches M as $t \rightarrow \infty$.

LaSalle's theorem and Barbalat's Lemma will be utilized in the subsequent nonlinear control development.

2.2.1 Integrator Backstepping

Backstepping was developed in the early 1990s by Petar V. Kokotovic and others to stabilize a class of nonlinear cascade systems (Kokotovic, 1992). It was based on hierarchical method of control design suggested in (V. Utkin, Drakunov, Izosimov, Lukjanovand, & Utkin, 1984; Drakunov, Izosimov, Lukjanov, Utkin, & Utkin, 1991a, 1991b), also known as block control principle. This special class of systems contains coupled subsystems such that all subsystems are affected by the control input, but only some or one of the subsystems are directly influenced by the control input. Backstepping is a recursive scheme that starts with the design of a virtual control input(s) to stabilize the subsystem(s) that do not explicitly contain the control input, and then using the virtual control(s) in the final control input design to stabilize the entire system. The following example below demonstrates the backstepping technique.

Consider the system

$$\dot{\eta} = f(\eta) + g(\eta)\xi \quad (2.18)$$

$$\dot{\xi} = u, \quad (2.19)$$

where $\eta(t) \in \mathbb{R}^n$, $\xi \in \mathbb{R}$, $f : D \rightarrow \mathbb{R}^n$, $g : D \rightarrow \mathbb{R}^n$, and $u(t) \in \mathbb{R}$ is the control input. The functions $f(\eta)$ and $g(\eta)$ are smooth in the domain $D \in \mathbb{R}^n$ that contains $f(\eta=0) = 0$. It is assumed that the functions $f(\eta)$ and $g(\eta)$ are known. The control objective is to design a state feedback control law that stabilizes the origin $(\eta=0, \xi=0)$. Suppose that there exists a state feedback control law $\xi = \phi(\eta)$, with $\phi(0) = 0$, that stabilizes subsystem (2.18) in the sense that the origin of

$$\dot{\eta} = f(\eta) + g(\eta)\phi(\eta) \quad (2.20)$$

is asymptotically (Khalil, 2002). Suppose further that there exists a positive definite function $V_1(\eta)$ that satisfies the inequality

$$\dot{V}_1 = \frac{\partial V_1}{\partial \eta} [f(\eta) + g(\eta)\phi(\eta)] \leq -W(\eta) \quad \forall \eta \in D, \quad (2.21)$$

where $W(\eta)$ is a positive definite function. Adding and subtracting $g(\eta)\phi(\eta)$ to the right hand side of (2.18) yields

$$\dot{\eta} = [f(\eta) + g(\eta)\phi(\eta)] + g(\eta)[\xi - \phi(\eta)] \quad (2.22)$$

$$\dot{\xi} = u, \quad (2.23)$$

By using the change of variables

$$z = \xi - \phi(\eta), \quad (2.24)$$

the system (2.22) - (2.23) can be expressed as

$$\dot{\eta} = [f(\eta) + g(\eta)\phi(\eta)] + g(\eta)z \quad (2.25)$$

$$\dot{z} = u - \dot{\phi} \quad (2.26)$$

The time-derivative of the function $\phi(\eta)$ can be obtained as

$$\dot{\phi} = \frac{\partial \phi}{\partial \eta} [f(\eta) + g(\eta)\xi], \quad (2.27)$$

where (2.18) was utilized. To express the system to the cascade connection, let $v = u - \dot{\phi}$, and the system can be rewritten as

$$\dot{\eta} = [f(\eta) + g(\eta)\phi(\eta)] + g(\eta)z \quad (2.28)$$

$$\dot{z} = v \quad (2.29)$$

The system in (2.28) and (2.29) is similar to the original system, but now subsystem (2.28) has an asymptotically stable origin when the input v is zero. Consider the Lyapunov function candidate

$$V_2(\eta, \xi) = V_1(\eta) + \frac{1}{2}z^2. \quad (2.30)$$

Taking the time derivative of $V_2(\eta, \xi)$ along trajectories of (2.28) and (2.29) yields

$$\dot{V}_2 = \frac{\partial V_1}{\partial \eta} [f(\eta) + g(\eta)\phi(\eta)] + \frac{\partial V_1}{\partial \eta} g(\eta)z + zv \quad (2.31)$$

$$\leq -W(\eta) + \frac{\partial V_1}{\partial \eta} g(\eta)z + zv. \quad (2.32)$$

Choosing the control input v as

$$v = -\frac{\partial V_1}{\partial \eta} g(\eta) - kz, \quad (2.33)$$

where $k > 0$ is a positive constant, \dot{V}_2 can be upper bounded as

$$\dot{V}_2 \leq -W(\eta) - kz^2. \quad (2.34)$$

The inequality in (2.34) shows that the origin ($\eta = 0, \xi = 0$) is asymptotically stable. The system presented has two subsystems, but the technique can be extended to systems containing n subsystems.

Example Consider the system

$$\dot{x}_1 = x_1 + x_2 \quad (2.35)$$

$$\dot{x}_2 = x_2^2 + x_1 + u, \quad (2.36)$$

where $x_1(t) \in \mathbb{R}$, $x_2(t) \in \mathbb{R}$ are the states, and $u(t) \in \mathbb{R}$ is the scalar control input.

A positive definite function is chosen as

$$V_n = \frac{1}{2}x_1^2 + \frac{1}{2}x_2^2. \quad (2.37)$$

After taking the time derivative of $V_n(x_1, x_2)$ and substituting (2.35), \dot{V}_n can be expressed as

$$\dot{V}_n = x_1^2 + x_1x_2 + x_2(x_2^2 + x_1 + u). \quad (2.38)$$

From (2.38), the control input $u(t)$ cannot be designed to cancel the x_1^2 term due to the presence of the input-multiplicative term $x_2(t)u(t)$. It is undesirable to design the control input with the term x_2^{-1} , because $u(t)$ would approach infinity as $x_2(t) \rightarrow 0$.

To implement the backstepping technique, the first step is to consider $x_2(t)$ as the virtual control input $\phi(x_1)$ such that

$$\dot{x}_1 = x_1 + \phi(x_1) \quad (2.39)$$

is asymptotically stable. Choosing the positive definite function

$$V_{11} = \frac{1}{2}x_1^2, \quad (2.40)$$

it follows that designing $\phi(x_1)$ as

$$\phi(x_1) = -2x_1, \quad (2.41)$$

renders the time derivative of V_{11} negative definite as

$$\dot{V}_{11} = -x_1^2. \quad (2.42)$$

Hence, $x_1(t)$ is asymptotically stable and approaches zero exponentially.

The next objective is for $x_2(t)$ to converge to $\phi(x_1)$. To achieve this objective, consider the change of variables

$$z = x_2 - \phi(x_1). \quad (2.43)$$

By substituting (2.41) into (2.35), adding and subtracting $\phi(x_1)$, then using the definition of $z(t)$ above, the dynamics in (2.35) - (2.36) can be expressed as

$$\dot{x}_1 = -x_1 + z \quad (2.44)$$

$$\dot{z} = x_2^2 - x_1 + z + u. \quad (2.45)$$

If the control input can be designed to stabilize $z(t)$ to the origin, it follows from (2.44) that $x_2(t) \rightarrow \phi(x_1)$, thereby achieving the objective. Consider the positive definite function

$$V_{22} = \frac{1}{2}x_1^2 + \frac{1}{2}z^2. \quad (2.46)$$

After taking the time derivative of $V_{22}(x_1, z)$ and substituting (2.44) - (2.45), \dot{V}_{22} can be expressed as

$$\dot{V}_{22} = x_1(-x_1 + z) + z(x_2^2 - x_1 + z + u). \quad (2.47)$$

Based on (2.47), the control input $u(t)$ is designed as

$$u = -x_2^2 - (k+1)z. \quad (2.48)$$

where $k > 0$ is a control gain. After substituting the control input $u(t)$ into (2.47), the following is obtained:

$$\dot{V}_{22} = -x_1^2 - kz^2 < 0. \quad (2.49)$$

The expression in (2.49) can be used to prove that $x_1(t) \rightarrow 0$ and $z(t) \rightarrow 0$ as $t \rightarrow \infty$.

Based on the transformation in (2.43), (2.49) implies that

$$x_1, z \rightarrow 0 \Rightarrow 0 \Rightarrow x_2 \rightarrow \phi(0) \Rightarrow x_2 \rightarrow 0. \quad (2.50)$$

Thus, the objective is achieved.

The integrator backstepping technique demonstrated in this section is provided for the purpose of comparing it with the control technique presented in the subsequent chapter dealing with parallel systems. Integrator backstepping can be applied to cascade systems with a scalar control input in only one of the subsystems. However, for parallel system that have a scalar control present in all of the subsystems, more advanced techniques are required in the control design. The previous demonstration of backstepping is based on the assumptions that all states are measurable and that the system dynamics are known exactly. How can the control design be modified to compensate for uncertainty in the model dynamics?

2.2.2 Adaptive Control

To adapt means to adjust to new or different environments. Adaptive control, as the name implies, is a control method that is used to automatically compensate for uncertainty present in a system's dynamics. To be more specific, (Lyapunov-based) adaptive control is an algorithm that uses time-varying parameters in the control law, which generate online parameter estimates that can be used to compensate for uncertainty to stabilize a system.

Adaptive control was developed in the early 1950s for autopilots to stabilize high-performance aircrafts operating in different flight conditions, where constant-gain

feedback laws are insufficient to cope with the wide range of operating conditions (Ioannou & Fidan, 2006). Since then, various developments on adaptive control allow the technique to cover a wide class of systems containing uncertainty, including systems with parametric uncertainty premultiplying the control input. The following example demonstrates the effectiveness of adaptive control to compensate for input-multiplicative uncertainty.

Control Design

Consider the system

$$\dot{x} = f(x) + bu, \quad (2.51)$$

where $x(t) \in \mathbb{R}$, $f : \mathbb{R} \rightarrow \mathbb{R}$, $u(t) \in \mathbb{R}$ is the control input, and $b \in \mathbb{R}$ is an unknown constant. The objective is to drive the dynamics in (2.51) to the origin $x = 0$. To facilitate the adaptive control design, the control term $bu(t)$ will be linearly parameterized as

$$bu = Y\theta, \quad (2.52)$$

where $Y(t) \in \mathbb{R}$ is a measurable regressor, and $\theta \in \mathbb{R}$ is an unknown constant (i.e., θ contains the parametric uncertainty in b). Equation (2.52) can be re-parameterized as

$$\Omega u = Y\theta, \quad (2.53)$$

where $\Omega \in \mathbb{R}$ contains the uncertainty premultiplying $u(t)$. The motivation for defining multiple parameterizations is based on the desire to use standard notation in the following adaptive control design example; in this simplified example, multiple parametrizations are not really necessary. To facilitate the adaptive control design,

an estimate $\hat{\Omega}$ of the uncertain term Ω is defined via the parameterization

$$\hat{\Omega}u = Y\hat{\theta}, \quad (2.54)$$

where $\hat{\theta}(t) \in \mathbb{R}$ is an adaptive estimate of Ω . By substituting (2.52) in to (2.51) and adding and subtracting the term $Y\hat{\theta}$, the open-loop dynamics can be expressed as

$$\dot{x} = f(x) + Y\theta - Y\hat{\theta} + Y\hat{\theta} \quad (2.55)$$

$$= f(x) + Y\tilde{\theta} + \hat{\Omega}u, \quad (2.56)$$

where the parameter estimate mismatch $\tilde{\theta}(t) \in \mathbb{R}$ is defined as

$$\tilde{\theta} \triangleq \theta - \hat{\theta}. \quad (2.57)$$

Based on the subsequent Lyapunov-based stability analysis, the control input is designed as

$$u = -\hat{\Omega}^{-1}(f(x) + kx), \quad (2.58)$$

where $k \in \mathbb{R}$ is a positive constant control gain. Based on the subsequent stability analysis, the adaptive estimate $\hat{\theta}(t)$ is designed via the adaptive update law

$$\dot{\hat{\theta}} = \text{proj}\{Yx\}, \quad (2.59)$$

where $\text{proj}(\cdot)$ is a standard projection algorithm, which is utilized to ensure that the estimate $\hat{\theta}(t)$ remains within a certain prescribed limits (i.e., to ensure that $\hat{\theta}(t) \in L_\infty \forall t$).

Remark 1 *It should be noted that the adaptive update law in (2.59) is designed to stabilize the system based on the following Lyapunov-based analysis; it is not designed to identify the value of the unknown parameter b . To actually estimate the value of the unknown parameter, more advanced techniques are required (e.g., utilizing the persistence of excitation condition).*

Stability Analysis

To analyze the stability of the adaptive control law in (2.58) and (2.59), a positive definite function is defined as

$$V(x, \tilde{\theta}) = \frac{1}{2}x^2 + \frac{1}{2}\tilde{\theta}^2. \quad (2.60)$$

After taking the time derivative of (2.60) and using the fact that $\dot{\tilde{\theta}}(t) = -\dot{\hat{\theta}}(t)$, \dot{V} can be expressed as

$$\dot{V} = x \left(f(x) + Y\tilde{\theta} + \hat{\Omega}u \right) - \tilde{\theta}\dot{\tilde{\theta}} \quad (2.61)$$

where (2.56) was utilized. After substituting (2.58) and (2.59) into (2.61), the following is obtained:

$$\dot{V}(t) = -kx^2 \leq 0. \quad (2.62)$$

The inequality in (2.62) implies that $\dot{V}(t)$ is negative *semidefinite*. To prove that $x(t) \rightarrow 0$, Barabalat's lemma can be utilized. To this end, it is first pointed out that

$$\dot{V}(t) \leq 0 \Rightarrow V(t) \in L_2 \forall t.$$

After integrating both sides of (2.62), the following is obtained

$$\begin{aligned} \int_0^t \dot{V}(\tau) d\tau &\leq -k \int_0^t \|x(\tau)\|^2 d\tau \\ \int_0^t \|x(\tau)\|^2 d\tau &\leq \frac{1}{k} (V(0) - V(t)) < \infty. \end{aligned} \quad (2.63)$$

Since $V(t)$ is always constant or decreasing from $V(0)$, taking the limit as $t \rightarrow \infty$ infinity yields

$$\lim_{t \rightarrow \infty} \int_0^t \|x(\tau)\|^2 d\tau \leq \lim_{t \rightarrow \infty} \frac{1}{k} (V(0) - V(t)) < \infty. \quad (2.64)$$

Thus, the inequality in (2.64) implies that $x(t) \in L_2$.

Since $V(t)$ is bounded, it follows that $x(t), Y(x) \in L_\infty$. Given that $Y(x) \in L_\infty$ and $x(t) \in L_\infty$, the assumption that $x(t) \in L_\infty \Rightarrow f(x) \in L_\infty$ can be used along with the fact that $\hat{\theta}(t) \in L_\infty$ to prove that $u(t) \in L_\infty$ from (2.58). Since $u(t), f(x), \hat{\theta}(t), Y(x) \in L_\infty$, (2.56) can be used to show that $\dot{x}(t) \in L_\infty$. Thus, $x(t)$ is uniformly continuous. Since $x(t) \in L_2$ and $x(t)$ is uniformly continuous, Barbalat's lemma can be invoked to conclude that $\|x(t)\| \rightarrow 0$.

A challenge with adaptive control is that the estimate $\hat{\theta}(t)$ might cross zero during adaptation, which would lead to a singularity from dividing by zero. There is no guarantee that this would not happen if the adaptive estimate is initialized with a sign that is opposite the sign of the actual unknown parameter $\theta(t)$. For example, if the unknown parameter $\theta(t) = -1$, the estimate $\hat{\theta}(t)$ might be initialized at $+1$ because the sign of $\theta(t)$ is unknown. If this happens, then the adaptive estimate $\hat{\theta}(t)$ could cross zero during adaptation, since the projection region must include the value

–1.

Although adaptive control can be utilized to achieve good control performance in the presence of parametric uncertainty, the controller structure is complicated due to the additional loop required to implement the adaptive update law (i.e., see Equation (2.59)). Moreover, the adaptive control algorithm presented here can only compensate for constant or slowly time-varying parametric uncertainty. A block diagram of the adaptive control system presented here is given in Figure 2.6. The next section describes a sliding mode control (SMC) design and demonstrates the capability of SMC to compensate for unknown bounded disturbances and state- and time-varying unknown control input direction.

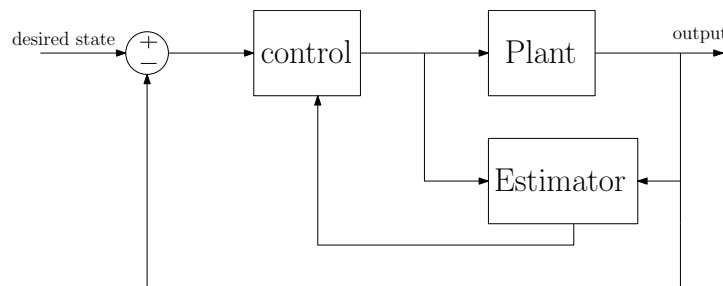


Figure 2.6: Block diagram of adaptive control

2.2.3 Variable Structure Control (VSC)

Detailed analysis of variable structure systems (VSS) appeared at Moscow University and Institute of Control Sciences, USSR, in the late 50s and early 60s (V. I. Utkin, 1992). The analysis showed that new trajectories can be obtained by allowing the control to instantaneously switch between members of a set of possible continuous functions of the state. The challenges of variable structure control (VSC) design entail selecting appropriate control structure parameters and defining proper switching

logics. The strength of VSC lies in the combination of useful properties of multiple individual structures. Specifically, the resulting VSS can exhibit new properties that are not present in the individual structures. For example, a VSS consisting of two structures could yield asymptotic stability, even though neither of the constituent structures is asymptotically stable. The following demonstrates the advantages of VSC.

Controller Structure

Consider the second-order system

$$\ddot{x} = -ux, \quad (2.65)$$

where $u(t) \in \mathbb{R}$ is the control input, and $x(t) \in \mathbb{R}$ is the state. The system or plant in (2.65) has two possible controller structures $u = \alpha_1^2$ and $u = \alpha_2^2$, where $\alpha_1^2 > \alpha_2^2$. Figure 2.7(a) illustrates the path of the structure α_1^2 , and Figure 2.7(b) shows the path of α_2^2 , where neither structure is asymptotically stable (V. Utkin, 1977). By combining the two structures with a switching logic as

$$u = \begin{cases} \alpha_1^2 & \text{if } x\dot{x} > 0 \\ \alpha_2^2 & \text{if } x\dot{x} < 0 \end{cases}$$

the origin of the system is now asymptotically stable, as shown in Figure 2.7(c); and the VSC switching logic drives the state space to a chosen sliding surface and maintains the state along the trajectory.

One possible control form used in VSC is the saturation function $\text{sat}(u)$ (see Fig.

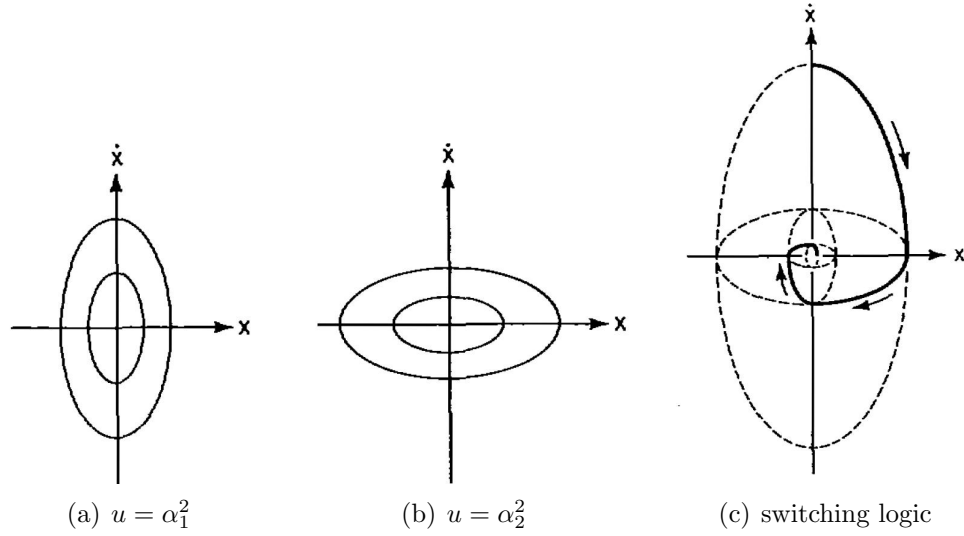


Figure 2.7: Possible path of system (2.65) for different α_1 (Adapted from (V. Utkin, 1977))

2.9(b)):

$$\text{sat}(u) = \begin{cases} u & \text{if } |u| \leq \epsilon \\ \pm 1 & \text{if } |u| > \epsilon \end{cases} \quad (2.66)$$

where ϵ is positive constant. The saturation function does not require infinite bandwidth, unlike the sign function shown in Fig. 2.9(b), but asymptotic stability is generally not achievable in the presence of norm-bounded disturbances. The trade-off between the *sign* and *sat* functions can be illustrated through Lyapunov analysis.

VSC Design Example

The *sat* function, despite its advantage over the *sign* function in terms of finite bandwidth, generally cannot achieve asymptotic stability in the presence of norm-

bounded disturbances. To show this, consider the system

$$\begin{aligned}\dot{x}_1 &= x_2 \\ \dot{x}_2 &= u + d(t)\end{aligned}\tag{2.67}$$

where $d(t) \in \mathbb{R}$ is a norm-bounded disturbance satisfying $|d(t)| \leq d_1$, $x_1(t), x_2(t) \in \mathbb{R}$ are the states, $u(t) \in \mathbb{R}$ is the control input, and $d_1 \in \mathbb{R}$ is a positive bounding constant. The control objective is to force the states $x_1(t)$ and $x_2(t)$ to zero. One of the possible sliding surfaces $\sigma \in \mathbb{R}$ is chosen as $\sigma = x_1 + x_2$. The surface is chosen so that when the sliding manifold is reached, $\sigma = 0$, resulting in $x_2(t) = -x_1(t)$, which implies that $x_1 = x_0 e^{-t}$, where x_0 is the initial condition.

A Lyapunov-based analysis will be utilized to demonstrate the performance of a VSC design. After taking the time derivative of the Lyapunov function

$$V = \frac{1}{2}\sigma^2,\tag{2.68}$$

where $x = \begin{bmatrix} x_1 & x_2 \end{bmatrix}^T$, the following is obtained:

$$\begin{aligned}\dot{V} &= \sigma \left(\frac{\partial \sigma}{\partial x} \right) \dot{x} \\ &= \sigma \begin{bmatrix} 1 & 1 \end{bmatrix} \begin{bmatrix} \dot{x}_1 \\ \dot{x}_2 \end{bmatrix} \\ &= \sigma(x_2 + u + d(t)).\end{aligned}\tag{2.69}$$

By designing $u = -x_2 - k\text{sat}(\sigma)$, the Lyapunov derivative can be expressed as

$$\begin{aligned}\dot{V} &= \sigma(-k\text{sat}(\sigma) + d(t)) \\ &\leq |\sigma|d_1 - k\sigma\text{sat}(\sigma)\end{aligned}\tag{2.70}$$

Based on (2.66) and (2.70), it can be seen that for $|\sigma| < 1$, k cannot compensate for $d(t)$ as σ approaches zero. Figure 2.8 shows that as σ approaches zero, the term σ^2 cannot dominate $|\sigma|d_1$. This illustrates the limitation of using the *sat* function. Figure 2.8 shows that as $\epsilon \rightarrow 0$, the *sat* function will behave like a *sign* function.

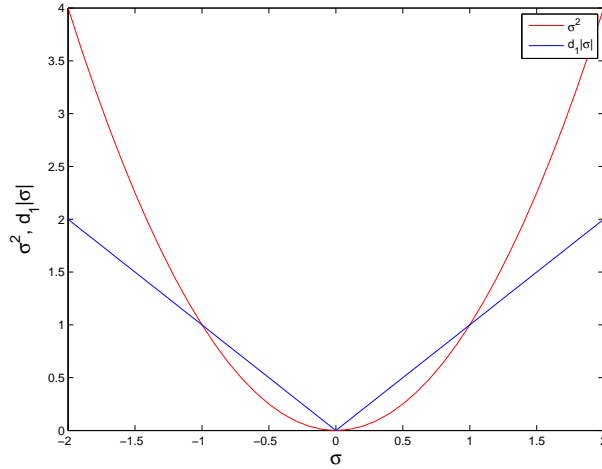


Figure 2.8: Comparison of σ^2 vs. σ and $|\sigma|d_1$ vs. σ

2.2.4 Sliding Mode Control (SMC)

SMC is a form of VSC that changes the dynamics of linear and nonlinear systems by applying a discontinuous control signal that forces the original system to “slide” along the intersections of designed manifolds. The feedback law of SMC use high-

frequency control switching to change from one continuous structure to another based on the current state of the system. SMC's high bandwidth provides the means to design effective and robust control of linear and nonlinear plants, allowing rejection of bounded disturbances in the system's model, making it desirable in control design. Despite the practical drawback of SMC in requiring infinite bandwidth, the high-speed switching achievable using modern-day circuitry and technology have made implementation of SMC a more feasible and attractive option.

The time during which the system's trajectory is approaching the sliding surface is referred to as the *reaching phase*. Once the trajectory reaches the sliding surface, the system has reached the *sliding mode*. Once the system is in sliding mode, convergence to the desired state is inevitable.

SMC uses the *sign* function to express the switching among surfaces. The *sign* function can be expressed as (see Figure 2.9(a))

$$\text{sign}(u) = \begin{cases} 1 & \text{if } u > 0, \\ 0 & \text{if } u = 0, \\ -1 & \text{if } u < 0, \end{cases} \quad (2.71)$$

Note that this is a simplification of the *sign* function to simplify the Lyapunov-based analysis. The official definition of the *sign* function is that the value at zero is contained in the set $(-1, 1)$. Using the *sign* definition would require Filippov-based arguments, which includes differential inclusions (Filippov, 1964).

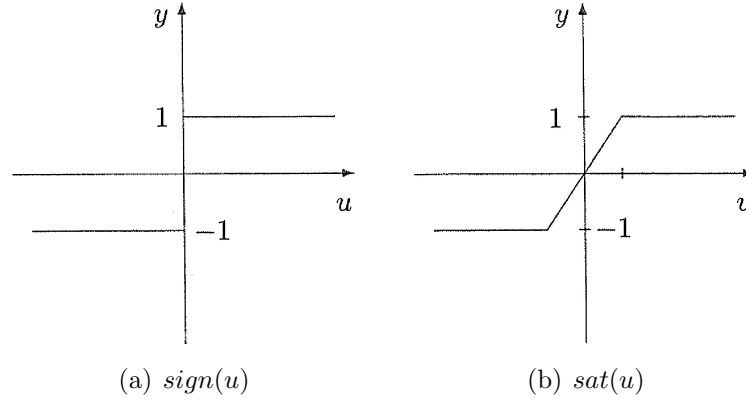


Figure 2.9: The signum and saturation functions (Adapted from (Khalil, 2002))

Existence and Uniqueness of SMC

The existence of a sliding mode implies that the plant intersects the sliding surface at t_0 , and sliding motion exists for $t \geq t_0$, provided that $\sigma(x(t_0)) = 0$. In other words, sliding mode existence implies that

$$\sigma(x) = 0, \quad \frac{\partial \sigma}{\partial x} \dot{x} = 0. \quad (2.72)$$

Sliding mode control, despite its inherent property to reject disturbances, produces a discontinuous right-hand side of (2.67), which fails to satisfy classical theorems on existence and uniqueness of solutions. One of the earlier conceptual proofs of the existence of a sliding mode utilizes the method of Filippov. Conceptually, the resulting behavior, from the method of Filippov, of the system from the discontinuous controller moving along the trajectory $\sigma(x) = 0$ is approximated by the smooth dynamics of $\dot{\sigma}(x) = 0$ (DeCarlo et al., 1988). The method of Filippov can be briefly described as follows: Take an n th order system with single input (DeCarlo et al., 1988)

$$\dot{x}(t) = f(t, x, u), \quad (2.73)$$

with a control strategy of

$$u = \begin{cases} u^+(t, x) & \text{if } \sigma(x) > 0 \\ u^-(t, x) & \text{if } \sigma(x) < 0. \end{cases} \quad (2.74)$$

From (Filippov, 1964), it can be shown that the state trajectories in (2.73) with the control in (2.74) on $\sigma(x) = 0$ are the solutions to

$$\dot{x}(t) = \alpha f^+ + (1 - \alpha)f^- = f^0, \quad 0 \leq \alpha \leq 1,$$

where α is a parameter that depends on the vector as f^+ , f^- ; and $\text{grad } \sigma$ denotes the gradient of $\sigma(x)$, shown in Figure (2.10). The functions

$$f^+ = f(t, x, u^+) \quad f^- = f(t, x, u^-) \quad (2.75)$$

and f^0 are the velocity vectors of the state trajectory resulting from sliding mode. Solving $\langle \text{grad } \sigma, f^0 \rangle = 0$ for α , i.e., where $\text{grad } \sigma$ is perpendicular to the vector f^0 , yields

$$\alpha = \frac{\langle \text{grad } \sigma, f^- \rangle}{\langle \text{grad } \sigma, (f^- - f^+) \rangle}, \quad (2.76)$$

where $\langle a, b \rangle$ denotes the inner product of a and b , provided that

$$\text{a) } \langle \text{grad } \sigma, (f^- - f^+) \rangle > 0 \quad \text{b) } \langle \text{grad } \sigma, f^+ \rangle \leq 0 \quad \text{c) } \langle \text{grad } \sigma, f^- \rangle \geq 0. \quad (2.77)$$

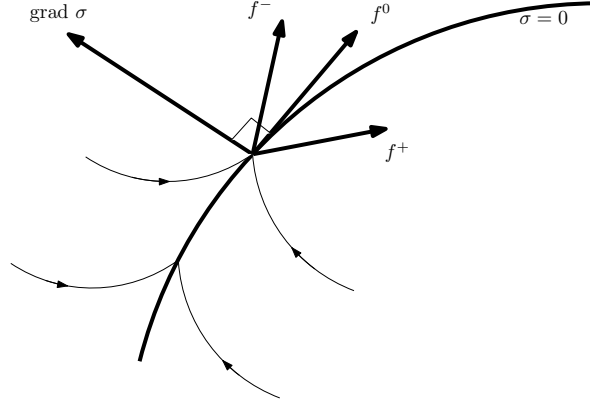


Figure 2.10: Illustration of Filippov method for determining the desired velocity vector in sliding mode (Adapted from (DeCarlo et al., 1988))

Thus, on average, the solution of equation (2.73) with the control in (2.74) exists and is unique on the sliding surface $\sigma(x) = 0$. Filippov's method is one of the techniques used to determine the sliding motion of a system; but the method of equivalent control, which will be discussed later, is more straightforward to apply for multi-input systems. The next section uses Lyapunov-based analysis to demonstrate the robustness of the *sign* function.

Lyapunov-based Convergence Analysis of SMC

To analyze the performance characteristics of SMC, consider the system

$$\begin{aligned}\dot{x}_1 &= x_2, \\ \dot{x}_2 &= u + d(t)\end{aligned}\tag{2.78}$$

where $x_1(t), x_2(t) \in \mathbb{R}$ denote the states, $u(t) \in \mathbb{R}$ is the control input, and $d(t)$ is a disturbance that is bounded as $|d(t)| \leq d_1$, where $d_1 \in \mathbb{R}$ is a positive bounding

constant. Based on the dynamics in (2.78), the sliding surface $\sigma(x)$ is selected as

$$\sigma = x_1 + x_2. \quad (2.79)$$

To design the controller and analyze the stability of the closed-loop system, a positive definite function (i.e., a Lyapunov function candidate) is defined as

$$V = \frac{1}{2}\sigma^2. \quad (2.80)$$

Taking the time derivative of (2.80) along trajectories of (2.78) yields

$$\begin{aligned} \dot{V} &= \sigma \dot{\sigma} \\ &= \sigma (x_2 + u + d(t)). \end{aligned} \quad (2.81)$$

Based on the expression in (2.81), the sliding mode controller is designed as

$$u = -x_2 - k \operatorname{sgn}(\sigma)$$

where $k > d_1$. Note here that the *sign* function is written in shorthand as *sgn*. After substituting $u(t)$ into (2.81), the Lyapunov derivative can be upper bounded as follows:

$$\begin{aligned} \dot{V} &= -k\sigma \operatorname{sgn}(\sigma) + \sigma d \\ &\leq -|\sigma| (k - d_1) \\ &\leq -\sqrt{2k_1} V^{1/2}, \end{aligned} \quad (2.82)$$

where $k_1 \triangleq k - d_1$. By defining $W = V^{1/2}$, the time derivative of W can be obtained as

$$\dot{W} = \frac{1}{2} \frac{\dot{V}}{V^{1/2}}. \quad (2.83)$$

Equation (2.82) can be rewritten as

$$\dot{W} \leq -\frac{\sqrt{2}k_1}{2}, \quad (2.84)$$

and solving for W yields

$$W(V(t)) \leq -\frac{\sqrt{2}k_1}{2}t + W(V(0)). \quad (2.85)$$

Since $V \geq 0$, $W = V^{1/2} \geq 0$, and W has to reach $W = 0$ in finite time, which implies that V reaches 0 in finite time. Thus,

$$\sigma = x_1 + x_2 \rightarrow 0 \Rightarrow \dot{x}_1 = -x_1.$$

Hence, $x_1(t) \rightarrow x_1(0)e^{-t}$, and $x_1(t) \rightarrow 0$ as $t \rightarrow \infty$. The *sign* controller allows the system to have uniform stability and causes the closed-loop system to reach the sliding surface $\sigma(x) = 0$ in finite time in the presence of disturbances. This is an advantage over the *sat* function, which generally yields convergence to a small neighborhood of the origin.

Advantages and Disadvantages of Sliding Mode

The inherent robustness of SMC makes it an attractive control method for systems with unknown disturbances. However, there are both advantages and disadvantages

in implementing sliding mode control. One of the advantages of sliding mode control is its ability to reject bounded disturbances. It also reduces the system order by one and restricts the plant's trajectories to the sliding manifold (V. I. Utkin, 1992). Consider the system

$$\begin{bmatrix} \dot{x}_1 \\ \dot{x}_2 \end{bmatrix} = \begin{bmatrix} 0 & 1 \\ 0 & 0 \end{bmatrix} \begin{bmatrix} x_1 \\ x_2 \end{bmatrix} + \begin{bmatrix} 0 \\ 1 \end{bmatrix} u, \quad (2.86)$$

and define the sliding surface as $\sigma = s_1 x_1 + x_2$, where s_1 is a positive constant. Small values of s_1 yield the trajectory shown in Figure 2.11(a), and large values of s_1 yield a different trajectory as shown in Figure 2.11(b) (DeCarlo et al., 1988). The system's behavior depends only on the slope s_1 on the sliding line $\sigma = 0$. Solving for $x_1(t)$ from $\sigma = 0 = s_1 x_1 + x_2$ yields

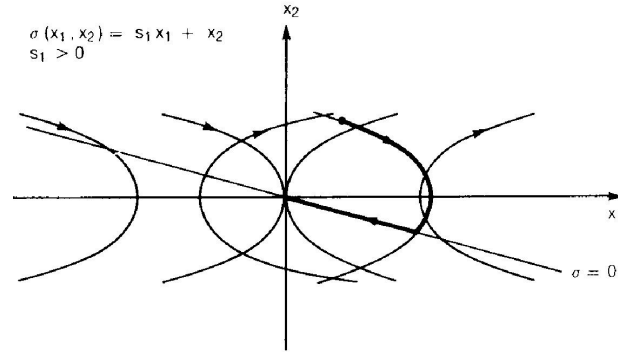
$$x_1 = x_0 e^{-s_1 t}, \quad (2.87)$$

where x_0 is a constant. Equation 2.87 implies that the system is insensitive to any perturbations or variations within the plant parameter in (2.86).

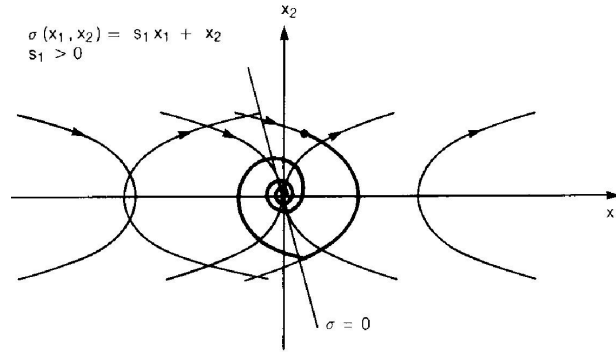
The limitations of SMC are the requirements for infinite bandwidth during its sliding phase and the chattering caused by the discontinuous structure of the controller. In a realistic system, no motors can switch infinitely fast. Thus, the discontinuous signum function is not practically implementable. Work has been done in twisting control (Levant, Taleb, & Plestan, 2011), integral SMC, and other methods to reduce the bandwidth requirement of the controller.

In digital implementation, the finite-time convergence and close to sliding motion without chattering can be achieved by using a continuous approximation of the dis-

continuous *sign* function in a small ε -vicinity of the sliding manifold. The correct choice of ε will result in convergence to the vicinity of the sliding manifold that may be sufficient for practical purposes.



(a) The system's trajectory for small s_1



(b) The system's trajectory for large s_1

Figure 2.11: Phase planes of the closed-loops system for different s_1 (Adapted from (DeCarlo et al., 1988)).

2.2.5 Integral Sliding Mode

Integral SMC is an extension of the standard SMC method that has the benefit of being continuous. Integral SMC (ISMC) eliminates the need for infinite bandwidth in SMC while retaining robustness with respect to norm-bounded disturbances. Figure

2.12 shows the block diagram of a general robust controller structure. It can be seen that robust control is simpler in structure than that of the adaptive control design in Figure 2.6 due to the single-loop structure in the closed-loop system.

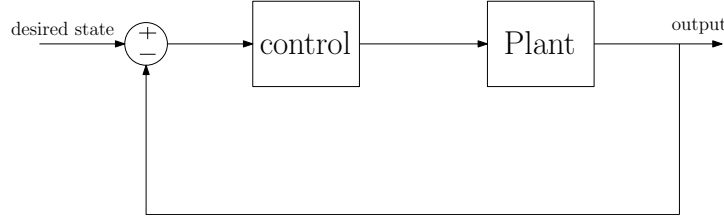


Figure 2.12: Block diagram of robust control

To demonstrate the convergence and disturbance rejection properties of ISMC, consider the second-order system

$$\dot{x}_1 = x_2 \quad (2.88)$$

$$\dot{x}_2 = u + d(t), \quad (2.89)$$

where $x_1(t), x_2(t) \in \mathbb{R}$ are the system states, $d(t) \in \mathbb{R}$ is an unknown nonlinear disturbance, and $u(t) \in \mathbb{R}$ is the control input. The control objective is to force the system state $x_1(t)$ to track the desired state $x_d(t)$. To quantify the control objective, the state tracking error and filtered tracking errors are defined as (Zhang & Zhang, 2010)

$$e_1 \triangleq x_1 - x_d, \quad e_2 \triangleq \dot{e}_1 + \alpha_1 e_1, \quad r \triangleq \dot{e}_2 + \alpha_2 e_2. \quad (2.90)$$

The open-loop tracking error dynamics can be developed by taking the time derivative of $r(t)$ and utilizing the expressions in (2.88) and (2.90) to obtain the following expression

$$\dot{r}(t) = \alpha_1 \ddot{e}_1 + \alpha_2 \dot{e}_2 - \ddot{x}_d + \dot{u} + \dot{d}(t). \quad (2.91)$$

To facilitate the following analysis, it will be assumed that the desired trajectory and its first four derivatives are bounded (i.e., $x_d(t), \dot{x}_d(t), \dots, x_d^{(4)}(t) \leq \zeta_0$, where ζ_0 is a known bounding constant). It will also be assumed that the disturbance $d(t)$ is sufficiently smooth in the sense that

$$\|d(t)\| \leq \zeta_1, \quad \|\dot{d}(t)\| \leq \zeta_2, \quad \|\ddot{d}(t)\| \leq \zeta_3, \quad (2.92)$$

where $\zeta_1, \zeta_2, \zeta_3 \in \mathbb{R}$ are known, positive bounding constants. Equation (2.91) can be rewritten as

$$\dot{r} = N_d + \tilde{N} + \dot{u} - e_2, \quad (2.93)$$

where $N_d(x_d, t) \in \mathbb{R}$ and $\tilde{N}(x, x_d, e_1, e_2, \dot{e}_1, \dot{e}_2, t) \in \mathbb{R}$ are unknown, unmeasurable auxiliary functions defined as

$$N_d \triangleq \dot{d}(t) - \ddot{x}_d, \quad (2.94)$$

$$\tilde{N} \triangleq \alpha_1 \ddot{e}_1 + \alpha_2 \dot{e}_2 + e_2. \quad (2.95)$$

The motivation for defining the auxiliary terms in (2.94) and (2.95) is based on the fact that the quantities $\tilde{N}(x, x_d, e_1, e_2, \dot{e}_1, \dot{e}_2)$ and $N_d(x_d, \dot{x}_d, \ddot{x}_d, t)$ and the time derivative of $N_d(x_d, \dot{x}_d, \ddot{x}_d, t)$ can be upper bounded as

$$\tilde{N} \leq \rho(\|z\|) \|z\|, \quad N_d \leq \zeta_{N_d}, \quad \dot{N}_d \leq \zeta_{\dot{N}_d}, \quad (2.96)$$

where $\zeta_{N_d}, \zeta_{\dot{N}_d} \in \mathbb{R}$ are known positive bounding constants, and $z(t) \in \mathbb{R}^{3 \times 1}$ is

defined as

$$z \triangleq \begin{bmatrix} e_1 & e_2 & r \end{bmatrix}^T. \quad (2.97)$$

In (2.96), $\rho(\cdot) \in \mathbb{R}$ is a positive, globally invertible, nondecreasing function. Based on the expression in (2.93) and the subsequent stability analysis, the control input is designed via

$$\dot{u} = -\beta \operatorname{sgn}(e_2) - (k_1 + 1)r, \quad (2.98)$$

where $\beta, k_1 \in \mathbb{R}$ are positive constant control gains. Note that the sliding surface in this design is taken to be $e_2(t) \triangleq \dot{e}_1(t) + \alpha_1 e_1(t)$. Note also that if $e_2(t) \rightarrow 0$, then $e_1(t) \rightarrow 0$, and $x(t) \rightarrow x_d(t)$.

Remark 2 *Integration by parts can be used in (2.98) to show that the control input $u(t)$ requires measurements of $x(t)$ and $\dot{x}(t)$ only; no acceleration measurements are necessary.*

After substituting (2.98) into (2.93), the closed-loop error system is obtained as

$$\dot{r}(t) = N_d + \tilde{N} - \beta \operatorname{sgn}(e_2) - (k_1 + 1)r - e_2. \quad (2.99)$$

Although the system under consideration (i.e., (2.88) and (2.89)) is only second order, it is trivial to extend this control methodology to n -order systems. For higher-order system, additional filtered tracking errors must be defined; the overall control structure would remain the same. By integrating both sides of (2.98), it follows that the control input $u(t)$ contains its integral, thereby resulting in a continuous signal. This eliminates the requirement for infinite bandwidth, which is inherent in standard SMC. In the Lyapunov analysis, it can be proven, using Theorem 8.4 of Khalil (Khalil,

2002), that the closed-loop system is asymptotically stable; and it can be shown that all system signals remain bounded throughout closed-loop controller operation.

Theorem 1 *The controller given in (2.98) ensures semiglobal asymptotic trajectory tracking in the sense that*

$$\|e_1(t)\| \rightarrow 0 \quad \text{as} \quad t \rightarrow \infty, \quad (2.100)$$

provided the control gain k_1 introduced in (2.98) is selected sufficiently large, and β is selected according to the sufficient condition

$$\beta > \zeta_{N_d} + \frac{\zeta \dot{N}_d}{\alpha_2}, \quad (2.101)$$

where $N_d(t)$ and $\dot{N}_d(t)$ are introduced in (2.94), and α_2 is introduced in (2.90). The control gains α_1 , α_2 , β , and k are selected to yield desirable performance characteristics in terms of overshoot, settling time, tracking accuracy, etc.

To facilitate the following analysis, an auxiliary function $P(t) \in \mathbb{R}$ is defined as the generalized solution to the differential equation

$$\dot{P}(t) = -L(t), \quad (2.102)$$

$$P(0) = \beta |e_2(0)| - N_d^T(0) e_2(0), \quad (2.103)$$

where the auxiliary function $L(t) \in \mathbb{R}$ is defined as

$$L(t) = r(N_d - \beta \operatorname{sgn}(e_2)). \quad (2.104)$$

Lemma 1 *If β satisfies the gain condition in (2.101), then the integral*

$$\int_0^t L(\tau) d\tau \leq \beta |e_2(0)| - N_d^T(0) e_2(0). \quad (2.105)$$

Hence, (2.105) can be used to prove that $P(t) \geq 0$.

Similar proof of Lemma 1 is provided in Appendix (A).

Proof. (See Theorem 1) Consider the nonnegative function

$$V(w, t) \triangleq \frac{1}{2} e_1^2 + \frac{1}{2} e_2^2 + \frac{1}{2} r^2 + P, \quad (2.106)$$

where

$$w(t) \triangleq \begin{bmatrix} z^T & \sqrt{P(t)} \end{bmatrix}^T. \quad (2.107)$$

The function $V(w, t)$ satisfies the inequality

$$U_1(w) \leq V(w, t) \leq U_2(w), \quad (2.108)$$

where the positive definite functions $U_1(w), U_2(w) \in \mathbb{R}$ are defined as

$$U_1 \triangleq \frac{1}{2} \|w\|^2, \quad U_2 \triangleq \|w\|^2. \quad (2.109)$$

After taking the time derivative of (2.106) along trajectories of (2.99), canceling common terms and utilizing the bounding arguments in (2.96), the upper bound on

$\dot{V}(t)$ can be expressed as

$$\dot{V}(w, t) \leq - \left(\lambda_0 - \frac{\rho^2(\|z\|)}{4k_1} \right) \|z\|^2, \quad (2.110)$$

where $k_1 > 0$, and $\lambda_0 \triangleq \min \left\{ \alpha_1 - \frac{1}{2}, \alpha_2 - \frac{1}{2}, 1 \right\}$. ■

The following expression can be obtained from (2.110):

$$\dot{V}(w, t) \leq -U(w), \quad (2.111)$$

where $U(w) = c \|z\|^2$, for some positive constant $c \in \mathbb{R}$, is a continuous, positive semi-definite function that is defined on the following domain:

$$\mathcal{D} \triangleq \left\{ w \in \mathbb{R}^{2m+1} \mid \|w\| < \rho^{-1} \left(2\sqrt{\lambda_0 k_1} \right) \right\}. \quad (2.112)$$

It follows directly from Lyapunov analysis that $r(t), e_2(t), e_1(t) \in \mathcal{L}_\infty$ in \mathcal{D} . This implies that $\dot{e}_2(t), \dot{e}_1(t) \in \mathcal{L}_\infty$ in \mathcal{D} from the definitions given in (2.90). Given that $r(t), e_2(t), \dot{e}_1(t) \in \mathcal{L}_\infty$ in \mathcal{D} , it follows that $\ddot{e}_1(t) \in \mathcal{L}_\infty$ from (2.90). Since $e_1(t), \dot{e}_1(t), \ddot{e}_1(t) \in \mathcal{L}_\infty$ in \mathcal{D} , (2.90) can be used along with the assumption that the desired trajectories are bounded to show that $x_1(t), \dot{x}_1(t), \ddot{x}_1(t) \in \mathcal{L}_\infty$ in \mathcal{D} . Since $\ddot{x}_1(t) \in \mathcal{L}_\infty$ in \mathcal{D} , $\dot{x}_2(t) \in \mathcal{L}_\infty$ in \mathcal{D} , and (2.89) can be used along with (2.92) to show that $u(t) \in \mathcal{L}_\infty$ in \mathcal{D} . Since $r(t) \in \mathcal{L}_\infty$ in \mathcal{D} , (2.98) can be used to show that $\dot{u}(t) \in \mathcal{L}_\infty$ in \mathcal{D} . Given that $r(t), e_2(t), e_1(t) \in \mathcal{L}_\infty$, (2.99) can be used along with (2.96) and (2.97) to prove that $\dot{r}(t) \in \mathcal{L}_\infty$ in \mathcal{D} . Since $\dot{e}_1(t), \dot{e}_2(t), \dot{r}(t) \in \mathcal{L}_\infty$ in \mathcal{D} , $e_1(t), e_2(t)$, and $r(t)$ are uniformly continuous in \mathcal{D} . Thus, the definitions for $U(w)$ and $w(t)$ can be used to prove that $U(w)$ is uniformly continuous in \mathcal{D} .

Let $S \subset D$ denote a set defined as follows:

$$S \triangleq \left\{ w(t) \in D \mid U_2(w(t)) < \frac{1}{2} \rho^{-1} \left(2\sqrt{\lambda_0 k_1} \right)^2 \right\}. \quad (2.113)$$

Theorem 8.4 of Khalil (Khalil, 2002) can now be invoked to state that

$$c \|z\|^2 \rightarrow 0 \quad \text{as} \quad t \rightarrow \infty \quad \forall w(0) \in S. \quad (2.114)$$

Based on the definition of $z(t)$, (2.114) can be used to show that

$$\|e_1(t)\| \rightarrow 0 \quad \text{as} \quad t \rightarrow \infty \quad \forall w(0) \in S. \quad (2.115)$$

For the case where $\tilde{N} \leq \rho(\|z\|)\|z\|$, the result is semi-global asymptotic stability (SGAS), meaning that asymptotic stability is achieved provided the initial conditions are within a bounded region which can be made arbitrarily large by increasing the control gain k_1 . For the case where $\tilde{N} \leq \rho_0 \|z\|$, where ρ_0 is a constant, the result is global asymptotic stability (GAS). The drawback of this controller is the additional derivative required of the systems dynamics to prove convergence in the Lyapunov stability analysis. However, the benefit gained by using this controller structure is the elimination of the requirement for infinite bandwidth.

The example presented has unity input gain, whereas the quadrotor, introduced in the later chapter, has an uncertain input matrix. The advantage of robust control over adaptive control is the simple single-loop controller structure. An advantage of RISE over standard SMC is the continuous controller structure, which eliminates the need for infinite bandwidth.

2.2.6 Method of Equivalent Control

Another method to determine a system's trajectory on a sliding surface is through the method of equivalent control. The discontinuous right-hand side produced by SMC in (2.71) - (2.78) does not satisfy classical theorems on existence and uniqueness of solutions (V. Utkin, 1977). Various non-idealities such as time-delay, hysteresis, and other types should be taken into consideration to treat SMC carefully. These non-idealities determine how the real sliding mode behaves when it is in the vicinity of the discontinuity surface $\sigma(x) = 0$. If the non-idealities go to zero, the motion of the system goes to the ideal sliding mode.

The method of equivalent control is one possible technique used to determine equations of ideal sliding modes (V. Utkin, 1977). The technique involves differentiating the surface $\sigma(x)$ along the system trajectory and setting it equal to zero to solve for the control vector. The resulting control vector is called the equivalent control. Substituting the equivalent control into the original system results in equations of ideal sliding mode. The equivalent control method, from a geometric point of view, is the means to find a continuous control that directs the velocity vector along the intersection of the discontinuity surfaces.

Consider the system

$$\dot{x} = f(t, x) + B(t, x)u \quad (2.116)$$

$$u = k\sigma(x), \quad (2.117)$$

where $x(t) \in \mathbb{R}^{n \times 1}$, $f(t, x) \in \mathbb{R}^{n \times 1}$, $B \in \mathbb{R}^{n \times m}$, $u(t) \in \mathbb{R}^m$, $\sigma(x) \in \mathbb{R}^m$ are known and continuous. To solve for the equivalent control $u_{eq}(t)$, it is desirable to obtain

an equation for sliding mode in the manifold $\sigma(x) = 0$. The equivalent control is obtained by calculating the solution of $\dot{\sigma}(x) = 0$ with respect to $u(t)$ along trajectories of (2.116) as

$$\dot{\sigma} = \frac{\partial \sigma}{\partial x} \frac{\partial x}{\partial t} = \frac{\partial \sigma}{\partial x} (f(t, x) + B(t, x)u_{eq}) = 0 \quad (2.118)$$

$$u_{eq} = - \left[\frac{\partial \sigma}{\partial x} B(t, x) \right]^{-1} \frac{\partial \sigma}{\partial x} f(t, x). \quad (2.119)$$

Substituting (2.119) into (2.116), the motion with equivalent control can be written as

$$\dot{x} = \left[I - B(t, x) \left(\frac{\partial \sigma}{\partial x} B(t, x) \right)^{-1} \frac{\partial \sigma}{\partial x} \right] f(t, x). \quad (2.120)$$

Equation (2.120) is valid with the assumption that $[\partial \sigma / \partial x] B(t, x)$ is nonsingular for all t and x . When $[\partial \sigma / \partial x] B(t, x)$ is singular, the equivalent control is not unique, or it does not exist. For the first situation where the equivalent control is not unique, a variety of sliding modes may occur depending on the non-idealities or limiting processes of the plant. For the second situation when the equivalent control does not exist, sliding modes cannot appear, which implies that the state leaves the sliding surface. Also, for systems that are nonlinear with respect to the control, if a unique equivalent control does exist, the differential equations for sliding mode, in general, are not unique, depending on the limiting processes of the plant. Note that the motion on the sliding surface is governed by a reduced-order set of equations because of the set $\sigma(x) = 0$. One of the applications of equivalent control is the super-twisting control given in (Levant et al., 2011).

The next chapter uses the mathematical background developed in this chapter to

solve for underactuated parallel systems with single input.

Chapter 3

Dual Parallel Systems with Single Input

3.1 Introduction

There has been a great deal of research devoted to control design for underactuated systems in recent years. This class of systems has a variety of real world applications, including the inverted pendulum, cars, spacecraft, unmanned underwater vehicle, overhead cranes, and others. Control algorithm design for underactuated systems is particularly challenging due to the fact that there are fewer control actuators than there are degrees of freedom. While there have been several approaches to the underactuated control problem, there remains a need for novel control techniques that can achieve desirable performance for general underactuated dynamic systems consist of a single control input and multiple outputs.

There are many works that contribute to the control problem of underactuated

systems. A general approach was proposed in (Reyhanoglu, Schaft, McClamroch, & Kolmanovsky, 1999), where a theoretical control framework was developed for a general class of underactuated mechanical systems with nonintegrable dynamics. In (Cornejo & Alvarez-Icaza, 2007), a passivity-based control was designed to compensate for systems with nonlinear friction effects. In (Mnif & Ghommam, 2002), a special class of mechanical systems in nontriangular form was investigated, where general construction of the nonlinear control law was developed by defining a change of coordinates. Nordkvist et al. (Nordkvist & Bullo, 2008) proposed a novel control algorithm for a class of underactuated systems that are invariant on a Lie group. The design in (Nordkvist & Bullo, 2008) is based on iterative small-amplitude control forces. In (Olfati-Saber, 2000), a change of control is utilized to partially linearize an underactuated system to develop partially linear cascade normal forms, which are convenient in control design for underactuated systems. In (Shiriaev & Kolesnichenko, 2000), Shiriaev *et al.* proposed stabilizing a class of systems with respect to part of the state variables, where it is assumed that part of the state variable is directly affected by the control. In (Bullo & Lynch, 2001), Bullo *et al.* worked on underactuated systems where the motion of kinematically controllable underactuated mechanical systems for which it is possible to decouple trajectories planning between zero velocity states. This form the basis for efficient collision-free trajectory planning for a class of underactuated mechanical systems. In (Arai, Tanie, & Shiroma, 1998), Arai *et al.* considers stabilization of a 3-DOF planar underactuated manipulator. The technique is based on composite of translational trajectory segment and rotational trajectory segment. In (Pettersen & Egeland, 1996), Pettersen *et al.* developed a continuous periodic time-varying feedback law for underactuated surface vessel.

Other control method such as adaptive control has proven to be useful in controlling underactuated systems. In (An-Chyau & Yung-Feng, 2010), An-Chyau *et al.* utilized the method developed in (Olfati-Saber, 2000) to transform an underactuated system dynamics into a special cascade form, then a control algorithm, composed of an adaptive multiple-surface sliding mode that is based on function approximation techniques, was developed. In (Kung, Chen, & Huang, 2009), an underactuated system is divided into two subsystems, then sliding surfaces for each of the subsystems are defined. Fuzzy models are then employed to estimate an unknown function, and an adaptive fuzzy sliding-mode controller was developed. In (Han, Wei, & Li, 2008), Han *et al.* used adaptive neural network control for switched underactuated systems. It was shown that sudden changes in control gains at switching times could be overcome using a smooth approximation of the discontinuous adaptive controller. In (Kim, Kim, & Jun, 2012), Kim *et al.* utilized adaptive sliding mode control that uses slack variables to overcome the underactuated properties of the systems. In (Orlov, Aguilar, & Acho, 2005), Orlov *et al.* develops a quasi-homogeneous control algorithm that used switching controller to drive the pendubot to the origin. The idea is based on generating the pendubot zero dynamics by a reference model made from a modified Van Der Pol oscillator.

In addition to adaptive control techniques, backstepping and energy shaping approaches have been proposed to address the underactuated control problem (Rosas-Flores, Alvarez-Gallegos, & Castro-Linares, 2000; Ghommam, Bouterrea, Mnif, & Poisson, 2011; Choukchou-Braham, Cherki, & Djemai, 2011; Albu-Schaffer, Ott, & Hirzinger, 2005; Xin, 2009; Hu, Gans, & Dixon, 2007). In (Rosas-Flores et al., 2000), backstepping was used to develop a control algorithm for a class of systems after

a suitable change of coordinates was constructed. Other backstepping-based control approaches for underactuated systems are presented in (Ghommam et al., 2011; Choukchou-Braham et al., 2011). The energy shaping method was used to design a control law for a class of underactuated systems in (Albu-Schaffer et al., 2005). The idea was to shape a potential energy function via the introduction of a new control variable that is a function of the collocated state variables. In (Jiang, 2002), Jiang *et al.* proposed two control algorithms, passivity-based feedback and cascade-backstepping, through Lyapunov's direct method for an underactuated ships with only two propellers. The passivity-based feedback has better transient performance than the cascade-backstepping method. In (Xin & Kaneda, 2002), Xin *et al.* designed a swing up control for the acrobot based on energy approach. The idea is to force the system to converge to the potential energy of its top upright position, which cause the system to converge to a homoclinic orbit. Other energy shaping-based control methods for underactuated systems can be found in (Xin, 2009; Hu et al., 2007).

Sliding mode is a popular control strategy because of its robustness to bounded disturbances and uncertainty. Despite its robustness, SMC design for underactuated systems is still challenging because underactuated systems are usually made of several subsystems, and among these subsystems, the parameters have no obvious differential relationship among them, so common sliding mode surfaces might not be appropriate. In (Hao, Yi, & Zhao, 2008), Hao *et al.* however, was able to use sliding mode control to stabilize a class of underactuated system using a combination of different sliding surfaces. Similarly, in (W. Wang, Yi, Zhao, & Liu, 2004; Yi, Wang, Zhao, & Liu, 2005; S. H. Lee, Park, & Choi, 2009; Qian, Yi, & Zhao, 2007; Qian & Yi, 2010), sliding mode control was implemented by dividing the single-input multiple-output

(SIMO) underactuated system into subsystems so that hierarchical sliding surfaces could be manipulated. In (Yi et al., 2005), Yi *et al.* presented a sliding mode controller for large-scale underactuated systems. The large-scale system was divided into subsystems and the sliding surfaces was designed to include all of the subsystems. In (S. H. Lee et al., 2009), a hierarchical sliding mode approach was developed for a class of underactuated systems where the structure is divided into two layers: terminal sliding surfaces for each subsystem and a whole sliding surface that is a linear combination of the terminal sliding surfaces. In (Xu, Guo, & Lee, 2010), integral sliding mode control was utilized to stabilize a class of underactuated systems with uncertainty. Sliding mode control was also used in (Xu, Guo, & Lee, 2012), where the focus on the norm model was used to describe a class of underactuated systems. Also, a combination of fuzzy logic and sliding mode control was used for output tracking of uncertain underactuated systems (Chiang, 2012).

The contribution of this chapter is the design of a novel control method for a small class of underactuated system: parallel systems with SIMO (single-input multiple-output). The general control algorithm proposed is based on two steps: the first step is to drive subsystem 2 to a region of stability near the origin by tracking a bounded time-varying desired function; the second step is to indirectly drive subsystem 1 to the origin via the desired function. To facilitate the analysis, properties of a slowly time-varying desired function is exploited. The proposed controller is computationally inexpensive (i.e., a single feedback loop), requiring no online adaptive updates, or function approximators. This computationally minimal design is motivated by the desire to improve controller performance in implementation by reducing the required computation time.

3.2 Problem Formulation

Consider a class of underactuated systems whose dynamics can be expressed as

$$\dot{x}_1 = f_1(x_1, x_2) + b_1(x_1, x_2)u, \quad (3.1)$$

$$\dot{x}_2 = f_2(x_2) + b_2(x_2)u, \quad (3.2)$$

where $x_1 \in \mathbb{R}^{n_1}$ and $x_2 \in \mathbb{R}^{n_2}$ are the states, $f_1(x_1, x_2) \in \mathbb{R}^{n_1}$ and $f_2(x_2) \in \mathbb{R}^{n_2}$ are the drift terms, $b_1(x_2) \in \mathbb{R}^{n_1}$ and $b_2(x_2) \in \mathbb{R}^{n_2}$ are the input vectors, $u(t) \in \mathbb{R}$ is the scalar control input, and $n_1, n_2 \in \mathbb{Z}^+$. The system under consideration is illustrated in Fig. 3.1. The state $x_1(t)$ does not directly influence the dynamics in (3.2), however, the state $x_2(t)$ is inherent in both subsystems. This kind of system is difficult to control because there is only one control input, which directly affects both channels. The control goal is to drive the system in (3.1) and (3.2) to the origin. To overcome the challenges involved in controlling the underactuated parallel system in (3.1) and (3.2), the control algorithm is divided into two stages **1)** Drive the subsystem in (3.2) to an area of stability near the origin by tracking a desired function $x_2^* = x_2^*(x_1)$, **2)** stabilize Subsystem (3.1) through the bounded slowly state-varying desired function $x_2^*(x_1)$ while keeping (3.2) in an area of stability near the origin.

Assumption 1 *The dynamics are assumed to satisfy*

$$f_1(0, 0) = 0 \quad f_2(0) = 0. \quad (3.3)$$

Consider Fig. 3.2, where $B_3 \in B_2 \in B_1$, with $x_2(t), \dot{x}_2(t) \in B_1$. The objective is to drive $x_2(t)$ to $x_2^*(x_1)$ in Subsystem (3.2), thereby driving $x_2(t)$ from the set

B_1 to B_2 , where it will stay in B_2 . Then, the bounded slowly time-varying desired function $x_2^*(x_1)$ is designed to drive Subsystem (3.1) ($x_1(t)$) to zero. Once $x_1(t) = 0$, $x_2(t)$ approaches B_3 , and both states will converge to zero. Throughout this chapter, Subsystem (3.1) is referred to as Subsystem 1 and Subsystem (3.2) is referred to as Subsystem 2.

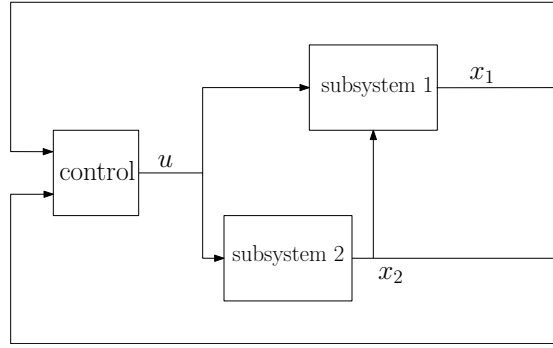


Figure 3.1: Block diagram of the considered system

3.3 Control Design

To stabilize Subsystem 2 to an area near the origin, the control $u(t)$ is designed as

$$u = g(x_2, x_2^*), \quad (3.4)$$

where $x_2^* = x_2^*(x_1)$ is a bounded slowly time-varying desired tracking state. The function $g(x_2, x_2^*)$ can be obtained from a variety of nonlinear control methods, such as sliding mode control, adaptive control, backstepping, and others.

Assumption 2 *There exists a control $g(x_2, x_2^*)$ in (3.4) that can track track $x_2^*(x_1)$ in the sense that $x_2(t) \rightarrow x_2^*(x_1)$, and there exists a control algorithm $u(x_2, x_2^*) =$*

$g(x_2, 0)$ that can stabilize Subsystem 2 to the origin.

For the first part of the control design, instead of driving Subsystem 2 to the origin, the goal is for $x_2(t)$ to track the desired state $x_2^*(x_1)$ such that

$$|x_2 - x_2^*| \rightarrow 0. \quad (3.5)$$

Based on (3.5), Subsystem 2 converges to $x_2^*(x_1)$ instead of directly going to origin. Once the tracking objective in (3.5) has been achieved, $x_2(t) = x_2^*(t)$, and Subsystem 2 can be expressed as

$$\dot{x}_2^* = f_2(x_2^*) + b_2(x_2^*)u_{eq}(x_2^*), \quad (3.6)$$

where $u_{eq}(x_2^*)$ is the equivalent control. To solve for $u_{eq}(x_2^*)$, Equation (3.6) is set equal to zero resulting in

$$u_{eq} = \psi(x_2^*) = -\frac{f_2(x_2^*)}{b_2(x_2^*)}. \quad (3.7)$$

The motivation for setting Equation (3.6) to zero to solve for $u_{eq}(x_2^*)$ is based on equivalent control analysis in sliding mode control, which can be found in (V. I. Utkin, 1992). For the method proposed in this chapter, the equivalent control $u_{eq}(x_2^*)$ governs the behavior of Subsystem 1 when Subsystem 2 is at the origin, thus allowing the design of the *fictitious control* $x_2^*(x_1)$ to drive Subsystem 1 to the origin by forcing $x_2(t)$ to track the function $x_2^*(x_1)$.

Remark 3 *If $g(x_2, x_2^*)$ is continuous, then $\psi(x_2^*) = g(x_2^*, x_2^*)$; if $g(x_2, x_2^*)$ is discontinuous, then $\psi(x_2^*) = \{g(x_2, x_2^*)\}_{eq}$.*

After Substituting $u_{eq}(x_2^*)$ into Subsystem 1, Equation (3.1) becomes

$$\dot{x}_1 = f_1(x_1, x_2^*) + b_1(x_1, x_2^*) \psi(x_2^*). \quad (3.8)$$

The control $u(x_2^*)$ in Subsystem 1 is replaced by the equivalent control $u_{eq}(x_2^*)$, because $x_2(t)$ is tracking $x_2^*(x_1)$ once the tracking objective in (3.5) has been achieved.

Assumption 3 *There exists a function $x_2^*(x_1)$ that can stabilize Subsystem 1 to the origin.*

The function $x_2^*(x_1)$ can be obtained by selecting appropriate linear or nonlinear control methods based on the dynamics in (3.8).

Based on preliminary analysis, the desired state $x_2^*(x_1)$ should meet the properties below.

Properties of $x_2^*(x_1)$

1. $|x_2^*(x_1)| \leq c_1$, where $c_1 > 0$ and c_1 is small,
2. $x_2^*(x_1)$ is slowly changing such that $x_2(t)$ can track it, i.e. $x_2(t) = x_2^*(x_1)$,
3. $x_2^*(0) = 0$,
4. When the state $x_1(t)$ is far away from the origin, $|x_2^*(x_1)|$ behaves like a constant.

There are several functions that satisfy the properties in (1)-(4). An example of a function that satisfies the properties above is the hyperbolic tangent function $\tanh(\cdot)$. When the argument (\cdot) is far away from the origin, $\tanh(\cdot)$ behaves like a constant,

and when the argument (\cdot) is close to the origin, $\tanh(\cdot)$ behaves like a linear system. When $x_2^*(x_1)$ is far away from the origin, $x_2(t)$ tracks $x_2^*(x_1)$ like a constant that can drive the dynamics in Subsystem 1 toward the vicinity of the origin; when Subsystem 1 is close to the origin, the dynamics can be linearized to see that $x_2^*(x_1)$ stabilizes Subsystems 1 and 2 to the origin at the same time.

This method is not backstepping. Traditional backstepping cannot be used to solve the parallel system presented. In backstepping, the design parameters are used to stabilize all the variables by branching out until the actual control is reached, but in this method, Subsystem 1 is stabilized to an area of stability near the origin, then the desired function $x_2^*(x_1)$ indirectly drives Subsystem 2 to the origin. Note here that the *fictitious control* is the state $x_2^*(x_1)$, not the equivalent control $u_{eq}(x_2)$. As Subsystem 2 decreases and goes to some vicinity around the origin, the designed $x_2^*(x_1)$ forces Subsystem 1 to go to the origin at the same time. Eventually, as Subsystem 1 goes to the origin, so does Subsystem 2. Additionally, the backstepping method has the control input in one of the subsystems and indirectly affects the other subsystems via the states. In the parallel system, the scalar control input is in all of the subsystems and directly affects all the states at once, making it a highly challenging problem to overcome.

3.3.1 Stability Proof

To prove the stability of the general method described above, a positive definite function is defined as

$$V_1 = V_1(x_1, x_2^*). \quad (3.9)$$

Taking the time derivative of (3.9), $\dot{V}_1(x_1, x_2^*)$ can be expressed as

$$\dot{V}_1 = \frac{\partial V_1}{\partial x_1} \dot{x}_1 + \frac{\partial V_1}{\partial x_2^*} \dot{x}_2^*, \quad (3.10)$$

where $\dot{x}_1(x_1, x_2^*)$ is obtained using (3.8). From Assumption (3), the fictitious control function $x_2^*(x_1)$ stabilizes (3.8) to the origin; thus, for a slowly time-varying function $x_2^*(x_1)$, Equation (3.10) satisfies the inequality

$$\dot{V}_1 < -W_1(x), \quad (3.11)$$

where $W(x)$ is a positive definite function, and $x \triangleq [x_1, x_2]^T$.

Consider a second candidate Lyapunov function

$$V_2 = V_2(x_2). \quad (3.12)$$

The time derivative of (3.12) can be expressed as

$$\dot{V}_2 = \frac{\partial V_2}{\partial x_2} \dot{x}_2, \quad (3.13)$$

where $\dot{x}_2(x_2)$ is obtained from (3.2). From Assumption 2, there exists a control $u(x_2, x_2^*) = g(x_2, 0)$ that stabilizes Subsystem 2, and Equation (3.13) can be upper bounded as

$$\dot{V}_2 \leq -W_2(x), \quad (3.14)$$

where $W_2(x)$ is a positive definite function.

After adding (3.9) and (3.12), a composite Lyapunov function is obtained as

$$V_3 = V_1 + V_2. \quad (3.15)$$

The control input $u(x_2, x_2^*)$ can be designed to track $x_2^*(x_1)$ to yield Inequality (3.11). Since the dynamics in (3.1)-(3.2) contain a scalar control in all the subsystems, one way to track $x_2^*(x_1)$ is through the state $x_2(t)$. Once $x_2(t) \rightarrow x_2^*(x_1)$ after some time interval $[0, t_1]$, the inequality in (3.11) is satisfied because of the equivalent control $\psi(x_2^*)$ in (3.8). This implies that $u(x_2, x_2^*) = g(x_2, 0)$ after another time interval $[t_1, t_2]$, so that Inequality (3.14) is satisfied. Therefore, the composite function V_3 satisfies the inequality

$$\dot{V}_3 < -W_3(x), \quad (3.16)$$

where $W_3(x)$ is a positive definite function. Based on the results in (3.9)-(3.16) and the fact that $x_2^*(x_1) \rightarrow 0$, the assumption that $x_2^*(0) = 0$ can be used to show that the system in (3.1) converges to the origin; and based on Assumption 2, Subsystem (3.2) also converges to the origin.

A more rigorous stability proof considering a mechanical system in the form of (3.1)-(3.2) is shown in the Simulation Results section.

The nature of this type of design is different from the integrator backstepping, where a scalar control appears in only one of the subsystems, which allows successful application of the recursive techniques developed by Petar V. Kokotovic. The method presented in this chapter has scalar control in all the subsystems, which makes backstepping algorithm not possible to apply. Instead of the standard backstepping technique, which uses the integral of the control input through successive

schemes, the proposed approach uses the state $x_2(t)$ to track $x_2^*(x_1)$ to stabilize the subsystems through equivalent control. Moreover, backstepping and other schemes start from Subsystem 1 and create a fictitious controller, then move on to Subsystem 2 to track the fictitious control in subsystem 1 if there is a scalar control only in Subsystem 2; the algorithm proposed in this chapter starts with Subsystem 2, where the control $u(x_2, x_2^*)$ stabilizes it around some region around the origin, then designed a fictitious controller that manipulates $x_1(t)$ by manipulating the behavior of $x_2(t)$. These are two completely different approaches.

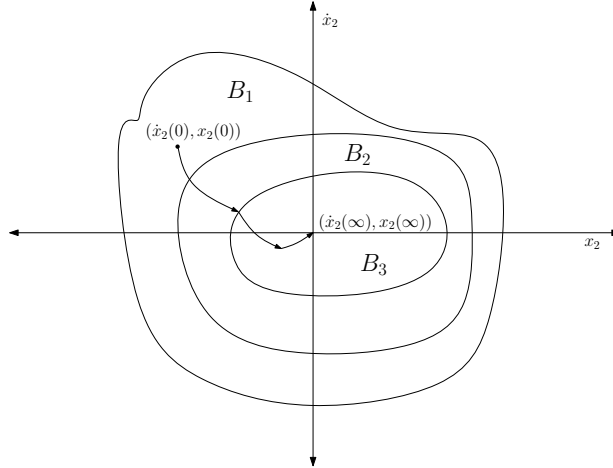


Figure 3.2: Sketch of the Lyapunov function regions

3.4 Simulation Results

The proposed control algorithm can be implemented using a variety of nonlinear control methods, but in this example, the authors use sliding mode control to stabilize the inverted pendulum system. Consider the inverted pendulum mechanical system

that has the form in (3.1) and (3.2) with the definitions (Wie, 2008)

$$\begin{aligned} b_1(x_1, x_2) &= \begin{bmatrix} 0 \\ b_{11}(x_2) \end{bmatrix} & b_2(x_1, x_2) &= \begin{bmatrix} 0 \\ b_{22}(x_2) \end{bmatrix}, \\ f_1(x_1, x_2) &= \begin{bmatrix} \dot{z} \\ f_{11}(x_2) \end{bmatrix} & f_2(x_1, x_2) &= \begin{bmatrix} \dot{\theta} \\ f_{22}(x_2) \end{bmatrix}, \end{aligned} \quad (3.17)$$

where $x_1 = \begin{bmatrix} z & \dot{z} \end{bmatrix}^T \in \mathbb{R}^2$ are the horizontal position and velocity, and $x_2 = \begin{bmatrix} \theta & \dot{\theta} \end{bmatrix}^T \in \mathbb{R}^2$ are the angular position and angular velocity. The states are illustrated in Fig. 3.3. The drift and input vector functions $f_{11}(x_1, x_2)$, $b_{11}(x_2)$, $f_{22}(x_2)$, and $b_{22}(x_2)$ are defined as

$$f_{11}(\theta, \dot{\theta}) = \frac{ml\dot{\theta}^2 \sin \theta - mg \sin \theta \cos \theta}{(M + m) - m \cos^2 \theta}, \quad (3.18)$$

$$b_{11}(\theta) = \frac{1}{(M + m) - m \cos^2 \theta}, \quad (3.19)$$

$$f_{22}(\theta, \dot{\theta}) = \frac{ml\dot{\theta}^2 \sin \theta \cos \theta - (M + m)g \sin \theta}{l(m \cos^2 \theta - (M + m))}, \quad (3.20)$$

$$b_{22}(\theta) = \frac{\cos \theta}{l(m \cos^2 \theta - (M + m))}, \quad (3.21)$$

where $M, m, l, g \in \mathbb{R}$ denote the cart mass, ball mass, pendulum length, and gravity, respectively.

Assumption 4 *The states $(x, \dot{x}, \theta, \dot{\theta})$ are measurable.*

The equivalent control u_{eq} in (3.6) is obtained by setting \dot{x}_2 to zero, yielding

$$u_{eq} = -\frac{f_{22}(x_2^*)}{b_{22}(x_2^*)}. \quad (3.22)$$

Substituting u_{eq} into (3.1) gives

$$\ddot{z}^* = f_{11}(x_2^*) - b_{11}(x_2^*) \frac{f_{22}(x_2^*)}{b_{22}(x_2^*)}. \quad (3.23)$$

From (3.23), $x_2^*(x_1) \in \mathbb{R}^2$ can be designed to stabilize the subsystem 1. After utilizing (3.18) - (3.21) and working out the algebra, equation (3.23) becomes

$$\ddot{z}^* = g \tan(\theta) = g \tan(\theta_1^*(x_1)). \quad (3.24)$$

Now, the desired function $x_2^*(x_1)$ can be designed as

$$x_2^* = \begin{bmatrix} \theta_1^*(x_1) \\ 0 \end{bmatrix}, \quad (3.25)$$

where $|\theta_1^*(x_1)| \leq c_1$ and $c_1 > 0$. In the equation (3.25), the bottom element of $x_2^*(x_1)$ is zero because $\theta_1^*(x_1)$ is slowly time-varying and it is a desired state. Based on (3.24), the desired states and sliding surfaces are defined as

$$\theta_1^*(z, \dot{z}) = -k \tanh(\sigma), \quad (3.26)$$

$$\sigma = \dot{z} + k_2 \tanh z, \quad (3.27)$$

$$s = \dot{\theta} + \theta - \theta_1^*(z, \dot{z}), \quad (3.28)$$

where $k, k_2 > 0$ are positive small constants, and $s(\theta, \theta_1^*)$ is the sliding surface. The desired state $\theta_1^*(x_1)$ is chosen as a hyperbolic tangent because Equation (3.24) has the $\tan(\cdot)$ function. Based on the properties of the $\tan(\cdot)$ function, the $\tanh(\cdot)$ function is chosen to ensure the upper limit on the magnitude of $\theta_1^*(z, \dot{z})$. Since $\theta_1^*(z, \dot{z})$ is limited in magnitude, and based on the subsequent analysis, $\theta_1^*(z, \dot{z})$ is designed to be small so that (3.24) behaves like a second order system, which can be analyzed by finding appropriate gains k, k_2 that can stabilize (3.24) to the origin. The sliding surface $s(\theta, \theta_1^*)$ is chosen so that the $\theta(t)$ can track $\theta_1^*(z, \dot{z})$. After taking the time derivative of the sliding surface $s(\theta, \theta_1^*)$ in (3.28) and based on Lyapunov arguments, the control law is proposed as

$$u_1 = -\frac{f_{22} + \dot{\theta} + h(x) \operatorname{sech}^2 \sigma + M_1 \operatorname{sgn}(s)}{b_{22} + kb_{11} \operatorname{sech}^2 \sigma}, \quad (3.29)$$

$$h(x) = kf_{11} + kk_2 \dot{z} \operatorname{sech}^2 z,$$

$$\gamma = b_{22} + kb_{11} \operatorname{sech}^2 \sigma, \quad (3.30)$$

where $M_1 > 0$ is a user-defined positive constant or function, and $\operatorname{sgn}(\cdot)$ is a *sign*(\cdot) function. The control in (3.29) is obtained from the Lyapunov function below.

Remark 4 *Singularity Issues* Based on (3.29), singularity occurs when the denominator γ is zero. To ensure that the control law $u(\theta, \theta_1^*)$ is singularity-free, the control signal is designed as

$$u = \begin{cases} \delta & \text{if } |\gamma| < |\delta| \\ u_1 & \text{otherwise} \end{cases} \quad (3.31)$$

where $\delta \in \mathbb{R}$ is a small parameter.

Proof. The proof is divided into two parts. The first part of the proof is to show convergence of the surface $s(x_2, x_2^*)$ in (3.28) is attractive to ensure that x_2 can track $x_2^*(x_1)$. The second part is to show the design of the fictitious control $x_2^*(x_1)$ in (3.26) can stabilize subsystem 1.

Consider the surface $s(x_2, x_2^*)$ to be

$$s = \dot{\theta} + \theta - \theta_1^*(x_1). \quad (3.32)$$

A Lyapunov candidate function is selected as

$$V_1 = \frac{1}{2}s^2. \quad (3.33)$$

Taking the time derivative of (3.33) and substituting (3.29) yields

$$\begin{aligned} \dot{V}_{1a} &= s\dot{s} \\ &= s\left(\ddot{\theta} + \dot{\theta} - \dot{\theta}_1^*(x_1)\right) \\ &= s\left(f_{22} + b_{22}u + \dot{\theta} - \dot{\theta}_1^*(x_1)\right) \\ &= -M_1 |s|. \end{aligned} \quad (3.34)$$

The expressions in (3.33) and (3.34) can be used to show that $s(x_2, x_2^*) \rightarrow 0$ in finite time. Thus, (3.32) can be used to show that $\dot{\theta} + \theta - \theta_1^*(x_1) \rightarrow 0$ in finite time. It then follows that $\dot{\theta} + \theta \rightarrow 0$ provided $\theta_1^*(x_1) \rightarrow 0$. In the subsequent analysis, it will be shown that $z(t) \rightarrow 0$ as $t \rightarrow \infty$, from which it follows directly from (3.26) that $\theta_1^*(x_1) \rightarrow 0$.

It follows from equation (3.24) and properties in 1)-4 from the previous section, the function $|\theta_1^*(x_1)| \leq c_1$, where c_1 is small, then base on the property of the trigonometric tangent function $\tan(\cdot) \approx (\cdot)$ for small values (\cdot) near the origin, thus the translational acceleration in (3.24) can be approximated as

$$\begin{aligned}\ddot{z}^* &= g \tan(\theta) = g \tan(\theta_1^*(x_1)), \\ &= g \tan(-k \tanh(\dot{z} + k_2 \tanh z)), \\ &\approx -gk \tanh(\dot{z} + k_2 \tanh z).\end{aligned}\tag{3.35}$$

Consider another positive definite function

$$V_{2a} = \ln \cosh(\dot{z} + k_2 \tanh z)\tag{3.36}$$

Take the time derivative of (3.36) and substituting (3.35) yields

$$\begin{aligned}\dot{V}_{2a} &= (\ddot{z} + k_2 \dot{z} \operatorname{sech}^2 z) \tanh(\dot{z} + k_2 \tanh z), \\ &= (-gk \tanh(\dot{z} + k_2 \tanh z) + k_2 \dot{z} \operatorname{sech}^2 z) \cdot \\ &\quad \tanh(\dot{z} + k_2 \tanh z), \\ &= -gk \tanh^2(\dot{z} + k_2 \tanh z) + k_2 \dot{z} \operatorname{sech}^2 z \cdot \\ &\quad \tanh(\dot{z} + k_2 \tanh z).\end{aligned}\tag{3.37}$$

Based on (3.35), when $\dot{z}(t)$ is large

$$\ddot{z}^* = -gk \operatorname{sign}(\dot{z})\tag{3.38}$$

thus, $\dot{z}(t)$ decreases and goes toward some constant until it no longer dominates $k_2 \tanh z$, i.e $\dot{z}(t) \rightarrow |\dot{z}(t)| \leq |k_2 \tanh z|$. When $\dot{z}(t)$ decreases toward some position $z(t) \rightarrow c_2$; if c_2 is large, and based on the property of the function $\text{sech}(\cdot)$, when (\cdot) is large, $\text{sech}(\cdot) \approx 0$, then from (3.37)

$$\dot{V}_{2a} < 0. \quad (3.39)$$

Based on (3.36)-(3.37) and (3.39), the translational velocity can written as

$$\dot{z} = -k_2 \tanh z, \quad (3.40)$$

therefore, $\dot{z}(t)$ and $z(t)$ will head toward some small vicinity around the origin $(0, 0)$.

Based on (3.38), (3.39), and (3.40), equation (3.35) can be approximated as

$$\frac{\ddot{z}}{gk} = -\dot{z} - k_2 z, \quad (3.41)$$

$$0 = \frac{\ddot{z}}{gk} + \dot{z} + k_2 z, \quad (3.42)$$

Based on the second order differential equation in (3.42), small value of k and k_2 can be chosen in such a way that

$$r_i = \frac{-1 \pm \sqrt{1 - 4\frac{k_2}{gk}}}{\frac{2}{gk}} = \frac{-gk \pm gk\sqrt{1 - 4\frac{k_2}{gk}}}{2} < 0, \quad (3.43)$$

where $i = 1, 2$; then the solution to (3.42) can be solved as

$$z(t) = c_3 e^{r_1 t} \cos(\beta t) + c_4 e^{r_2 t} \sin(\beta t). \quad (3.44)$$

where β is a constant. If the real part of the constants r_1, r_2 satisfy the condition (3.43), then based equation (3.44) $z(t) \rightarrow 0$ as $t \rightarrow \infty$. Hence based on the fact that $s \rightarrow 0$ in finite time can be used along with (3.32) to prove that $\theta \rightarrow 0$ as $t \rightarrow \infty$, which satisfies Assumption 2-3. Base on the analysis in (3.9)-(3.16), subsystems 1 and 2 go to the origin, achieving our objective. ■

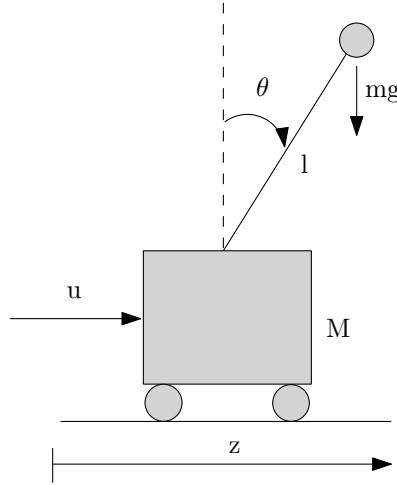


Figure 3.3: The Inverted Pendulum

A numerical simulation was created to demonstrate the performance of the proposed controller. The plant model utilized in the simulation is given by (3.17). The physical parameters of the inverted pendulum were chosen as in (Wie, 2008)

$$M = 0.5kg \quad m = 0.2kg \quad l = 0.3m \quad g = 9.8m/s^2$$

The control gain parameters were chosen as

$$k = \frac{5\pi}{180} \quad k_2 = 0.21 \quad M_1 = 0.1$$

The initial conditions used in the simulation are

$$\begin{aligned}\theta(0) &= -3.61 \text{ deg} & \dot{\theta}(0) &= -11.75 \text{ deg/s} \\ z(0) &= 0.725 \text{ m} & \dot{z}(0) &= 0.715 \text{ m/s}\end{aligned}$$

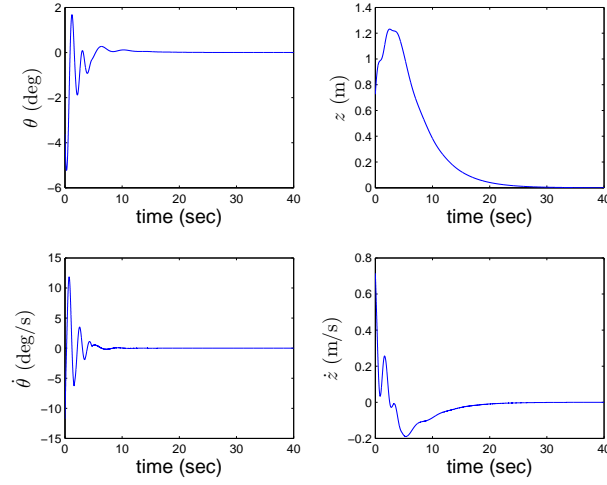


Figure 3.4: States versus time

3.4.1 Discussion of Results

From Fig. 3.4, for the first 15 seconds, the angle θ oscillates around the origin until it reaches zero, which in turn causes θ_1^* in Fig. 3.5 to be zero around the same moment. Since $\theta_1^* = 0$, it causes (z, \dot{z}) to converge to the origin around the 30th second. The control plot in Fig. 3.5 shows the control input, and the control commands remain within reasonable limits.

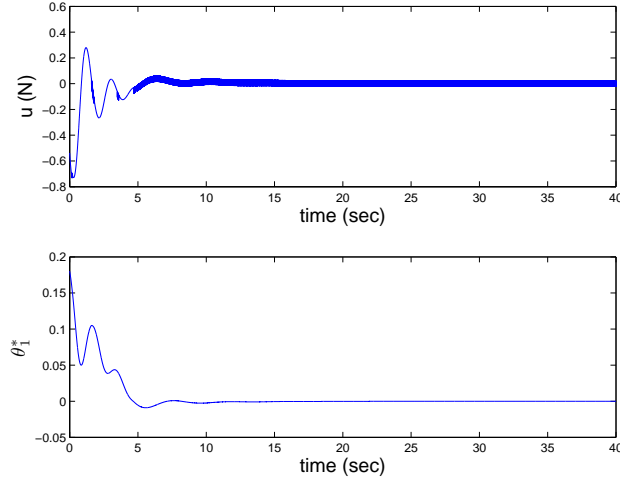


Figure 3.5: Control input u and tracking state θ_1^* versus time

3.5 Conclusion

The contribution of this chapter is the design of a novel control method that is based on two steps: the first step is to drive one subsystem to a region of stability near the origin by tracking a bounded time-varying desired function; the second step is to indirectly drive the second subsystem to the origin via the desired function. To facilitate the analysis, properties of a slowly time-varying desired function is exploited. The proposed controller is computationally inexpensive (i.e., a single feedback loop), requiring no observers, online adaptive updates, or function approximators. A detailed mathematical analysis is utilized to prove the theoretical result. An inverted pendulum system is presented as a numerical example to demonstrate the effectiveness of the proposed control algorithm.

This chapter has presented a novel SMC algorithm to stabilize a class of underactuated parallel systems. Future work involves extending the current result to n -parallel systems. The technique presented in this chapter deals with a challeng-

ing underactuated parallel system that does not containing parametric uncertainty. Systems that contain disturbances and uncertainty in the control input require a different approach from what is presented. In the next chapter, systems containing norm-bound disturbances and parametric uncertainty in the input matrix is compensated by using robust integral of the signum error (RISE). Specifically, the system is derived for a second order dynamics of the quadrotor.

Chapter 4

Robust Attitude Tracking Control of a Quadrotor Helicopter in the Presence of Uncertainty

4.1 Introduction

This chapter develops a robust nonlinear control algorithm for quadrotor systems that contain parametric uncertainty and disturbances. The following work can be found in (Ton & Mackunis, 2012).

Unmanned four-rotor helicopters (quadrotors) have been an increasingly popular research topic in recent years due their low cost, maneuverability, and ability to perform a variety of tasks, including reconnaissance, search and rescue, area mapping, and more. Although several quadrotor control methods have been proposed in literature, design of nonlinear tracking controllers for quadrotors in the presence of

system uncertainty, unmodeled disturbances, and actuator failures remains a challenging task.

While linear, PID-based control approaches have been successful at controlling quadrotor systems (e.g., see (Salih et al., 2010) and (Huang et al., 2009)), a variety of nonlinear control techniques have also been presented in controls literature. A dynamic inversion (DI)-based technique was presented in Wang et al. (J. Wang et al., 2011) to develop a two-loop controller that allows direction position commands. In the scheme in (J. Wang et al., 2011), the inner loop controls the angular rate, while the outer loop controls the position. The approach in (J. Wang et al., 2011) enabled decoupling of the quadrotor dynamics without compromising controller robustness, and it eliminated singularities in attitude control when the pitch angle is 90 degrees. A DI-based technique was also used in Das et al. (Das et al., 2009) to create a robust controller that guarantees stabilization of the internal dynamics. Backstepping-based quadrotor control designs have been investigated by many researchers (Al-Younes et al., 2010), (Vries & Subbarao, 2010), (Mian & Daobo, 2008). Younes et al. (Al-Younes et al., 2010) developed an adaptive integral backstepping-based nonlinear control law, which was shown to achieve an improved dynamic response over PID and LQR. Additionally, Vries et al. (Vries & Subbarao, 2010) developed multi-loop control laws based on backstepping and tested them via both linear and nonlinear simulations. In (Mian & Daobo, 2008), feedback linearization was used for the translational portion of the system, and a Lyapunov-based backstepping approach was used for the rotational portion of the controller. In (Dydek et al., 2010), adaptive control was utilized to augment an existing linear controller through Lyapunov stability arguments. The controller in (Dydek et al., 2010) used full system feedback, assuming

availability of position, angular velocity, and angular acceleration measurements. In (Gillula et al., 2010), a Hamilton-Jacobi differential game formulation was utilized to construct reachable sets so that complex maneuvers could be discretized into safe and feasible maneuvers. The technique in (Gillula et al., 2010) was implemented to enable a quadrotor to perform backflips. Zhu et al. (Zhu & Huo, 2010) divided the quadrotor model into four subsystems (i.e., position kinematics, attitude kinematics, position dynamics, and attitude dynamics), then designed a controller based on trajectory linearization control by neglecting the gyroscopic dynamic effects. In (Tayebi & McGilvray, 2006), a quaternion-based control law was presented, which achieves attitude stabilization in vertical takeoff and landing of a quadrotor. Although the aforementioned quadrotor control techniques performed well in their respective tasks, tracking control for quadrotors in the presence of input-multiplicative parametric uncertainty and unmodeled, nonlinear, nonvanishing disturbances remains a challenging task. While sliding mode control (SMC) techniques can be applied to compensate for norm-bounded disturbances, the inherent requirement of infinite bandwidth presents limitations in practical implementation.

Various practical factors can hinder the operation of quadrotors and create challenges in the control design. To achieve reliable and accurate tracking control of quadrotors over a wide envelope of operating conditions, controllers must be designed to compensate for model uncertainty, external disturbances, motor failures, and partial actuator failures. Various control techniques have been proposed in literature to address these difficulties. In (Waslander & Wang, 2009), a wind model and on-board sensors were utilized to estimate wind disturbances and adjust the controller to take the appropriate actions. This is especially necessary when the quadrotors

are flying near obstacles or in formation. A controller based on backstepping and a sliding mode observer was developed in (Madani & Benallegue, 2007), which yielded good performance in the presence of wind disturbances. In (Achtelik et al., 2011), a model reference adaptive control (MRAC) technique was utilized in a nonlinear control structure based on dynamic inversion. The control design in (Achtelik et al., 2011) was robust enough to handle power loss in one of the motors, but requires a fast update rate of 1 kHz. MRAC was also utilized in (Chamseddine et al., 2011) to compensate for partial loss in one of the rotors, partial damage of a propeller, and partial loss in total thrust. The scheme in (Chamseddine & Zhang, 2010) utilized an optimal trajectory planning approach along with an adaptive control law. Lyapunov-based robust control and backstepping were also utilized in (D. Lee et al., 2009) to compensate for parametric uncertainty in the quadrotor model. In (Dierks & Jagannathan, 2010), a nonlinear controller for a quadrotor was developed using neural networks and output feedback. The controller in (Dierks & Jagannathan, 2010) was designed to learn the dynamics of the quadrotor online, and the effectiveness of the controller was demonstrated in the presence of unknown, nonlinear dynamics and disturbances. The control methods presented in the aforementioned research are capable of compensating for parametric uncertainty and disturbances; however, the problem of purely robust tracking control for quadrotors with minimal computational complexity remains a challenging problem.

The contribution in this chapter is the design of a continuous robust controller, which achieves asymptotic attitude trajectory tracking for a quadrotor in the presence of input-multiplicative uncertainty and unknown, nonlinear, nonvanishing disturbances. The advantage of the controller is its ability to compensate for unknown

multiplicative uncertainty in the control input and nonvanishing additive disturbance without an observer or adaptive updates used in (Waslander & Wang, 2009; Madani & Benallegue, 2007; Achtelik et al., 2011; Chamseddine et al., 2011; D. Lee et al., 2009; Dierks & Jagannathan, 2010). Input-multiplicative parametric uncertainty in the quadrotor dynamics can significantly hinder controller effectiveness. This difficulty is mitigated through careful algebraic manipulation in the error system development along with a robust feedback control term. A robust integral sliding mode technique is also employed to compensate for model uncertainty and disturbances. The controller is designed to be practically implementable, requiring no observers, function approximators, or online adaptive updates, allowing the control to update quickly and be computationally efficient. Moreover, the proposed approach demonstrates robust performance in the presence of significant input-multiplicative parametric uncertainty using only position and velocity measurements for feedback. Another benefit of the proposed control design is that it completely rejects norm-bounded disturbances using a continuous control structure; it does not explicitly contain the discontinuous signum term that is inherent in standard sliding mode approaches. A Lyapunov-based stability analysis is utilized to prove the theoretical result, and numerical simulation results are provided to demonstrate the performance of the proposed controller in the presence of exogenous disturbances and high levels of input-multiplicative parametric uncertainty.

4.2 Quadrotor Model and Properties

The dynamic model for the quadrotor helicopter under consideration in this chapter can be expressed as (Achtelik et al., 2011), (Chamseddine & Zhang, 2010), (Besnard et al., 2007):

$$\ddot{x} = f(x, \dot{x}) + g(x)u + d(t), \quad (4.1)$$

where $f(x, \dot{x}) \in \mathbb{R}^n$ denotes an unknown, nonlinear vector function, $g(x) \in \mathbb{R}^{n \times n}$ is an uncertain input matrix, $u(t) \in \mathbb{R}^n$ is a vector of control inputs, and $d(t) \in \mathbb{R}^n$ is an unknown, nonlinear disturbance. In (4.1), $x(t) \in \mathbb{R}^n$ denotes the configuration vector, which is defined as

$$x \triangleq \begin{bmatrix} z_1 & \phi & \theta & \psi \end{bmatrix}^T, \quad (4.2)$$

where $z_1(t) \in \mathbb{R}$ denotes altitude, and $\phi(t)$, $\theta(t)$, $\psi(t) \in \mathbb{R}$ denote roll, pitch, and yaw angles, respectively. Also in (4.1), the functions $f(x, \dot{x})$ and $g(x)$ are defined as

(Zhang & Zhang, 2010)

$$f(x, \dot{x}) = \begin{bmatrix} -g \\ \frac{-\dot{\theta}\dot{\psi}(J_z - J_y)}{J_x} \\ \frac{-\dot{\phi}\dot{\psi}(J_x - J_z)}{J_y} \\ \frac{-\dot{\theta}\dot{\phi}(J_y - J_x)}{J_z} \end{bmatrix}, \quad (4.3)$$

$$g(x) = \begin{bmatrix} \frac{\cos \theta \cos \phi}{m} & 0 & 0 & 0 \\ 0 & \frac{l}{J_x} & 0 & 0 \\ 0 & 0 & \frac{l}{J_y} & 0 \\ 0 & 0 & 0 & \frac{l}{J_z} \end{bmatrix}, \quad (4.4)$$

where $m, l \in \mathbb{R}$ denote the uncertain quadrotor mass and arm length; and $J_x, J_y, J_z \in \mathbb{R}$ represent the uncertain moments of inertia.

Remark 5 *The explicit definition of $f(x, \dot{x})$ in (4.3) is provided for completeness in defining the dynamic model only. In the subsequent controller development and stability analysis, $f(x, \dot{x})$ is assumed to be an unknown nonlinear function and is not used in the control design.*

Assumption 1: The roll and pitch angles $\theta(t)$ and $\phi(t)$ are assumed to satisfy the following inequalities:

$$-\frac{\pi}{2} < \theta(t) < \frac{\pi}{2}, \quad -\frac{\pi}{2} < \phi(t) < \frac{\pi}{2}.$$

Assumption 2: The disturbance $d(t)$ is sufficiently smooth and bounded in the sense that

$$\|d(t)\| \leq \zeta_1, \quad \|\dot{d}(t)\| \leq \zeta_2, \quad \|\ddot{d}(t)\| \leq \zeta_3,$$

where ζ_i are known bounding constants for $i = 1, 2, 3$. The disturbance needs to be bounded, otherwise the system in (4.1) becomes uncontrollable.

Assumption 1 is mild in the sense that, due to the geometry of the system, violation of the assumption results in loss of controllability of the quadrotor (Zhang & Zhang, 2010).

4.3 Control Development

In this section, a continuous robust control technique is presented, which yields asymptotic tracking for a quadrotor helicopter in the presence of parametric uncertainty in a state-varying input matrix in addition unknown, nonlinear, non-vanishing disturbances. The subsequent development is based on the assumption that $x(t)$ and $\dot{x}(t)$ (i.e., position and velocity only) are measurable. By utilizing minimal system knowledge and a feedforward estimate of the uncertain input matrix, a continuous robust integral sliding mode control structure is developed to compensate for the disturbances and input-multiplicative uncertainty.

4.3.1 Control Objective

The objective is to design a robust tracking controller, which ensures that the system track a desired time-varying trajectory $x_d(t) \in \mathbb{R}^n$ despite uncertainty and norm-bounded disturbances present in the dynamic model. To quantify this objective, a position tracking error, denoted by $e_1(t) \in \mathbb{R}^n$, is defined as

$$e_1 \triangleq x - x_d. \quad (4.5)$$

To facilitate the subsequent analysis, filtered tracking errors, denoted by $e_2(t)$, $r(t) \in \mathbb{R}^n$, are also defined as

$$e_2 \triangleq \dot{e}_1 + \alpha_1 e_1, \quad r \triangleq \dot{e}_2 + \alpha_2 e_2, \quad (4.6)$$

where $\alpha_1, \alpha_2 \in \mathbb{R}$ denote positive, constant control gains. The filtered tracking error $r(t)$ is not measurable since the expression in (4.6) depends on $\ddot{x}(t)$. Note that, based on the definitions in (4.6), $r(t) \rightarrow 0 \Rightarrow e_2(t) \rightarrow 0 \Rightarrow e_1(t) \rightarrow 0$.

Based on the tracking error definition in (4.5), the control objective can be stated as

$$\|e_1(t)\| \rightarrow 0. \quad (4.7)$$

4.3.2 Error System Development

The open-loop tracking error dynamics can be developed by taking the time derivative of $r(t)$ and utilizing the expressions in (4.1), (4.5), and (4.6) to obtain the following expression:

$$\begin{aligned} \dot{r}(t) = & \dot{f}(x, \dot{x}) - \dot{f}(x_d, \dot{x}_d) + \alpha_1 \ddot{e}_1 + \dot{g}(x)u + g(x)\dot{u} \\ & + \alpha_2 \dot{e}_2 + \dot{f}(x_d, \dot{x}_d) + \dot{d}(t) - \ddot{x}_d. \end{aligned} \quad (4.8)$$

Assumption 3: The desired trajectory $x_d(t)$ is bounded and sufficiently smooth in the sense that

$$\|x_d(t)\|, \|\dot{x}_d(t)\|, \|\ddot{x}_d(t)\| \leq \zeta_4, \quad (4.9)$$

where $\zeta_4 \in \mathbb{R}$ is a known positive bounding constant.

4.3.3 Controller Formulation

A challenge in the control design is that the control input is premultiplied by a state-varying matrix containing parametric uncertainty. To compensate for the uncertainty premultiplying the control input, the matrix $g(x)$ will be segregated in terms of a known, nominal matrix $g_o(x) \in \mathbb{R}^{n \times n}$ and an uncertain constant matrix $\Delta g \in \mathbb{R}^{n \times n}$ as follows:

$$g(x) = g_o(x)\Delta g. \quad (4.10)$$

Assumption 4: The uncertain constant matrix Δg in (4.10) is assumed to satisfy the inequalities

$$1 - \varepsilon \leq \|\Delta g\|_{i\infty} \leq 1 + \varepsilon, \quad (4.11)$$

where $\varepsilon \in (0, 1)$ is a known positive bounding constant, and $\|\cdot\|_{i\infty}$ denotes the induced infinity norm of a matrix. The uncertain constant matrix Δg is a diagonal matrix that represents parametric uncertainty in J_x , J_y , J_z , m , and l .

Remark 6 *Preliminary results show that Assumption 4 is mild in the sense that (4.11) is satisfied for a wide range of parametric uncertainty in $g(x)$.*

After using the decomposition in (4.10), the open loop error system in (4.8) can be rewritten as

$$\dot{r} = N_d + \tilde{N} + \Delta g(\dot{g}_o(x)u + g_o(x)\dot{u}) - e_2, \quad (4.12)$$

where $N_d(t, x_d) \in \mathbb{R}^n$ and $\tilde{N}(x, x_d, e_1, e_2, \dot{e}_1, \dot{e}_2) \in \mathbb{R}^n$ are auxiliary functions defined

as

$$N_d \triangleq \dot{d}(t) + \dot{f}(x_d, \dot{x}_d) - \ddot{x}_d, \quad (4.13)$$

$$\tilde{N} \triangleq \dot{f}(x, \dot{x}) - \dot{f}(x_d, \dot{x}_d) + \alpha_1 \ddot{e}_1 + \alpha_2 \dot{e}_2 + e_2. \quad (4.14)$$

In (4.12), the quantities \tilde{N} and N_d and the time derivative of N_d can be upper bounded as follows (Xian, Dawson, Queiroz, & Chen, 2004), (Patre, MacKunis, Makkar, & Dixon, 2008):

$$\tilde{N} \leq \rho(\|z\|) \|z\|, \quad N_d \leq \zeta_{N_d}, \quad \dot{N}_d \leq \zeta_{\dot{N}_d}, \quad (4.15)$$

where $\zeta_{N_d}, \zeta_{\dot{N}_d} \in \mathbb{R}$ are known positive bounding constants, and $z(t) \in \mathbb{R}^{3n}$ is defined as

$$z \triangleq \begin{bmatrix} e_1^T & e_2^T & r^T \end{bmatrix}^T.$$

In (4.15), $\rho(\cdot) \in \mathbb{R}$ is a positive, globally invertible, nondecreasing function. Based on the expression in (4.12) and the subsequent stability analysis, the control input is designed via

$$\dot{u} = -g_o(x)^{-1}(\beta \operatorname{sgn}(e_2) + (k_1 + 1)r + \dot{g}_o(x)u), \quad (4.16)$$

where $\beta, k_1 \in \mathbb{R}^{n \times n}$ are positive constant control gain matrices.

Remark 7 *The control design in (4.16) does not require knowledge of $f(x, \dot{x})$ in (4.1). Note that equation (4.14) can be bounded by mean value theorem.*

Remark 8 *Integration by parts can be used in (4.16) to show that the control input $u(t)$ requires measurements of $x(t)$ and $\dot{x}(t)$ only; no acceleration measurements are necessary.*

After substituting (4.16) into (4.12), the close-loop error system is obtained as

$$\dot{r}(t) = N_d + \tilde{N} + \Delta g(-\beta \operatorname{sgn}(e_2) - (k_1 + 1)r) - e_2. \quad (4.17)$$

4.4 Stability Analysis

Theorem 1 *The controller given in (4.16) ensures asymptotic trajectory tracking in the sense that*

$$\|e_1(t)\| \rightarrow 0 \quad \text{as} \quad t \rightarrow \infty, \quad (4.18)$$

provided the control gain k_1 introduced in (4.16) is selected sufficiently large, and β is selected according to the sufficient condition

$$\beta > \frac{1}{1 - \varepsilon} \left(\zeta_{N_d} + \frac{\zeta_{\dot{N}_d}}{\alpha_2} \right), \quad (4.19)$$

where $N_d(t)$ and $\dot{N}_d(t)$ are introduced in (4.13), ε is introduced in (4.11), and α_2 is introduced in (4.6). The control gains $\alpha_1, \alpha_2, \beta$, and k are selected to yield desirable performance characteristics such as overshoot, settling, tracking accuracy, etc.

The following lemma is utilized in the proof of Theorem 1.

Lemma 1 *Let $\mathcal{D} \subset \mathbb{R}^{3n+1}$ be a domain containing $w(t) = 0$, where $w(t) \in \mathbb{R}^{2n+1}$ is defined as*

$$w(t) \triangleq \begin{bmatrix} z^T & \sqrt{P(t)} \end{bmatrix}^T. \quad (4.20)$$

In (4.20), the auxiliary function $P(t) \in \mathbb{R}$ is the generalized solution to the differential

equation

$$\dot{P}(t) = -L(t), \quad (4.21)$$

$$P(0) = \Delta g \beta |e_2(0)| - N_d^T(0) e_2(0), \quad (4.22)$$

where the auxiliary function $L(t) \in \mathbb{R}$ is defined as

$$L(t) = r^T (N_d(t) - \Delta g \beta \operatorname{sgn}(e_2)). \quad (4.23)$$

Provided the sufficient conditions in (4.19) is satisfied, the following inequality can be obtained:

$$\int L(\tau) d\tau \leq \Delta g \beta |e_2(0)| - N_d^T(0) e_2(0). \quad (4.24)$$

Hence, equation (4.24) can be used to conclude that $P(t) \geq 0$.

Proof of the bound in (4.24) can be found in Appendix A or (Ton & Mackunis, 2012).

Proof. (See Theorem 1) Let $V(w, t) : \mathcal{D} \times [0, \infty) \rightarrow \mathbb{R}$ be defined as the nonnegative function

$$V(w, t) \triangleq \frac{1}{2} e_1^T e_1 + \frac{1}{2} e_2^T e_2 + \frac{1}{2} r^T r + P, \quad (4.25)$$

where $e_1(t)$, $e_2(t)$, and $r(t)$ are defined in (4.5) and (4.6), respectively; and the positive definite function $P(t)$ is defined in (4.21). The function $V(w, t)$ satisfies the inequality

$$U_1(w) \leq V(w, t) \leq U_2(w), \quad (4.26)$$

provided the sufficient condition introduced in (4.19) is satisfied, where the positive

definite functions $U_1(w)$, $U_2(w) \in \mathbb{R}$ are defined as

$$U_1 \triangleq \frac{1}{2} \|w\|^2, \quad U_2 \triangleq \|w\|^2. \quad (4.27)$$

After taking the time derivative of (4.25) and utilizing (4.5), (4.6), (4.17), and (4.21), $\dot{V}(w, t)$ can be expressed as

$$\begin{aligned} \dot{V}(w, t) &= e_1^T (e_2 - \alpha_1 e_1) + e_2^T (r - \alpha_2 e_2) + r^T (\tilde{N} + N_d - \Delta g \beta \operatorname{sgn}(e_2)) \\ &\quad - \Delta g (k_1 + 1) r - e_2) - r^T (N_d - \Delta g \beta \operatorname{sgn}(e_2)). \end{aligned} \quad (4.28)$$

After canceling common terms and rearranging, (4.28) can be rewritten as

$$\dot{V}(w, t) = -\alpha_1 \|e_1\|^2 - \alpha_2 \|e_2\|^2 + e_1^T e_2 + r^T \tilde{N} - \Delta g (k_1 + 1) r^T r. \quad (4.29)$$

After using (4.15) and (4.11), (4.29) can be upper bounded as

$$\begin{aligned} \dot{V}(w, t) &\leq -\left(\alpha_1 - \frac{1}{2}\right) \|e_1\|^2 - \left(\alpha_2 - \frac{1}{2}\right) \|e_2\|^2 - \varepsilon_0 \|r\|^2 \\ &\quad - \varepsilon_0 k_1 \|r\|^2 + \rho (\|z\|) \|z\| \|r\|, \end{aligned} \quad (4.30)$$

where $\varepsilon_0 \triangleq 1 - \varepsilon$, and the fact that $e_1^T e_2 \leq \frac{1}{2} \|e_1\|^2 + \frac{1}{2} \|e_2\|^2$ was utilized. After completing the squares in (4.30), the upper bound on $\dot{V}(w, t)$ can be expressed as

$$\begin{aligned} \dot{V}(w, t) &\leq -\left(\alpha_1 - \frac{1}{2}\right) \|e_1\|^2 - \left(\alpha_2 - \frac{1}{2}\right) \|e_2\|^2 - \varepsilon_0 \|r\|^2 \\ &\quad - \varepsilon_0 k_1 \left(\|r\| - \frac{\rho(\|z\|)}{2\varepsilon_0 k_1} \|z\| \right)^2 + \frac{\rho^2(\|z\|)}{4\varepsilon_0 k_1} \|z\|^2. \end{aligned} \quad (4.31)$$

Since $\varepsilon_0, k_1 > 0$, the upper bound in (4.31) can be expressed as

$$\dot{V}(w, t) \leq - \left(\lambda_0 - \frac{\rho^2(\|z\|)}{4\varepsilon_0 k_1} \right) \|z\|^2, \quad (4.32)$$

where $\lambda_0 \triangleq \min \left\{ \alpha_1 - \frac{1}{2}, \alpha_2 - \frac{1}{2}, \varepsilon_0 \right\}$.

The following expression can be obtained from (4.32):

$$\dot{V}(w, t) \leq -U(w), \quad (4.33)$$

where $U(w) = c \|z\|^2$, for some positive constant $c \in \mathbb{R}$, is a continuous, positive semi-definite function that is defined on the following domain:

$$\mathcal{D} \triangleq \left\{ w \in \mathbb{R}^{2m+1} \mid \|w\| < \rho^{-1} \left(2\sqrt{\varepsilon_0 \lambda_0 k_1} \right) \right\}. \quad (4.34)$$

It follows directly from Lyapunov analysis that $r(t), e_2(t), e_1(t) \in \mathcal{L}_\infty$ in \mathcal{D} . This implies that $\dot{e}_2(t), \dot{e}_1(t) \in \mathcal{L}_\infty$ in \mathcal{D} from the definitions given in (4.6). Given that $r(t), e_2(t), \dot{e}_1(t) \in \mathcal{L}_\infty$ in \mathcal{D} , it follows that $\ddot{e}_1(t) \in \mathcal{L}_\infty$ from (4.6). Since $e_1(t), \dot{e}_1(t), \ddot{e}_1(t) \in \mathcal{L}_\infty$ in \mathcal{D} , (4.5) can be used along with Assumption 4 to show that $x(t), \dot{x}(t), \ddot{x}(t) \in \mathcal{L}_\infty$ in \mathcal{D} . Since $\dot{x}(t) \in \mathcal{L}_\infty$, then (4.2) and (4.3) can be used to show that $f(x) \in \mathcal{L}_\infty$. Given that $\ddot{x}(t), f(x) \in \mathcal{L}_\infty$, Assumptions 1 and 2 can be used along with (4.1) to prove that $u(t) \in \mathcal{L}_\infty$ in \mathcal{D} . Since $r(t), u(t) \in \mathcal{L}_\infty$, (4.16) can be used along with Assumption 1 to show that $\dot{u}(t) \in \mathcal{L}_\infty$ in \mathcal{D} . Given that $r(t), e_2(t), e_1(t), \dot{x}(t), x(t), \dot{u}(t) \in \mathcal{L}_\infty$, (4.15) can be used along with (4.12) and Assumption 4 to prove that $\dot{r}(t) \in \mathcal{L}_\infty$ in \mathcal{D} . Since $\dot{e}_1(t), \dot{e}_2(t), \dot{r}(t) \in \mathcal{L}_\infty$ in \mathcal{D} , $r(t), e_2(t), e_1(t)$ are uniformly continuous in \mathcal{D} . Thus, the definitions for $U(w)$ and $w(t)$ can be used

to prove that $U(w)$ is uniformly continuous in \mathcal{D} .

Let $S \subset D$ denote a set defined as follows:

$$S \triangleq \left\{ w(t) \in D \mid U_2(w(t)) < \frac{1}{2}\rho^{-1} \left(2\sqrt{\varepsilon_0\lambda_0k_1} \right)^2 \right\}. \quad (4.35)$$

Theorem 8.4 of Khalil (Khalil, 2002) can now be invoked to state that

$$c \|z\|^2 \rightarrow 0 \quad \text{as} \quad t \rightarrow \infty \quad \forall w(0) \in S. \quad (4.36)$$

Based on the definition of $z(t)$, (4.36) can be used to show that

$$\|e_1(t)\| \rightarrow 0 \quad \text{as} \quad t \rightarrow \infty \quad \forall w(0) \in S. \quad (4.37)$$

■

4.5 Simulation Results

4.5.1 Simulation Model

A numerical simulation was created to demonstrate the performance of the proposed controller. The plant model utilized in the simulation is given by (4.1), (4.3), and (4.4), where $f(x, \dot{x}) \in \mathbb{R}^{4 \times 1}$, $g(x) \in \mathbb{R}^{4 \times 4}$, $u(t) \in \mathbb{R}^{4 \times 1}$, and $d(t) \in \mathbb{R}^{4 \times 1}$. The physical parameters used in the simulation are based on the experimentally determined parameters of the Embry-Riddle quadrotor test bed.

In order to develop a realistic stepping stone to actual experimental demonstration of the proposed quadrotor controller, the simulation parameters were selected

based on detailed data analyses and specifications. The thrust limit and the quadrotor's physical properties were determined via model testing. Each of the four rotors has a thrust limit of approximately 38 N , yielding a total maximum thrust limit of approximately 152 N . The uncertain matrix Δg is defined as

$$\Delta g = \begin{bmatrix} b_1 & 0 & 0 & 0 \\ 0 & b_2 & 0 & 0 \\ 0 & 0 & b_3 & 0 \\ 0 & 0 & 0 & b_4 \end{bmatrix}, \quad (4.38)$$

where $b_i \in (0, 1) \forall i = 1, \dots, 4$ denote subsequently defined uncertain parameters that represent the uncertainty in the parameters J_x , J_y , J_z , m , and l . The quadrotor physical properties are selected as follows:

$$\begin{aligned} J_x &= 0.6768 \text{ kg} \cdot \text{m}^2, & J_y &= 0.6768 \text{ kg} \cdot \text{m}^2, \\ J_z &= 0.011 \text{ kg} \cdot \text{m}^2, & l &= 0.6768 \text{ m}, \\ m &= 6.804 \text{ kg}. \end{aligned}$$

The initial conditions used in the simulation are

$$\begin{aligned} x(0) &= \begin{bmatrix} 0 \text{ m} & 0.1 \text{ rad} & 0.1 \text{ rad} & 0.1 \text{ rad} \end{bmatrix}^T, \\ \dot{x}(0) &= \begin{bmatrix} 0 \text{ m} & 0 \text{ rad} & 0 \text{ rad} & 0 \text{ rad} \end{bmatrix}^T. \end{aligned}$$

The nonlinear disturbance term $d(t)$ introduced in (4.1) is modeled as noise drawn from the normal (Gaussian) distribution in the simulation. The disturbance $d(t)$ can

be explicitly defined as

$$d(t) = \begin{bmatrix} \mathcal{N}(0, 1) \\ \mathcal{N}(0, 0.5) \\ \mathcal{N}(0, 0.5) \\ \mathcal{N}(0, 0.5) \end{bmatrix}$$

The function $f(x, \dot{x})$ and the disturbance $d(t)$ are utilized in the simulation to develop the plant model only, they are not used in the control law. The robust elements in the control law compensate for these effects.

The objective is to force the state $x(t)$ to follow the desired time-varying trajectory $x_d(t)$ given by

$$x_d = \begin{bmatrix} 0.1t + 6 \\ \frac{20\pi}{180} \sin(\frac{t}{10}) \\ \frac{20\pi}{180} \sin(\frac{t}{10} + \frac{\pi}{3}) \\ \frac{20\pi}{180} \sin(\frac{t}{10} + \frac{\pi}{6}) \end{bmatrix}. \quad (4.39)$$

The control gains for the robust controller were selected such that the controller exhibits the best possible performance (e.g., in terms of settling time, overshoot, steady state error). Figs. 4.1 and 4.2 show the simulation results of the closed-loop system with control gains selected as follows:

$$\begin{aligned} k_1 &= \text{diag}(1, 6, 3, 3), & \beta &= \text{diag}(1, 1, 1, 1), \\ \alpha_1 &= \text{diag}(1, 1, 1, 1), & \alpha_2 &= \text{diag}(1, 1, 1, 1), \end{aligned}$$

where $\text{diag}(\cdot)$ denotes the diagonal matrix. Fig. 4.1 shows the time evolution of the height, roll angle, pitch angle, and yaw angle errors, and Fig. 4.2 shows the

commanded control inputs during closed-loop operation.

4.5.2 Simulation Results

In the following simulation results, the uncertain elements of the Δg matrix (see (4.38)) are selected as $b_1 = 0.8$, $b_2 = 0.5$, $b_3 = 0.7$, $b_4 = 0.6$. These values correspond to 20% – 50% uncertainty in the mass and inertia parameters. From Fig. 4.1, the altitude (i.e., $z_1(t)$) tracking error converges in approximately 10 seconds, and the attitude (i.e., $\phi(t)$, $\theta(t)$, $\psi(t)$) tracking errors also converge after approximately 10 seconds. The maximum rate and magnitude of the control inputs in Fig. 4.2 are well within practical control limits. The control input and performance of the quadrotor is well within acceptable region when compared to experimental work done in (Huang et al., 2009), (Dydek et al., 2010), (Achtelik et al., 2011), (Chamseddine & Zhang, 2010). Real-time applications of the controller should be computationally efficient because there is no online learning.

4.5.3 Discussion of Results

Based on the results from the error plots, the proposed controller is capable of achieving accurate trajectory tracking. The input-multiplicative uncertainty is compensated at the cost of a slightly higher feedback gain β (i.e., see (4.19)); however, the maximum control command is less than 152 N as seen in Fig. 4.2, which is well within the actuator limits of the Embry-Riddle quadrotor test bed. The robust structure of the controller enables the closed loop system to converge, even when the unknown parameters $b_i \forall i = 1, \dots, 4$ are off from nominal by up to 50%. The chattering in the control is largely due to the Gaussian noise injected into the system. The simu-

lation yields satisfactory results despite various unknown, nonlinear disturbances in the dynamic model and parametric uncertainty.

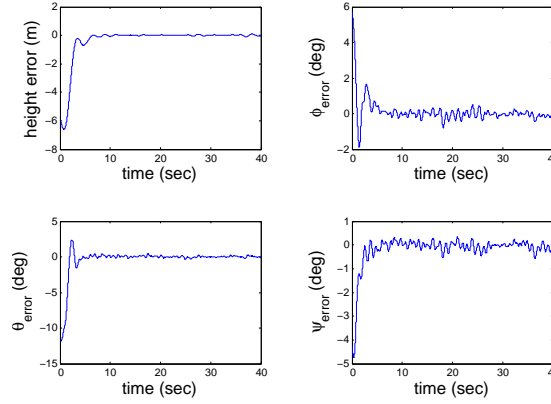


Figure 4.1: Tracking error response achieved during closed-loop controller operation.

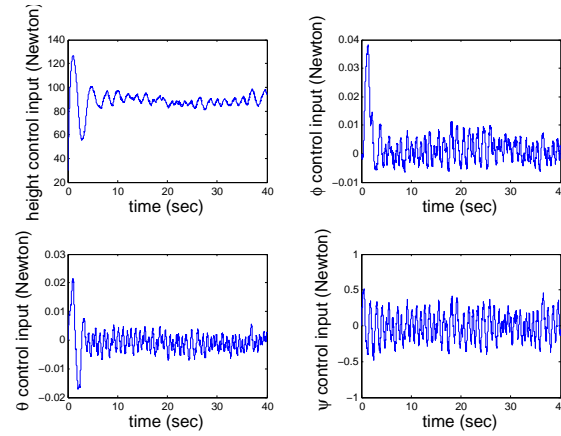


Figure 4.2: Control commands used during closed-loop controller operation.

4.6 Conclusion

A tracking controller for a quadrotor is presented, which achieves asymptotic tracking, where the dynamic model contains input-multiplicative parametric uncertainty

and norm-bounded nonlinear disturbances. Moreover, the result is achieved using a control law that is computationally inexpensive, requiring no observers, function approximators, or online adaptive update laws. A robust integral sliding mode control technique is employed to compensate for parametric input uncertainty and unknown, nonlinear, non-vanishing disturbances. The proposed control design has the advantage of being continuous, eliminating the need for infinite actuator bandwidth. A Lyapunov-based stability analysis is provided to verify the theoretical result, and simulation results are provided to demonstrate the performance of the controller in the presence of significant parametric uncertainty and exogenous perturbations. Future work will focus on improving controller robustness with respect to complete loss of effectiveness in one or more actuators.

Chapter 5

Robust Nonlinear Aircraft Tracking Control Using Synthetic Jet Actuators

5.1 Introduction

In this chapter, a robust nonlinear tracking control method is presented for aircraft systems equipped with synthetic jet actuators. This work can be found in (MacKunis et al., 2013).

Due to their small size, ease of operation, and low cost, synthetic jet actuators (SJA) are promising tools for aircraft tracking control and flow control applications. SJA transfer linear momentum to a flow system by using a vibrating diaphragm, which creates trains of vortices through the alternating ejection and suction of fluid through a small orifice. Since these vortices (i.e., jets) are formed entirely from the

fluid (i.e., air) of the flow system, a key benefit of SJA is that they achieve this transfer of momentum with zero net mass injection across the flow boundary. Thus, SJA do not require space for a fuel supply. SJAs can be utilized to modify the boundary layer flow field near the surface of an aircraft wing, which can improve aerodynamic performance. Moreover, synthetic jet actuators can expand the usable range of angle of attack, which can improve maneuverability (Amitay, Smith, Kibens, Parekh, & Glezer, 2001). In addition to flow control applications, arrays consisting of several SJAs can be employed to achieve tracking control of aircraft, possibly eliminating the need for mechanical control surfaces. The benefits of utilizing SJAs on aircraft as opposed to mechanical control surfaces include reduced cost, weight, and mechanical complexity.

Uncertainties inherent in the dynamics of SJA present significant challenges in control design, however. Specifically, the input-output characteristic of each SJA is nonlinear and contains parametric uncertainty. Additional challenges exist in control design in low Reynolds number (low-Re) flight conditions inherent in the dynamics of smaller, lighter aircraft (e.g., small unmanned aerial vehicles). While much research has addressed SJA-based flow and flight control design, the majority of the recently developed SJA-based control designs are typically investigated using computational fluid dynamics-based numerical methods, without detailed mathematical performance analysis (e.g., see (Hong, 2012; Kim, Kim, Kim, Kim, & Kim, 2011; Kim et al., 2012; Kotapati et al., 2010; Kourta & Leclerc, 2013; Liu et al., 2006; Mejia, Moser, Brzozowski, & Glezer, 2011; Luo, Xia, & Xie, 2007; Ozawa, Lesbros, & Hong, 2010; Tamburello & Amitay, 2008; Ozawa, Lesbros, & Hong, 2012; Travnicek, Nemcova, Kordik, Tesar, & Kopecky, 2012; Tseng, Yang, & Lin, 2011; Vukasinovic, Glezer,

Gordeyev, Jumper, & Kibens, 2009; Zhang & Zhang, 2010)). While computational methods have proven useful in analyzing the complex dynamics inherent in control of fluid flow and SJA-based fight tracking control, one of the contributions of the research presented in this chapter is theoretical development of a SJA-based aircraft tracking controller that includes rigorous analysis of controller performance.

While nonlinear methods are popularly utilized in control system design, nonlinear control techniques are not often applied to SJA-based control systems. Recently developed nonlinear SJA-based control designs utilize online adaptive control algorithms, neural networks, and/or complex fluid dynamics computations in the feedback loop (e.g., see (Tchieu et al., 2008; Mondschein et al., 2011; Deb et al., 2005a, 2005b, 2006, 2007, 2008; Liu et al., 2006; Singhal et al., 2009; Tao, 1996; Jee et al., 2009)). In (Muse et al., 2009) a low-order model was utilized to develop a neural network-based adaptive output feedback control scheme using SJA. The control design in (Muse et al., 2009) achieves uniformly ultimately bounded model reference tracking in the presence of actuator disturbances; the controller performance was demonstrated via computer simulation and experiment. In (Jee et al., 2009), a neural network is coupled with a computational fluid dynamics model to develop SJA-based flow and pitching and plunging control laws for an airfoil. The controller performance in (Jee et al., 2009) is demonstrated via numerical computer simulation. The aforementioned neural network-based control laws are shown to perform well at their respective tasks; however, neural networks can increase the computational complexity of feedback control systems.

Adaptive control is another method that is popularly utilized in SJA-based control design. An adaptive approach is presented in (Mondschein et al., 2011), which

is shown to compensate for synthetic jet actuator nonlinearities and disturbances. The approach in (Mondschein et al., 2011) utilizes a linear time-invariant dynamic model containing actuator nonlinearities and non-constant disturbances, and it is proven that the adaptive controller achieves asymptotic trajectory tracking. Adaptive inverse schemes are utilized in (Deb et al., 2005a, 2006, 2007, 2008) to achieve tracking performance in the presence of synthetic jet actuator nonlinearities. In (Deb et al., 2005a) and (Deb et al., 2005b), an adaptive inverse technique is utilized to compensate for the SJA nonlinearity, and a Lyapunov-based analysis is provided to prove asymptotic trajectory tracking using a linear time-invariant plant model in the absence of disturbances. Adaptive control methods can achieve good control performance in the presence of uncertainty at a reduced computational cost as compared to neural network-based methods. The research presented in this chapter seeks an answer to the question: *Can a computationally minimal robust feedback control strategy be utilized to achieve SJA-based tracking control performance that is comparable to adaptive or neural network-based methods?*

The contribution in this chapter is the development of a robust nonlinear control method, which is proven to achieve accurate flight tracking control in the presence of SJA nonlinearities, parametric uncertainty and external disturbances (e.g., wind gusts). The structure of the control law is continuous, making the proposed design amenable to practical application. Moreover, the control method presented in this chapter is designed to be inexpensively implemented, requiring no online adaptive laws, function approximators, or complex fluid dynamics computations in the feedback loop. A matrix decomposition technique is utilized along with innovative manipulation in the error system development to compensate for the dynamic SJA

uncertainty. The robust controller is designed with an implicit learning law, which is shown to compensate for bounded disturbances. A Lyapunov-based stability analysis is utilized to prove global asymptotic trajectory tracking in the presence of external disturbances, actuator nonlinearities, and parametric uncertainty in the system and actuator dynamics. Numerical simulation results are provided to complement the theoretical development.

5.2 Dynamic Model and Properties

The uncertain aircraft dynamic model under consideration in this chapter is assumed to contain parametric uncertainty due to linearization errors and unmodeled nonlinearities. Specifically, the aircraft system can be modeled via a linear time-invariant system as (Mondschein et al., 2011; Deb et al., 2005a, 2007, 2008; Nelson, 1998; Tchieu et al., 2008; Singhal et al., 2009)

$$\dot{x} = Ax + Bu + f(x, t) \quad (5.1)$$

where $A \in \mathbb{R}^{n \times n}$ denotes the uncertain state matrix, $B \in \mathbb{R}^{n \times m}$ represents the uncertain input matrix, and $f(x, t) \in \mathbb{R}^n$ is a state- and time-dependent unknown, nonlinear disturbance. For example, $f(x, t)$ could include exogenous disturbances (e.g., due to wind gusts) or nonlinearities not captured in the linearized dynamic model. Also in (5.1), the control input $u(t) \triangleq \begin{bmatrix} u_1(t) & u_2(t) & \cdots & u_m(t) \end{bmatrix}^T \in \mathbb{R}^m$ represents the virtual surface deflections due to m arrays of synthetic jet actuators (SJA). Based on experimental data, the dynamics of the SJA can be modeled as (Deb

et al., 2008, 2005a, 2006, 2007)

$$u_i = \theta_{2i}^* - \frac{\theta_{1i}^*}{v_i}, \quad i = 1, 2, \dots, m \quad (5.2)$$

where $v_i(t) = A_{ppi}^2(t) \in \mathbb{R}$ denotes the peak-to-peak voltage acting on the i^{th} SJA array, and $\theta_{1i}^*, \theta_{2i}^* \in \mathbb{R}$ are unknown positive physical parameters. One of the control design challenges is that the control terms $u_i(t)$ depend nonlinearly on the voltage signal $v_i(t)$ and contain parametric uncertainty due to θ_{1i}^* and θ_{2i}^* . This challenge will be handled using a robust, continuous nonlinear control technique.

Using the expressions in (5.2) and (5.1), the dynamics can be expressed in terms of the i^{th} SJA array as

$$\dot{x} = Ax + \sum_{i=1}^m b_i u_i + f(x, t). \quad (5.3)$$

In (5.3), $b_i \triangleq \begin{bmatrix} b_{1i} & b_{2i} & \dots & b_{ni} \end{bmatrix}^T \in \mathbb{R}^n \forall i = 1, 2, \dots, m$, where b_{ij} denotes the $(i, j)^{th}$ element of the matrix B in (5.1).

Assumption 1: If $x(t) \in L_\infty$, then $f(x, t)$ is bounded. Moreover, if $x(t) \in \mathcal{L}_\infty$, then the first and second partial derivatives of the elements of $f(x, t)$ with respect to $x(t)$ exist and are bounded.

5.2.1 Robust Nonlinearity Inverse

The contribution in this chapter is development that shows how a purely robust feedback control strategy can be utilized to compensate for the control input nonlinearity and input parametric uncertainty in (5.2). To this end, a robust inverse $v_i(t)$ will be utilized, which contains constant feedforward “best-guess” estimates of the uncertain

parameters θ_{1i}^* and θ_{2i}^* . The robust inverse that compensates for the uncertain jet array nonlinearities in (5.2) can be expressed as

$$v_i(t) = \frac{\hat{\theta}_{1i}}{\hat{\theta}_{2i} - u_{di}(t)}, \quad i = 1, \dots, m \quad (5.4)$$

where $\hat{\theta}_{1i}, \hat{\theta}_{2i} \in \mathbb{R}^+$ are constant feedforward estimates of θ_{1i}^* and θ_{2i}^* , respectively, and $u_{di}(t) \in \mathbb{R} \forall i = 1, \dots, m$ are subsequently defined auxiliary control signals.

Remark 9 *Singularity Issues* Based on (5.4), the control signal $v_i(t)$ will encounter singularities when $u_{di}(t) = \hat{\theta}_{2i}$. To ensure that the control law in (5.4) is singularity-free, the control signals $u_{di}(t)$ for $i = 1, 2, \dots, m$ will be designed using the following algorithm (Mondschein et al., 2011):

$$u_{di}(t) = \begin{cases} \hat{\theta}_{2i} - \delta & \text{if } g(\mu_0(t), \mu_1(t)) \geq \hat{\theta}_{2i} - \delta \\ g(\mu_0(t), \mu_1(t)) & \text{otherwise} \end{cases} \quad (5.5)$$

where $\delta \in \mathbb{R}^+$ is a small parameter, $g(\cdot)$ is a subsequently defined function, and $\mu_0(t), \mu_1(t) \in \mathbb{R}^m$ are subsequently defined feedback control terms. Note that the parameter δ can be selected arbitrarily small such that the subsequent stability analysis remains valid for an arbitrarily large range of positive control voltage signals $v_i(t)$.

In addition, the control terms $u_i(t)$ in (5.2) will encounter singularities when $v_i(t) = 0$, which occurs when $\hat{\theta}_{1i} = 0$ for any i . Since $\hat{\theta}_{1i}$ is a constant, user-defined feedforward estimate of the uncertain parameter θ_{1i}^* , the singularity at $v_i(t) = 0$ can be easily avoided by selecting $\hat{\theta}_{1i} > 0$ for $i = 1, 2, \dots, m$.

Remark 10 Preliminary results show that the auxiliary control signal $u_{di}(t)$ in (5.4) can be designed to achieve asymptotic tracking control and disturbance rejection for

the uncertain dynamic model in (5.1) and (5.2) over a wide range of feedforward estimates $\hat{\theta}_{ji} \neq \theta_{ji}^*$, $j = 1, 2$.

5.2.2 Control Development

The control objective is to force the system state $x(t)$ to track the state of a model reference system. Based on (5.1), a reference model is selected as

$$\dot{x}_m = A_m x_m + B_m \delta \quad (5.6)$$

where $x_m(t) \in \mathbb{R}^n$ denotes the reference state, $A_m \in \mathbb{R}^{n \times n}$ is a Hurwitz state matrix, $B_m \in \mathbb{R}^n$ denotes the reference input matrix, and $\delta(t) \in \mathbb{R}$ is the reference input signal. The reference model in (5.6) is designed to exhibit desirable performance characteristics.

Assumption 2: The model reference state $x_m(t)$ is bounded and sufficiently smooth in the sense that $x_m(t), \dot{x}_m(t), \ddot{x}_m(t), \dddot{x}_m(t) \in \mathcal{L}_\infty \forall t \geq 0$.

To quantify the control objective, the tracking error $e(t) \in \mathbb{R}^n$ is defined as

$$e = x - x_m. \quad (5.7)$$

To facilitate the subsequent analysis, a filtered tracking error $r(t)$ is also defined as

$$r = \dot{e} + \alpha e \quad (5.8)$$

After taking the time derivative of (5.8) and using (5.1) and (5.7), the open loop

tracking error dynamics are obtained as

$$\dot{r} = A\dot{e} + A\dot{x}_m + \sum_{i=1}^m b_i \left(\frac{\theta_{1i}^*}{\hat{\theta}_{1i}} \dot{u}_{di}(t) \right) + \dot{f}(x, t) - \ddot{x}_m + \alpha \dot{e} \quad (5.9)$$

Remark 11 *Although the constant portion of the control input term vanishes upon taking the time derivative of the dynamics as in (5.9), the plant model used in the subsequent numerical simulation retains the complete actuator dynamics. In the simulation, the control input $u_i(t)$ is generated using (5.2) and (5.4); thus, the simulation model includes the complete actuator dynamics.*

The expression in (5.9) can be rewritten as

$$\dot{r} = \tilde{N} + N_d + \Omega \dot{u}_d(t) - Se \quad (5.10)$$

where $\Omega \in \mathbb{R}^{n \times m}$ denotes a constant uncertain matrix, $S \in \mathbb{R}^{n \times n}$ is a subsequently defined uncertain matrix and the control vector $u_d(t)$

$$u_d(t) \triangleq \begin{bmatrix} u_{d1}(t) & u_{d2}(t) & \cdots & u_{dm}(t) \end{bmatrix}^T \in \mathbb{R}^m \quad (5.11)$$

In (5.10), the unknown, unmeasurable auxiliary functions $\tilde{N}(t)$ and $N_d(t)$ are defined as

$$\tilde{N} \triangleq A\dot{e} + \alpha \dot{e} + Se + \left(\dot{f}(x, t) - \dot{f}(x_m, t) \right) \quad (5.12)$$

$$N_d \triangleq A\dot{x}_m - \ddot{x}_m + \dot{f}(x_m, t) \quad (5.13)$$

The selective grouping of terms in (5.12) and (5.13) is motivated by the fact that

Assumptions 1 and 2 can be utilized to develop the following inequalities:

$$\left\| \tilde{N} \right\| \leq \rho_0 \|z\|, \quad \|N_d\| \leq \zeta_{N_d}, \quad \left\| \dot{N}_d \right\| \leq \zeta_{\dot{N}_d} \quad (5.14)$$

where $\rho_0, \zeta_{N_d}, \zeta_{\dot{N}_d} \in \mathbb{R}^+$ are known bounding constants and $z(t) \in \mathbb{R}^{2n}$ is defined as

$$z \triangleq \begin{bmatrix} e^T & r^T \end{bmatrix}^T. \quad (5.15)$$

5.2.3 Closed-loop Error System

Based on the open-loop error system in (5.10), the auxiliary control $u_d(t)$ is designed as

$$u_d(t) = \hat{\Omega}^\# (\mu_0 - \mu_1) \quad (5.16)$$

where $\hat{\Omega} \in \mathbb{R}^{n \times m}$ is a constant, best-guess estimate of the uncertain matrix Ω , and $[\cdot]^\#$ denotes the pseudoinverse of a matrix. In (5.16) $\mu_0(t), \mu_1(t) \in \mathbb{R}^n$ are subsequently defined feedback control terms. After substituting the time derivative of (5.16) into (5.10), the error dynamics can be expressed as

$$\dot{r} = \tilde{N} + N_d + \tilde{\Omega} (\dot{\mu}_0 - \dot{\mu}_1) - Se \quad (5.17)$$

where the constant uncertain matrix $\tilde{\Omega} \in \mathbb{R}^{n \times n}$ is defined as

$$\tilde{\Omega} = \Omega \hat{\Omega}^\#. \quad (5.18)$$

Assumption 3: Bounds on the uncertain matrix Ω are known such that the

feedforward estimate $\hat{\Omega}$ can be selected such that the product $\tilde{\Omega}$ can be decomposed as (Morse, 1993)

$$\tilde{\Omega} = ST \quad (5.19)$$

where $S \in \mathbb{R}^{n \times n}$ is a positive definite symmetric matrix, and $T \in \mathbb{R}^{n \times n}$ is a unity upper triangular matrix, which is diagonally dominant in the sense that

$$\varepsilon \leq |T_{ii}| - \sum_{k=i+1}^n |T_{ik}| \leq Q, \quad i = 1, \dots, n-1. \quad (5.20)$$

In inequalities (5.20), $\varepsilon \in (0, 1)$ and $Q \in \mathbb{R}^+$ are known bounding constants, and $T_{ik} \in \mathbb{R}$ denotes the (i, k) th element of the matrix T .

Remark 12 *Preliminary results show that Assumption 3 is mild in the sense that (5.20) is satisfied over a wide range of $\hat{\Omega} \neq \Omega$. Specifically, simulation results show that the auxiliary control signal $u_{di}(t)$ in (5.4) and (5.16) can be designed to achieve asymptotic tracking control and disturbance rejection for the uncertain dynamic model in (5.1) and (5.2) when the mean values of the constant feedforward estimates $\hat{\theta}_{j1}$ and $\hat{\theta}_{j2} \forall j = 1, \dots, 6$ differ from the mean values of the actual parameters θ_{j1}^* and $\theta_{j2}^* \forall j = 1, \dots, 6$ as*

$$\begin{aligned} \text{mean}(\hat{\theta}_{j1}) &= 14.05, & \text{mean}(\theta_{j1}^*) &= 25.28 \\ \text{mean}(\hat{\theta}_{j2}) &= 7.25, & \text{mean}(\theta_{j2}^*) &= 12.08 \end{aligned}$$

The values for $\hat{\theta}_{j1}$ and $\hat{\theta}_{j2} \forall j = 1, \dots, 6$ used in the simulation can be found in Table 1 of Section 5.4. This preliminary result demonstrates the capability of the robust control design to compensate for significant dynamic uncertainty using only a simple

feedback controller structure.

After utilizing the decomposition in (5.19), the error dynamics in (5.17) can be expressed as

$$S^{-1}\dot{r} = \tilde{N}_1 + N_{d1} + T(\dot{\mu}_0 - \dot{\mu}_1) - e \quad (5.21)$$

where

$$\tilde{N}_1 \triangleq S^{-1}\tilde{N}, \quad N_{d1} \triangleq S^{-1}N_d. \quad (5.22)$$

Since S is positive definite, $\tilde{N}_1(t)$ and $N_{d1}(t)$ satisfy the inequalities

$$\|\tilde{N}_1\| \leq \rho_1 \|z\|, \quad \|N_{d1}\| \leq \zeta_{N_{d1}}, \quad \|\dot{N}_{d1}\| \leq \zeta_{\dot{N}_{d1}} \quad (5.23)$$

where $\rho_1, \zeta_{N_{d1}}, \zeta_{\dot{N}_{d1}} \in \mathbb{R}^+$ are known bounding constants. By utilizing the fact that the uncertain matrix T is unity upper triangular, the error dynamics in (5.21) can be rewritten as

$$S^{-1}\dot{r} = \tilde{N}_1 + N_{d1} + \dot{\mu}_0 + \bar{T}\dot{\mu}_0 - T\dot{\mu}_1 - e \quad (5.24)$$

where $\bar{T} \triangleq T - I_{n \times n}$ is a strictly upper triangular matrix, and $I_{n \times n}$ denotes an $n \times n$ identity matrix. Based on the open-loop error system in (5.24), the auxiliary control terms $\mu_0(t)$ and $\mu_1(t)$ are designed as

$$\mu_0 = -(k_s + I_{n \times n})e(t) - (k_s + I_{n \times n})e(0) \quad (5.25)$$

$$\begin{aligned} & - \int_0^t \alpha(k_s + I_{n \times n})e(\tau) d\tau. \\ \mu_1 &= \int_0^t \beta \operatorname{sgn}(e(\tau)) d\tau \end{aligned} \quad (5.26)$$

where $\beta \in \mathbb{R}$ is a constant, positive control gain, $k_s \in \mathbb{R}^{n \times n}$ is a constant, positive

definite, diagonal control gain matrix, and α is introduced in (5.8). After substituting the time derivative of (5.25) into (5.24), the closed-loop error system is obtained as

$$S^{-1}\dot{r} = \tilde{N}_1 + \bar{T}\dot{\mu}_0 + N_{d1} - (k_s + I_{n \times n})r - T\dot{\mu}_1 - e. \quad (5.27)$$

After taking the time derivative of (5.25), the term $\bar{T}\dot{\mu}_0$ can be expressed as

$$\bar{T}\dot{\mu}_0 = \begin{bmatrix} \sum_{j=2}^n \bar{T}_{1j}\dot{\mu}_{0j} \\ \sum_{j=3}^n \bar{T}_{2j}\dot{\mu}_{0j} \\ \vdots \\ \bar{T}_{(n-1)n}\dot{\mu}_{0n} \\ 0 \end{bmatrix} = \begin{bmatrix} \Lambda_\rho \\ 0 \end{bmatrix} \quad (5.28)$$

where the auxiliary signal $\Lambda_\rho \triangleq \begin{bmatrix} \Lambda_{\rho 1} & \Lambda_{\rho 2} & \cdots & \Lambda_{\rho(n-1)} \end{bmatrix}^T \in \mathbb{R}^{n-1}$, with the individual elements defined as

$$\Lambda_{\rho i} \triangleq - \sum_{j=i+1}^n \bar{T}_{ij} (k_{sj} + 1) r_j \quad (5.29)$$

$\forall i = 1, \dots, n-1$ where the subscript j indicates the j th element of the vector. Based on the definitions in (5.25) and (5.28), Λ_ρ satisfies the inequality

$$\|\Lambda_\rho\| \leq \rho_{\Lambda 1} \|z\| \quad (5.30)$$

where $z(t)$ is defined in (5.15), and $\rho_{\Lambda 1} \in \mathbb{R}$ is a known positive bounding constant.

Remark 13 Note that based on (5.28) and (5.29), the bounding constant $\rho_{\Lambda 1}$ depends

only on elements $i + 1$ to n of the control gain matrix k_s due to the strictly upper triangular nature of \bar{T} . Thus, the element $\dot{\mu}_{01}(t)$ of the control vector $\dot{\mu}_0(t)$ does not appear in the term Λ_ρ . This fact will be utilized in the subsequent stability proof.

By utilizing (5.28), the error dynamics in (5.27) can be expressed as

$$S^{-1}\dot{r} = \tilde{N}_2 + N_{d1} - (k_s + I_{n \times n})r - T\dot{\mu}_1 - e \quad (5.31)$$

where

$$\tilde{N}_2 = \tilde{N}_1 + \begin{bmatrix} \Lambda_\rho \\ 0 \end{bmatrix}. \quad (5.32)$$

Based on (5.23), (5.30), and (5.32), $\tilde{N}_2(t)$ satisfies the inequality

$$\|\tilde{N}_2\| \leq \rho_2 \|z\| \quad (5.33)$$

where $\rho_2 \in \mathbb{R}$ is a known bounding constant.

To facilitate the subsequent stability analysis, the control gain β introduced in (5.26) is selected to satisfy

$$\beta > \frac{1}{\varepsilon} \left(\zeta_{N_{d1}} + \frac{1}{\alpha} \zeta_{\dot{N}_{d1}} \right) \quad (5.34)$$

where $\zeta_{N_{d1}}$ and $\zeta_{\dot{N}_{d1}}$ are introduced in (5.23), and ε is introduced in (5.20).

5.3 Stability Analysis

To facilitate the subsequent stability analysis, let $\mathcal{D} \subset \mathbb{R}^{2n+1}$ be a domain containing $w(t) = 0$, where $w(t) \in \mathbb{R}^{2n+1}$ is defined as

$$w(t) \triangleq \begin{bmatrix} z^T(t) & \sqrt{P(t)} \end{bmatrix}^T. \quad (5.35)$$

In (5.35), the auxiliary function $P(t) \in \mathbb{R}$ is defined as the generalized solution to the differential equation

$$\dot{P}(t) = -L(t), \quad P(0) = \beta Q |e(0)| - e^T(0) N_{d1}^T(0) \quad (5.36)$$

where the auxiliary function $L(t) \in \mathbb{R}$ is defined as

$$L(t) = r^T (N_{d1}(t) - T\dot{\mu}_1). \quad (5.37)$$

Lemma 2 *Provided the sufficient gain condition in (5.34) is satisfied, the following inequality can be obtained:*

$$\int_0^t L(\tau) d\tau \leq \beta Q |e(0)| - e^T(0) N_{d1}(0). \quad (5.38)$$

Hence, (5.38) can be used to conclude that $P(t) \geq 0$.

Proof of Lemma 2 is in Appendix (B) or (MacKunis et al., 2013), and it is omitted here for brevity.

Theorem 1 *The robust control law given by (5.4), (5.16), (5.25), and (5.26) ensures*

asymptotic trajectory tracking in the sense that

$$\|e(t)\| \rightarrow 0, \quad \text{as} \quad t \rightarrow \infty \quad (5.39)$$

provided the control gain matrix k_s introduced in (5.25) is selected sufficiently large (see the subsequent proof), and β is selected to satisfy the sufficient condition in (5.34).

Proof. Let $V(w, t) : \mathcal{D} \times [0, \infty) \rightarrow \mathbb{R}$ be a continuously differentiable, radially unbounded, positive definite function defined as

$$V = \frac{1}{2}e^T e + \frac{1}{2}r^T S^{-1}r + P. \quad (5.40)$$

After taking the time derivative of (5.40) and utilizing (5.8), (5.31), (5.36), and (5.37), $\dot{V}(t)$ can be expressed as

$$\dot{V} \leq - \left(\lambda_0 - \frac{\rho_2^2}{4\lambda_{\min}(k_s)} \right) \|z\|^2 \quad (5.41)$$

where $\lambda_0 \triangleq \min\{\alpha, 1\}$, and $\lambda_{\min}(\cdot)$ denotes the minimum eigenvalue of the argument.

Inequality (5.41) can be used to show that $V(w, t) \in \mathcal{L}_\infty$; hence, $e(t), r(t), P(t) \in \mathcal{L}_\infty$. Given that $e(t), r(t) \in \mathcal{L}_\infty$, (5.8) can be utilized to show that $\dot{e}(t) \in \mathcal{L}_\infty$. Since $e(t), \dot{e}(t) \in \mathcal{L}_\infty$, (5.7) can be used along with the assumption that $x_m(t), \dot{x}_m(t) \in \mathcal{L}_\infty$ to prove that $x(t), \dot{x}(t) \in \mathcal{L}_\infty$. Based on the fact that $x(t) \in \mathcal{L}_\infty$, Assumption 1 can be utilized to show that $f(x, t) \in \mathcal{L}_\infty$. Given that $x(t), \dot{x}(t), f(x, t) \in \mathcal{L}_\infty$, (5.1) can be used to show that $u(t) \in \mathcal{L}_\infty$. Since $e(t), r(t) \in \mathcal{L}_\infty$, the time derivative of (5.25) and (5.26) can be used to show that $\dot{\mu}_0(t), \dot{\mu}_1(t) \in \mathcal{L}_\infty$.

Given that $e(t), r(t), \dot{\mu}_1(t) \in \mathcal{L}_\infty$, (5.31) can be used along with (5.33) to show that $\dot{r}(t) \in \mathcal{L}_\infty$. Since $\dot{e}(t), \dot{r}(t) \in \mathcal{L}_\infty$, (5.15) can be used to show that $z(t)$ is uniformly continuous. Since $z(t)$ is uniformly continuous, $V(w, t)$ is radially unbounded, and (5.40) and (5.41) can be used to show that $z(t) \in \mathcal{L}_\infty \cap \mathcal{L}_2$. Barbalat's Lemma (Khalil, 2002) can now be invoked to state that

$$\|z(t)\| \rightarrow 0 \quad \text{as} \quad t \rightarrow \infty \quad \forall w(0) \in \mathbb{R}^{2n+1}. \quad (5.42)$$

Based on the definition of $z(t)$, (5.42) can be used to show that

$$\|e(t)\| \rightarrow 0 \quad \text{as} \quad t \rightarrow \infty \quad \forall w(0) \in \mathbb{R}^{2n+1}.$$

■

5.4 Simulation Results

A numerical simulation was created to verify the performance of the control law developed in (5.2), (5.4), (5.16), (5.25), and (5.26). The simulation is based on the dynamic model given in (5.1) and (5.2), where $n = 3$ and $m = 6$. Specifically, the control input $u_i(t)$, $i = 1, 2, \dots, 6$, consists of 6 synthetic jet arrays, and the 3-DOF state vector is defined in terms of the roll, pitch, and yaw rates as

$$x = \begin{bmatrix} x_1 & x_2 & x_3 \end{bmatrix}^T.$$

The state and input matrices A and B and reference system matrices A_m and B_m are defined based on the Barron Associates nonlinear tailless aircraft model (BANTAM) (for details of the sim model, see (Deb et al., 2007)).

The 3-DOF linearized model for the BANTAM was obtained analytically at the trim condition: Mach number $M = 0.455$, angle of attack $\alpha = 2.7$ deg, and side slip angle $\beta = 0$ (Deb et al., 2007). The linearized dynamic model does not produce the same result as the full nonlinear system with mechanical control surfaces, but the angular accelerations caused by the virtual surface deflections are predicted accurately using the matrix B . The actual (i.e., θ_{1i}^* and θ_{2i}^* , $i = 1, 2, \dots, 6$) and estimated (i.e., $\hat{\theta}_{1i}$ and $\hat{\theta}_{2i}$, $i = 1, 2, \dots, 6$) values of the SJA parameters (see (5.2) and (5.4)) are shown in Table 1.

Table 1

Array i	1	2	3	4	5	6
θ_{1i}^* [volt-deg]	32.9	29.8	26.7	24.0	20.5	17.8
θ_{2i}^* [deg]	14.7	13.8	12.8	11.7	10.0	9.5
$\hat{\theta}_{1i}$ [volt-deg]	16.5	15.9	14.5	13.4	12.1	11.9
$\hat{\theta}_{2i}$ [deg]	9.1	8.3	7.2	6.8	6.5	5.6

The external disturbance used in the simulation is given by

$$d = \begin{bmatrix} 0.2 \sin(0.5t) \\ 0.1 \sin(0.5t) + 0.2 \sin(0.5t) \\ 0.15 \sin(0.3t) \end{bmatrix}.$$

The reference input $\delta(t)$ used in the simulation is given by (Deb et al., 2007)

$$\delta(t) = \begin{cases} 0.5 \sin(t), & 0 \leq t \leq 50 \\ 0.5 \sin(t) + \sin(2t) & 50 < t \leq 100 \end{cases} \quad (5.43)$$

Figures 5.1-5.2 illustrate the performance of the proposed controller with control gains selected as

$$\alpha = 0.3, \quad \beta = \text{diag}\{3.3, 0.3, 0.8\}, \quad k_s = \text{diag}\{0.10, 0.15, 2.3\}$$

The first plot shows the tracking error response, which demonstrate the rapid convergence of the closed-loop system, and the final plot shows the control commands during closed-loop operation. The effects of the instantaneous change in the reference input $\delta(t)$ (i.e., see (5.43)) at $t = 50$ s are apparent in the $e_1(t)$ and $e_3(t)$ plots in Figure 5.1, but the tracking errors converge to zero quickly in spite of this sudden switch in the reference command. The control commands remain within reasonable limits, and the level of chattering is minimal.

5.5 Conclusion

A robust nonlinear control strategy is presented, which is capable of achieving accurate tracking for an aircraft using synthetic jet actuators. The proposed controller is shown to achieve global asymptotic tracking of a model reference system, where the plant dynamics contain input-multiplicative parametric uncertainty and actuator nonlinearities in addition to unknown, additive external disturbances. Moreover,

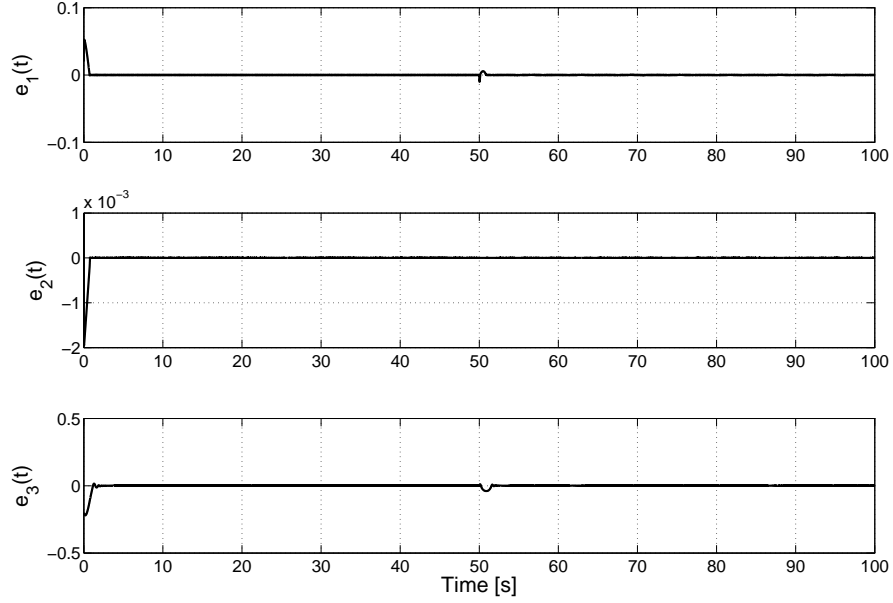


Figure 5.1: Tracking error plots achieved during closed-loop controller operation.

the structure of the control law is continuous, making the proposed design amenable to practical application. The controller is designed to be practically implementable, requiring no observers, function approximators or adaptive laws. By exploiting minimal knowledge of the structure of the SJA dynamic model, a matrix decomposition technique is utilized along with careful algebraic manipulation in the error system development to compensate for the input-multiplicative parametric uncertainty. A Lyapunov-based stability analysis is provided to prove the theoretical result, and numerical simulation results are provided to demonstrate the performance of the proposed controller. Future work will address simultaneous flow and flight control of using SJA.

A second order dynamic system with parametric uncertainty and disturbance is

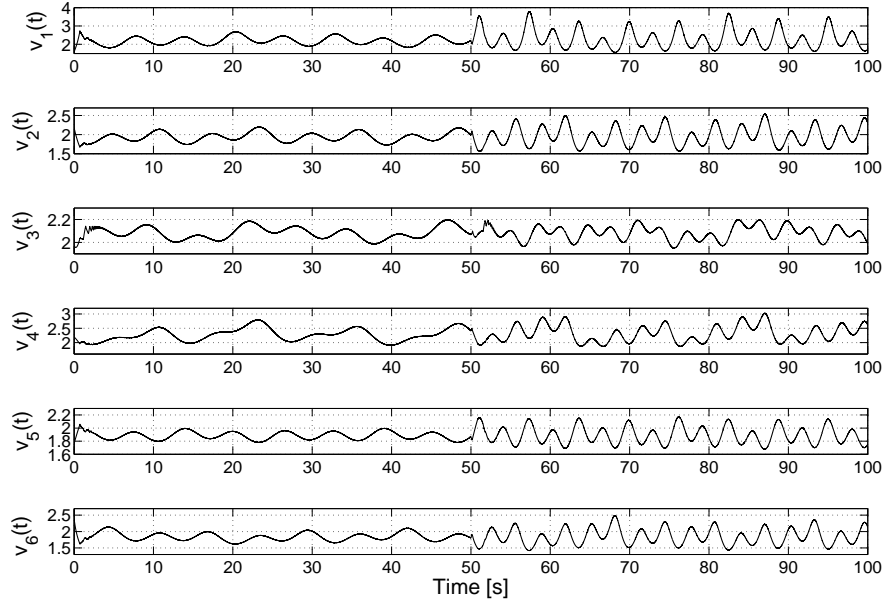


Figure 5.2: Control signals $v_i(t)$, $i = 1, \dots, 6$ [Volts] used during closed-loop controller operation.

presented in this chapter. To extend the current work to a more general class of systems that contain heavy uncertainty or unmodeled variations that manifest themselves as a priori unknown changes in the control direction, can the SMC technique presented in this section be extended to systems where the sign of the matrix $g(x)$ is unknown, i.e., unknown control direction? The next chapter presents an extension to handle a more general case where there is uncertainty in the control input direction.

Chapter 6

Self-Reconfigurable Control

6.1 Introduction

This chapter develops a sliding mode control algorithm that compensates for systems containing unknown control direction, and this work can be found in (Price, Ton, MacKunis, & Drakunov, 2013; Drakunov, 1994).

Systems with unknown control direction has been an interesting research area within the past two to three decades. The challenge of an unknown direction control vector has led to some creative ways to circumvent the problem. Various areas of research in adaptive control, sliding mode control (SMC), and robust control have contributed to the solution.

The problem of unknown control direction had an early interest in the area of adaptive control when Morse proposed a conjecture that one-dimensional linear systems with relaxed assumption in the control direction, i.e., unknown control sign, cannot be globally stabilized via adaptive control law (Morse, 1998). Nussbaum,

however, was able to show that linear systems with unknown signs can be stabilized through suitable adaptive control gain named *Nussbaum* function (Nussbaum, 1983). Although the Nussbaum function can stabilize systems with unknown control direction, it needs infinite bandwidth to compensate for the uncertainty in the dynamics.

Adaptive control has made further progress in the area of unknown control direction in the input matrix since Nussbaum's proposed control algorithm. In (Ferrara et al., 2009), Ferrara *et al.* has developed an adaptive sliding mode control for uncertain nonholonomic systems with unknown control direction. This method segregates the known states from the uncertain parameters, then an estimate for the uncertainty is designed. Lozano et al. have designed an updated version of the adaptive controller that does not require knowledge of the sign of the control direction, and the scheme is free from singularities (Lozano & Brogliato, 1992). In (Xudong & Jingping, 1998), a method using adaptive design is applied to n -order system. However, the design has the flaw of over parameterization, which decreases effect of parameter convergence and system robustness because of the controller's dynamic order. The system contains an unknown but constant sign direction. Their key idea is based on backstepping and implementing the Nussbaum-type function. Reference type functions are also defined in (Xudong & Jingping, 1998) to ease the analysis, and the result is a global adaptive control that can be designed for nonlinear systems with unknown parameters.

There are also novel algorithms invented to solve the problem of unknown control direction. A differential approach was used in (Kaloust & Qu, 1997), where the first and second derivative was used to detect sign changes, and the nominal system is

assumed to be stable, which restricts the applicable class of systems. This approach used the Lyapunov method to design a continuous robust control that has an online algorithm to identify the change in the control direction and a shifting law that smoothly changes the control. Since it is a robust controller, bounding of the unknown functions and on the rate of change of the control direction are required. Yang et al. divide up the state $x(t) \in \mathbb{R}$ into convergent and non-convergent sets and analyze where the signs will switch and the intervals in between the switching (Yang et al., 2009). The main analysis uses the Nussbaum-type function for periodic switching to allow convergence of the system. The important aspect of (Yang et al., 2009) is to prove the bounding of the Nussbaum-type gain where the unknown control directional is able to smoothly cross zero and change its sign for unlimited number of times. In (Yan & Xu, 2004; Yan et al., 2008), Yan et al. used a monitoring function that exponentially decays with time, and they test whether the error function intersects it. If an intersection happens, this implies that the controller sign is wrong, thus, switching occurs to change the direction; however, if the assumed control direction is correct, then the switching does not occur. This method is designed for a constant unknown sign. In (Hsu et al., 2006), Hsu et al. used variable structure for arbitrary relative degree n system. The unknown sign direction is constant, and the system does not have unlimited switching. The variable structure implementation control algorithm in (Hsu et al., 2006) has a direct advantage over (Yan et al., 2008) due to its insensitivity to measurement noise.

Sliding mode control, known for its robustness, has also been used to stabilize systems unknown control direction. In (Bartolini & Pisano, 2008; Bartolini et al., 2003, 2010, 2011), Bartolini *et al.* rely on a Lyapunov function to derive the control law for

systems with heavy uncertainty, i.e unknown control signs. In (Bartolini et al., 2003), Bartolini et al. also use sliding mode control to compensate for the uncertain control input direction with an observer designed to estimate the drift terms to ensure the attractiveness of the sliding surface. In (Drakunov, 1993), *self-reconfigurable* control was suggested to compensate the unknown control direction problem. The control algorithm presented in (Drakunov, 1993) uses a purely robust feedback technique to achieve finite-time convergence in the presence of unknown signs.

The contribution of this chapter is utilizing a control architecture similar to that (Drakunov, 1993) to compensate for unknown control direction for a general class of systems. This robust feedback control is computationally inexpensive due to the fact that it requires no monitoring functions, function approximations, or online adaptive update.

6.1.1 Multi-Manifold Sliding Mode Control

This section considers the application of sliding mode control, where uncertainty in the model contribute to unknown control direction. In section 2.2.2, it was shown that adaptive control is able to adjust itself to an unknown constant in the input matrix b in (2.51). Adaptive control is computationally expensive due to the online adaption that is required. Moreover, adaptive control can only compensate constant uncertainty. For the case where there is high uncertainties and the input matrix is state- and time-varying, adaptive control is not sufficient to stabilize the system. In such a case, SMC can be used to compensate for these uncertainty. In the following, sliding mode control is used to compensate for unknown control direction in a scalar control input.

Consider a nonlinear system

$$\dot{x} = f(t, x) + B(t, x)u, \quad (6.1)$$

where $x(t) \in \mathbb{R}^n$, $B(t, x) \in \mathbb{R}^{n \times m}$, $u(t) \in \mathbb{R}^m$. The objective is to design a control algorithm that does not require the knowledge of the input matrix $B(t, x)$. In SMC, the objective is to drive the state to the manifold

$$\mathbb{M} = [x \in \mathbb{R}^n | \sigma(x) = 0], \quad (6.2)$$

where

$$\sigma(x) = \begin{bmatrix} \sigma_1(x) & \sigma_2(x) & \dots & \sigma_m(x) \end{bmatrix}^T \quad (6.3)$$

is an m -dimensional smooth function such that the system (6.1) is stable when constrained to the manifold \mathbb{M} . The manifold \mathbb{M} can be considered as the intersection of hypersurfaces of the components $\sigma_i(x) \in \mathbb{R}$

$$\mathbb{M} = \bigcap_{i=1}^m \mathbb{M}_i \quad \mathbb{M}_i = \{x \in \mathbb{R}^n : \sigma_i(x) = 0\}, \quad (6.4)$$

where \mathbb{M}_i is the i^{th} switching surface.

Consider the time derivative of the sliding surface σ along trajectories of the system (6.1):

$$\dot{\sigma} = \frac{\partial \sigma(x)}{\partial x} B(t, x)u + \frac{\partial \sigma(x)}{\partial x} f(t, x). \quad (6.5)$$

The control function $u = u(\sigma; t, x)$ that provides stabilization to the surface σ is

defined by the property of the matrix

$$\frac{\partial \sigma(x)}{\partial x} B(t, x). \quad (6.6)$$

Consider the situation when the control designed for the system (6.1) is applied to the system with uncertainty

$$\dot{x} = \tilde{f}(t, x) + \tilde{B}(t, x)u. \quad (6.7)$$

In this situation, when $\tilde{B}(t, x) \equiv B(t, x)$, where there are no anomalies in the input matrix, Equation (6.7) can be rewritten as

$$\dot{x} = f(t, x) + \Delta f(t, x) + B(t, x)u, \quad (6.8)$$

where $\tilde{f}(t, x) = f(t, x) + \Delta f(t, x)$. The variable Δf is a perturbation of the function $f(t, x)$, and if Δf satisfies the matching condition (Drazenovic, 1969)

$$\Delta f \in \text{range}(B)$$

for all t and x , then sliding mode can make the closed-loop system invariant to the perturbation. The control $u = u(\sigma; t, x)$ based on the nominal system in (6.1) can still be applied to (6.7), provided that control amplitude is large enough dominate the first term in the equation

$$\dot{\sigma} = \frac{\partial \sigma(x)}{\partial x} B(t, x)u + \frac{\partial \sigma(x)}{\partial x} (f(t, x) + \Delta f(t, x)) \quad (6.9)$$

to guarantee convergence to the sliding surface \mathbb{M} .

For the case where $\tilde{B}(t, x) = B(t, x) + \Delta B(t, x)$, the system in (6.7) can be written as

$$\dot{x} = f(t, x) + \Delta f(t, x) + (B(t, x) + \Delta B(t, x))u. \quad (6.10)$$

The control designed for the system (6.1) can still be applied to (6.10) to achieve convergence to the manifold \mathbb{M} for certain variations of the matrix B that satisfy the matching condition

$$\Delta f + \Delta B(t, x)u \in \text{range} B.$$

However, if the uncertain input matrix $\tilde{B}(t, x)$ is too different from the nominal matrix $B(t, x)$, the existence of the sliding mode cannot be guaranteed. The time derivative of σ can be written

$$\dot{\sigma} = \frac{\partial \sigma(x)}{\partial x} \tilde{B}(t, x)u + \frac{\partial \sigma(x)}{\partial x} \tilde{f}(t, x). \quad (6.11)$$

and the control based on the matrix $B(t, x)$ from (6.1) can no longer guarantee that $\sigma \rightarrow 0$. There are many variations such as disturbances or unmodeled dynamics that can change the direction of the control actuation in the input matrix $B(t, x)$, which can cause instability in the system.

The following mathematical development focuses on one of the applications of sliding mode control to stabilize systems that control sign uncertainty in the matrix $B(t, x)$. The underlying idea is to define multiple alternating stable and unstable surfaces for the dynamic model. As the structure changes, i.e., the sign of $B(t, x)$ switches, the unstable surfaces will become stable and the stable surfaces will become unstable. The trajectory of the system will transition to the nearest sliding surface.

All of the surfaces are designed such that sliding on any of them will achieve the control objective. Thus, any changes in the sign of $B(t, x)$ will only create short-lived transients in the system before it converges back to its goal.

Applications of this control technique can be applied to micro-air vehicles that are susceptible to highly uncertain environmental conditions and vehicle orientation that produce forces in various combinations. In this situation, rather than resisting by constantly restructuring the control actions, the autopilot should use the flow to aid its mission. This strategy would allow a more efficient control actuation and energy conservation.

The following work provides the mathematical development for a scalar input with sign uncertainty in the input gain vector.

Scalar Case

The method proposed in (Drakunov, 1993, 1994) is based on partitioning hypersurfaces into cell-like structures. An illustration of a two dimensional hypersurfaces can be seen in in Figure 6.1. The hypersurfaces shown in Figure 6.1 are the cellular structure of the sliding manifolds implemented through periodic switching. These manifolds are parallel switching surfaces partitioned onto the state space as cells

$$\mathbb{M}_i = \{x \in \mathbb{R}^n : \tilde{\sigma}_i(x) = \sin(\sigma_i(x)) = 0\}, \quad (6.12)$$

where $\sigma_i(x) = 0$ is the traditional switching surface. For the case of the switching surfaces of equation (6.12), the switching set is the union of the one-component switching manifolds

$$\mathbb{M}_i^{(k)} = \{x \in \mathbb{R}^n : \sigma_i(x) = \pi k\}, \quad (6.13)$$

where

$$\mathbb{M}_i = \bigcup_{k=-\infty}^{\infty} \mathbb{M}_i^{(k)} \quad (6.14)$$

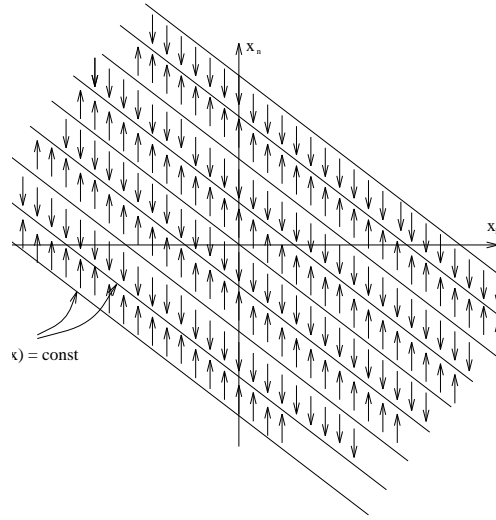


Figure 6.1: Multiple equilibrium manifolds in the state space for scalar case (Drakunov, 1994)

Consider the system in (6.1) for the case where the control input is a scalar:

$$\dot{x} = f(t, x) + b(t, x)u, \quad (6.15)$$

where $x(t) \in \mathbb{R}^n$, $b(t, x) \in \mathbb{R}^n$, $u(t) \in \mathbb{R}$. The objective is to stabilize the system to the desired manifold

$$\mathbb{M} = \{x : \sigma(x) = 0\}, \quad (6.16)$$

where

$$\sigma(x) \in \mathbb{R}^1. \quad (6.17)$$

The challenge of this system is the vector $b(t, x) = [b_1(t, x), \dots, b_n(t, x)]^T$ defining actuation direction is time- and state-dependent, and its sign is completely unknown. Taking the time derivative of the surface σ yields

$$\dot{\sigma} = G(x)f(t, x) + G(x)b(t, x)u, \quad (6.18)$$

where

$$G(x) = \frac{\partial \sigma(x)}{\partial x}. \quad (6.19)$$

To reach the sliding manifold \mathbb{M} without knowledge of the input vector $b(t, x)$, the proposed control law contains a periodic switching function as

$$u = M_0 \text{sign} \sin \left(\frac{\pi}{\epsilon} \tilde{\sigma} \right), \quad (6.20)$$

where

$$\tilde{\sigma} = \sigma(t) + \lambda \int_0^t \text{sign}(\sigma(\tau)) d\tau, \quad (6.21)$$

and $M_0 > 0$ is a positive control gain that can be a constant or a function, $\lambda \in \mathbb{R}$ is a positive constant that determines the rate of convergence of the manifolds, and $\epsilon \in \mathbb{R}$ is a positive constant that determines the spacing between the manifolds.

If for all $t > 0$ and $x(t) \in \mathbb{R}^n$ the function $b(t, x)$ satisfies

$$G(x)b(t, x) \neq 0, \quad (6.22)$$

then the control in Equation (6.20) can stabilize the surface σ to zero in finite time, provided the variable M_0 satisfies the inequality

$$|G(x)b(t, x)M_0(t, x)| > |G(x)f(t, x)| + \lambda + \delta, \quad (6.23)$$

where $\delta > 0$ is some positive constant. From (6.23), it is obvious that by increasing M_0 , the control law can compensate for a larger range of uncertainty. Differentiating $\tilde{\sigma}$ in (6.21) and substituting the control in (6.20) yields

$$\dot{\tilde{\sigma}} = Gf + Gb^T M_0 \text{sign} \left[\sin \left(\frac{\pi}{\varepsilon} \tilde{\sigma} \right) \right] + \lambda \text{sign}(\sigma). \quad (6.24)$$

In the neighborhoods of the points where

$$\tilde{\sigma} = k\varepsilon, \quad (6.25)$$

for $k = 0, \pm 2, \pm 4, \dots$, the following is obtained:

$$\text{sign} [\sin (\tilde{\sigma})] = \text{sign}(\tilde{\sigma} - k\varepsilon), \quad (6.26)$$

and for $k = \pm 1, \pm 3, \dots$, the following is obtained:

$$\text{sign} [\sin (\tilde{\sigma})] = -\text{sign}(\tilde{\sigma} - k\varepsilon). \quad (6.27)$$

Thus, if the inequality in (6.23) is satisfied, then sliding mode will occur on one of the manifolds in (6.25) for any sign of $G(x)b(t, x)M_0$. In fact, sliding mode occurs where

$\tilde{\sigma} = \text{constant}$ after some moment of time, and after differentiating (6.21) yields

$$\dot{\sigma} = -\lambda \text{sign}(\sigma). \quad (6.28)$$

Thus (6.28) guarantees that the manifold $\mathbb{M} = \{x : \sigma(x) = 0\}$ is reached in finite time.

The control law in (6.20) for a scalar case was designed without knowledge of the sign of $G(x)b(t, x)$. This sign is allowed to be different in different parts of the state space, which means that the system switches from one sliding manifolds to another. However, since the distance between the manifolds can be chosen to be arbitrarily small by the constant ϵ , the Equation (6.28) is violated for only a short period of time, provided that the inequality (6.23) does not coincide with the desired manifold.

From a geometric point of view, there are an infinite number of parallel switching surfaces partitioned into cells that have stable sliding manifolds for certain sign of $G(x)b(t, x)$. Thus, based on (6.28), all the parallel manifolds move in the direction of the manifold $\sigma = 0$ and, thus, sliding mode is reached in finite time.

6.2 Example

This section uses the dynamics of the quadrotor expressed in (4.1)

$$\ddot{x} = f(x) + g(x)u, \quad (6.29)$$

where $f(x, \dot{x}) \in \mathbb{R}^n$ denotes an unknown, nonlinear vector function, $g(x) \in \mathbb{R}^{n \times n}$ is an uncertain input matrix with unknown sign, $u(t) \in \mathbb{R}^n$ is a vector of control inputs,

and $d(t) \in \mathbb{R}^n$ is an unknown, nonlinear disturbance. The objective is to track the desired trajectory $x_d(t)$

$$x_d = \begin{bmatrix} 3 & \frac{20\pi}{180} \sin t & \frac{20\pi}{180} \sin \left(\frac{\pi}{3} + t \right) & \frac{20\pi}{180} \sin \left(\frac{\pi}{6} + t \right) \end{bmatrix}^T. \quad (6.30)$$

In this example, the magnitude of each element of the $g(x)$ is known but the sign is unknown. The sliding surface $\sigma(t)$ is chosen as

$$\sigma = (x - x_d) + \alpha(\dot{x} - \dot{x}_d), \quad (6.31)$$

and the control input $u(t)$ be

$$u = M_0 \operatorname{sgn} \left\{ \sin \left[\frac{\pi}{\varepsilon} \left(\sigma + \lambda \int \operatorname{sgn}(\sigma(\tau)) d\tau \right) \right] \right\}. \quad (6.32)$$

The gain matrix M_0 is

$$M_0 = \begin{bmatrix} 100 & 0 & 0 & 0 \\ 0 & 1 & 0 & 0 \\ 0 & 0 & 1 & 0 \\ 0 & 0 & 0 & 30 \end{bmatrix}. \quad (6.33)$$

The matrices α , ϵ , and λ are chosen as $\alpha = \operatorname{diag}(.01, .01, .01, .01)$, $\epsilon = \operatorname{diag}(.01, .01, .01, .01)$ and $\lambda = \operatorname{diag}(0.1, 0.1, 0.1, 0.1)$.

From Figure 6.2, it can be seen that the system in (6.29) converges around 20 seconds with nonlinear, bounded disturbances and unknown direction control.

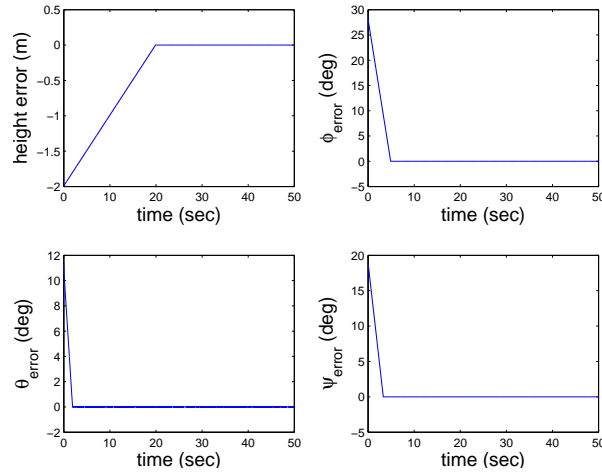


Figure 6.2: Quadrotor tracking error with unknown control direction

6.3 Conclusion

A sliding mode control law for a class of systems was presented, which achieves stability under unknown control direction. To achieve the result, multiple manifolds were created to adapt to the changing uncertainty in the control direction. The control algorithm is universal for a class of system where sign the control matrix is unknown.

Chapter 7

Conclusions

Two novel control methods are presented to deal with underactuated parallel systems, and dynamical systems containing parametric uncertainty and disturbances. Underactuated parallel systems were handled by driving a state to some area near the equilibrium point, then drive the second state to the origin through the design of a desired function. The dynamical system containing parametric uncertainty and norm-bound disturbances are dealt with by designing a continuous robust control law through the integral of the signum error. For systems containing heavy uncertainty such as unknown control direction input, a self-reconfiguration algorithm is proposed to adjust itself to the unknown changes. Simulations are shown to demonstrate the effectiveness of the proposed control laws.

Future research includes

- extending the underactuated dual parallel systems to n -parallel systems,
- design a more general case for second order dynamic with non-symmetric matrix and time-varying uncertainty,

- Apply pure sliding mode control to the synthetic jet actuators.

In conclusion, the contributions of this dissertation are

- design a novel technique to stabilize a class of underactuated dual parallel systems
- develop a robust control algorithm to compensate for systems with norm-bound disturbance and parametric uncertainty
- use sliding mode control to stabilize a class of systems with unknown control direction

Appendix A

Quadrotor

A.0.1 Proof of Lemma 1

Integrating both sides of (5.37) yields

$$\int_0^t L(\sigma) d\sigma = \int_0^t r^T(\sigma) (N_d(\sigma) - \Delta g \beta \operatorname{sgn}(e_2(\sigma))) d\sigma. \quad (\text{A.1})$$

After using (4.6), (A.1) can be rewritten as follows:

$$\begin{aligned} \int_0^t L(\sigma) d\sigma &= \int_0^t \left(\frac{\partial e_2(\sigma)}{\partial \sigma} \right)^T N_d(\sigma) d\sigma - \int_0^t \left(\frac{\partial e_2(\sigma)}{\partial \sigma} \right)^T \Delta g \beta \operatorname{sgn}(e_2(\sigma)) d\sigma \\ &\quad + \int_0^t \alpha_2 e_2^T(\sigma) (N_d(\sigma) - \Delta g \beta \operatorname{sgn}(e_2(\sigma))) d\sigma \end{aligned} \quad (\text{A.2})$$

After evaluating the first integral in (A.2) by parts, the following is obtained:

$$\begin{aligned}
\int_0^t L(\sigma) d\sigma &= N_d^T(\sigma) e_2(\sigma) \Big|_0^t - \int_0^t \left(\frac{\partial N_d(\sigma)}{\partial \sigma} \right)^T e_2(\sigma) d\sigma \\
&\quad - \Delta g \beta |e_2(\sigma)|_0^t + \int_0^t \alpha_2 e_2^T(\sigma) (N_d(\sigma) \\
&\quad - \Delta g \beta \operatorname{sgn}(e_2(\sigma))) d\sigma
\end{aligned} \tag{A.3}$$

where the fact that $\int_0^t \left(\frac{\partial e_2(\sigma)}{\partial \sigma} \right) \operatorname{sgn}(e_2(\sigma)) d\sigma = |e_2(\sigma)|_0^t$ was utilized. The expression in (A.3) can be upper bounded as

$$\begin{aligned}
\int_0^t L(\sigma) d\sigma &\leq \|e_2(t)\| (\zeta_{N_d} - (1 - \varepsilon) \beta) + \Delta g \beta |e_2(0)| - N_d^T(0) e_2(0) \\
&\quad + \int_0^t \alpha_2 \|e_2(\sigma)\| \left(\frac{1}{\alpha_2} \zeta_{\dot{N}_d} + \zeta_{N_d} - (1 - \varepsilon) \beta \right) d\sigma,
\end{aligned} \tag{A.4}$$

where (4.11) was utilized. Based on (A.4), inequality (4.24) is clearly satisfied provided the control gain β is selected to satisfy

$$\beta > \frac{1}{1 - \varepsilon} \left(\zeta_{N_d} + \frac{\zeta_{\dot{N}_d}}{\alpha_2} \right). \tag{A.5}$$

Appendix B

Synthetic Jets Actuator

B.0.2 Proof of Lemma 2

Integrating both sides of (5.37) yields

$$\int_0^t L(\tau) d\tau = \int_0^t r^T (N_{d1}(\tau) - T\dot{\mu}_1) d\tau. \quad (\text{B.1})$$

The expression in (B.1) can be rewritten as

$$\int_0^t L(\tau) d\tau = \int_0^t \sum_{i=1}^n r_i(\tau) \left(- \sum_{j=1}^n T_{ij} \dot{\mu}_{1_j}(\tau) + N_{d1_i}(\tau) \right) d\tau \quad (\text{B.2})$$

where $r_i(t)$, $N_{d1_i}(t)$, $\dot{\mu}_{1_i}(t) \in \mathbb{R}$ denote the i^{th} elements of $r(t)$, $N_{d1}(t)$, and $\dot{\mu}_1(t)$, respectively, and T_{ij} is introduced in (5.28). Substituting (5.8) into (B.2) yields

$$\begin{aligned} \int_0^t L(\tau) d\tau &= \sum_{i=1}^n e_i(t) N_{d1_i}(t) - \int_0^t \sum_{i=1}^n e_i(\tau) \frac{\partial N_{d1_i}(\tau)}{\partial \tau} d\tau \\ &\quad - \int_0^t \sum_{i=1}^n \frac{\partial e_i(\tau)}{\partial \tau} \beta \operatorname{sgn} \left(e_i(\tau) + \sum_{j=i+1}^n \bar{T}_{ij} \operatorname{sgn}(e_j(\tau)) \right) d\tau \\ &\quad + \int_0^t \sum_{i=1}^n \alpha e_i(\tau) (N_{d1_i}(\tau) - \beta (\operatorname{sgn}(e_i(\tau)) \\ &\quad + \sum_{j=i+1}^n \bar{T}_{ij} \operatorname{sgn}(e_j(\tau))) d\tau - \sum_{i=1}^n e_i(0) N_{d1_i}(0). \end{aligned} \quad (\text{B.3})$$

In (B.3), the fact that

$$\sum_{j=1}^n T_{ij} \dot{\mu}_{1_j}(t) = \beta \left(\operatorname{sgn}(e_i(\tau)) + \sum_{j=i+1}^n \bar{T}_{ij} \operatorname{sgn}(e_j(\tau)) \right)$$

$\forall i = 1, \dots, n-1$ was utilized (note that $\bar{T}_{nn} = 0$ since \bar{T} is strictly upper triangular).

Based on Assumption 2, the following equation holds $\forall i = 1, \dots, n-1$:

$$\operatorname{sgn}(e_i(t)) + \sum_{j=i+1}^n \bar{T}_{ij} \operatorname{sgn}(e_j(\tau)) = \phi \operatorname{sgn}(e_i(t)) \quad (\text{B.4})$$

where $\phi \in \mathbb{R}^+$ is a parameter satisfying $\varepsilon \leq \phi \leq Q$, with ε and Q defined as in (5.20).

After utilizing the fact that

$$\int_0^t \frac{\partial e_i(\tau)}{\partial \tau} \beta \phi \operatorname{sgn}(e_i(\tau)) d\tau = \beta \phi |e_i(t)| - \beta \phi |e_i(0)| \quad (\text{B.5})$$

and using (5.20) and (5.23), (B.3) can be upper bounded as

$$\begin{aligned} \int_0^t L(\tau) d\tau \leq & \int_0^t \sum_{i=1}^n \alpha |e_i(\tau)| \left(\zeta_{N_{d1}} + \frac{1}{\alpha} \zeta_{\dot{N}_{d1}} - \varepsilon \beta \right) d\tau + \sum_{i=1}^n |e_i(t)| (\zeta_{N_{d1}} - \varepsilon \beta) \\ & + \sum_{i=1}^n (\beta Q |e_i(0)| - e_i(0) N_{d1_i}(0)) \end{aligned} \quad (\text{B.6})$$

Thus, it is clear from (B.6) that if β satisfies (5.34), then (5.38) holds.

Bibliography

- Achtelik, M., Bierling, T., Wang, J., & Holzapfel, F. (2011, March). Adaptive Control of a Quadrotor in the Presence of large / complete Parameter Uncertainties. (2011-1485), 993-1007.
- Albu-Schaffer, A., Ott, C., & Hirzinger, G. (2005). Constructive energy shaping based impedance control for a class of underactuated euler-lagrange systems. In *2005. ICRA 2005. Proceedings of the 2005 IEEE International Conference on Robotics and Automation* (p. 1387-1393).
- Al-Younes, Y., Al-Jarrah, M., & Jhemi, A. (2010). Linear vs. nonlinear control techniques for a quadrotor vehicle. In *2010 7th International Symposium on Mechatronics and its Applications (ISMA)* (p. 1-10).
- Amitay, M., Smith, D. R., Kibens, V., Parekh, D. E., & Glezer, A. (2001). Aerodynamic flow control over an unconventional airfoil using synthetic jet actuators. *AIAA Journal*, 39(3), 361–370.
- An-Chyau, H., & Yung-Feng, C. (2010). Adaptive control for a class of underactuated systems with mismatched uncertainties. In *2010 29th Chinese Control Conference (CCC)* (p. 2053-2059).
- Arai, H., Tanie, K., & Shiroma, N. (1998). Nonholonomic control of a three-dof planar

- underactuated manipulator. *IEEE Transactions on Robotics and Automation*, 14(5), 681-695.
- Bartolini, G., Ferrara, A., & Giacomini, L. (2003). A switching controller for systems with hard uncertainties. *IEEE Transactions on Circuits and Systems I: Fundamental Theory and Applications*, 50(8), 984-990.
- Bartolini, G., & Pisano, A. (2008). Sliding mode control of nonlinear uncertain systems with relative degree two and uncertain control direction. In *VSS '08. International Workshop on Variable Structure Systems, 2008.* (p. 167-172).
- Bartolini, G., Punta, E., & Zolezzi, T. (2010, June). Multi-input sliding mode control of nonlinear systems with uncertain affine dependence on the control. *2010 11th International Workshop on Variable Structure Systems (VSS)*, 148–153.
- Bartolini, G., Punta, E., & Zolezzi, T. (2011). Multi-Input Sliding Mode Control of Uncertain Systems. *IFAC World Congress*, 1917–1921.
- Besnard, L., Shtessel, Y., & Landrum, B. (2007). Control of a quadrotor vehicle using sliding mode disturbance observer. In *American Control Conference, 2007. ACC '07* (p. 5230-5235).
- Bullo, F., & Lynch, K. (2001). Kinematic controllability for decoupled trajectory planning in underactuated mechanical systems. *IEEE Transactions on Robotics and Automation*, 17(4), 402-412.
- Chamseddine, A., & Zhang, Y. (2010, August). Adaptive Trajectory Planning for a Quad-rotor Unmanned Aerial Vehicle. *AIAA Guidance, Navigation, and Control Conference, 2010.* (AIAA 2010-8279)
- Chamseddine, A., Zhang, Y., Rabbath, C., Fulford, C., & Apkarian, J. (2011, March). Model Reference Adaptive Fault Tolerant Control of a Quadrotor UAV. *AIAA*

- Infotech@Aero-space Conference*. (AIAA 2011-1606)
- Chiang, C.-C. (2012, June). Output tracking control for uncertain underactuated systems based on fuzzy sliding mode control approach. *2012 IEEE International Conference on Fuzzy Systems*, 1–8.
- Choukchou-Braham, A., Cherki, B., & Djemai, M. (2011). A backstepping procedure for a class of underactuated system with tree structure. In *2011 International Conference on Communications, Computing and Control Applications (CCCA)* (p. 1-6).
- Cornejo, C., & Alvarez-Icaza, L. (2007). A nonlinear friction model for the passivity-based control of underactuated mechanical systems. In *2007 46th IEEE Conference on Decision and Control* (p. 3859-3864).
- Das, A., Subbarao, K., & Lewis, F. (2009). Dynamic inversion with zero-dynamics stabilisation for quadrotor control. *Control Theory Applications, IET*, 3(3), 303-314.
- Deb, D., Tao, G., Burkholder, J., & Smith, D. (2005a). An adaptive inverse control scheme for a synthetic jet actuator model. In *Proceedings of the 2005 American Control Conference* (p. 2646-2651 vol. 4).
- Deb, D., Tao, G., Burkholder, J. O., & Smith, D. R. (2005b, Sept. 26-29). An adaptive inverse control scheme for synthetic jet actuator arrays. *AIAA Infotech@Aerospace Conference*(AIAA 2005-7170).
- Deb, D., Tao, G., Burkholder, J. O., & Smith, D. R. (2006, June). Adaptive synthetic jet actuator compensation for a nonlinear tailless aircraft model at low angles of attack. In *American Control Conference, 2006* (p. 6 pp.-).
- Deb, D., Tao, G., Burkholder, J. O., & Smith, D. R. (2007, Mar.-Apr.). Adaptive

- compensation control of synthetic jet actuator arrays for airfoil virtual shaping. *AIAA Journal of Aircraft*, 44(2), 616–626.
- Deb, D., Tao, G., Burkholder, J. O., & Smith, D. R. (2008, Sept.). Adaptive synthetic jet actuator compensation for a nonlinear aircraft model at low angles of attack. *IEEE Transactions on Control Systems Technology*, 16(5), 983–995.
- DeCarlo, R., Drakunov, S., & Li, X. (2000). A unifying characterisation of robust sliding mode control: a lyapunov approach. *ASME Journal of Dynamics Systems, Measurement, and Control*, 122(4), 708–718.
- DeCarlo, R., Zak, S., & Matthews, G. (1988). Variable structure control of nonlinear multivariable systems: A tutorial. *Proceedings of the IEEE*, 76(3), 212–232.
- Dierks, T., & Jagannathan, S. (2010). Output feedback control of a quadrotor uav using neural networks. *IEEE Transactions on Neural Networks*, 21(1), 50–66.
- Drakunov, S. V. (1993, Dec.). Sliding mode control of the systems with uncertain direction of control vector. In *Proc. of IEEE Conf. on Decision and Control* (p. 2477–2478). San Antonio, TX.
- Drakunov, S. V. (1994, November). Sliding mode control with multiple equilibrium manifolds. , 55-1, 101–108.
- Drakunov, S. V., Izosimov, D., Lukjanov, A., Utkin, V. A., & Utkin, V. (1991a). Block control principle. part i. In *Automation and Remote Control* (Vols. 51, Nb 5, p. 601–608).
- Drakunov, S. V., Izosimov, D., Lukjanov, A., Utkin, V. A., & Utkin, V. (1991b). Block control principle. part ii. In *Automation and Remote Control* (Vols. 51, Nb 6, p. 737–746).
- Drakunov, S. V., & Utkin, V. (1992). Sliding mode control in dynamic systems. In

- International Journal of Control* (Vols. 55, 4, p. 1029-1037).
- Drazenovic, B. (1969). The invariance condition in variable structure systems. *Automatica*, 5, 287 - 295.
- Dydek, Z. T., Annaswamy, A. M., Company, T. B., & Beach, H. (2010, April). Adaptive Control of Quadrotor UAVs in the Presence of Actuator Uncertainties. *AIAA infotech@Aerospace 2010*, 1–9. (AIAA 2010-3416)
- Ferrara, A., Giacomini, L., & Vecchio, C. (2009). Adaptive sliding mode control of uncertain nonholonomic systems with unknown control direction. In *Control applications, (cca) intelligent control, (isic), 2009 ieee* (p. 290-295).
- Filippov, A. F. (1964). Differential equations with discontinuous right hand side. *Amer. Math. Soc. Transactions*, 42(2), 191–231.
- Ghommam, J., Bouterra, Y., Mnif, F., & Poisson, G. (2011). Distributed backstepping control for synchronization of networked class of underactuated systems: A passivity approach. In *2011 19th Mediterranean Conference on Control Automation (MED)* (p. 7-12).
- Gillula, J., Huang, H., Vitus, M., & Tomlin, C. (2010). Design of guaranteed safe maneuvers using reachable sets: Autonomous quadrotor aerobatics in theory and practice. In *Robotics and Automation (ICRA), 2010 IEEE International Conference on* (p. 1649-1654).
- Han, D.-P., Wei, Q., & Li, Z.-X. (2008, July). Kinematic control of free rigid bodies using dual quaternions. *International journal of Automation and Computing*, 5(3), 319–324.
- Hao, Y., Yi, J., & Zhao, D. (2008, June). Robust control using incremental sliding mode for underactuated systems with mismatched uncertainties. *2008 American*

- Control Conference*(1), 532–537.
- Hong, G. (2012). Numerical investigation to forcing frequency and amplitude of synthetic jet actuators. *AIAA Journal*, 50(4), 788–796.
- Hsu, L., Oliveira, T., & Peixoto a.J. (2006). Sliding Mode Control of Uncertain Non-linear Systems with Arbitrary Relative Degree and Unknown Control Direction. *International Workshop on Variable Structure Systems, 2006. VSS'06*.(2), 178–183.
- Hu, G., Gans, N., & Dixon, W. E. (2007, Oct.). Quaternion-based visual servo control in the presence of camera calibration error. *IEEE International Conference on Control Applications*, 1492–1497.
- Huang, H., Hoffmann, G., Waslander, S., & Tomlin, C. (2009, May). Aerodynamics and control of autonomous quadrotor helicopters in aggressive maneuvering. *2009 IEEE International Conference on Robotics and Automation*, 3277–3282.
- Ioannou, P., & Fidan, B. (2006). *Adaptive control tutorial*. Philadelphia, PA: Society for Industrial and Applied Mathematics.
- Jee, S. K., Lopez, O., Moser, R. D., Kutay, A. T., Muse, J. A., & Calise, A. J. (2009, June). Flow simulation of a controlled airfoil with synthetic jet actuators. In *AIAA Conf. on Computational Fluid Dynamics*. San Antonio TX. (AIAA 2009-3673)
- Jiang, Z.-P. (2002). Global tracking control of underactuated ships by lyapunov's direct method. *Automatica*, 38(2), 301 - 309.
- Kaloust, J., & Qu, Z. (1997, March). Robust control design for nonlinear uncertain systems with an unknown time-varying control direction. *IEEE Transactions on Automatic Control*, 42(3), 393–399.

- Khalil, H. K. (2002). *Nonlinear systems* (3rd Edition ed.). Upper Saddle River, NJ: Prentice Hall.
- Kim, M., Kim, S., Kim, W., Kim, C., & Kim, Y. (2011). Flow control of tiltrotor unmanned-aerial-vehicle airfoils using synthetic jets. *Journal of Aircraft*, 48(3).
- Kim, M., Kim, Y., & Jun, J. (2012). Adaptive sliding mode control using slack variables for affine underactuated systems. In *2012 IEEE 51st Annual Conference on Decision and Control (CDC)* (p. 6090-6095).
- Kokotovic, P. (1992). The joy of feedback: nonlinear and adaptive. *Control Systems, IEEE*, 12(3), 7-17.
- Kotapati, R. B., Mittal, R., Marxen, O., Ham, F., You, D., & Cattafesta III, L. N. (2010). Nonlinear dynamics and synthetic-jet-based control of a canonical separated flow. *Journal of Fluid Mechanics*, 654, 65–97.
- Kourta, A., & Leclerc, C. (2013). Characterization of synthetic jet actuation with application to Ahmed body wake. *Sensors and Actuators A: Physical*, 192, 13–26.
- Kung, C.-C., Chen, T.-H., & Huang, L.-C. (2009). Adaptive fuzzy sliding mode control for a class of underactuated systems. In *2009. FUZZ-IEEE 2009. IEEE International Conference on Fuzzy Systems* (p. 1791-1796).
- Lee, D., Burg, T., Dawson, D., Shu, D., Xian, B., & Tatlicioglu, E. (2009). Robust tracking control of an underactuated quadrotor aerial-robot based on a parametric uncertain model. In *2009. SMC 2009. IEEE International Conference on Systems, Man and Cybernetics* (p. 3187-3192).
- Lee, S. H., Park, J.-B., & Choi, Y.-H. (2009). Finite time control of nonlinear underactuated systems using terminal sliding surface. In *2009. IEEE International*

- Symposium on Industrial Electronics, 2009. ISIE* (p. 626-631).
- Levant, A., Taleb, M., & Plestan, F. (2011). Twisting-controller gain adaptation. In *2011 50th IEEE Conference on Decision and Control and European Control Conference (CDC-ECC)* (p. 7015-7020).
- Liapunov, A. M. (1992). *The general problem of the stability of motion* (A. T. Fuller, Trans.). London ; Washington, DC : Tayor and Francis.
- Liu, Y. (2008). Multivariable MRAC using Nussbaum gains for aircraft with abrupt damages. *2008 47th IEEE Conference on Decision and Control*, 2600–2605.
- Liu, Y., Ciuryla, M., Amitay, M., Kwan, C., Myatt, J. H., Zhang, X., et al. (2006). Integrated flight control and flow control using synthetic jet arrays. In *AIAA Guidance, Navigation, and Control Conference*. Keystone, CO. (AIAA 2006-6190)
- Lozano, R., & Brogliato, B. (1992). Adaptive control of a simple nonlinear system without a priori information on the plant parameters. *IEEE Transactions on Automatic Control*, 37(1), 30–37.
- Luo, Z.-B., Xia, Z.-X., & Xie, Y.-G. (2007). Jet vectoring control using a novel synthetic jet actuator. *Chinese Journal of Aeronautics*, 20(3), 193 - 201.
- MacKunis, W., Subramanian, S., Mehta, S., Ton, C., Curtis, J. W., & Reyhanoglu, M. (2013). Robust nonlinear aircraft tracking control using synthetic jet actuators. In *2013 IEEE 52st Annual Conference on Decision and Control (CDC)*. Florence, Italy.
- Madani, T., & Benallegue, A. (2007, July). Sliding Mode Observer and Backstepping Control for a Quadrotor Unmanned Aerial Vehicles. *2007 American Control Conference*, 5887–5892.

- Mejia, O. D. L., Moser, R. D., Brzozowski, D. P., & Glezer, A. (2011, Aug.). Effects of trailing-edge synthetic jet actuation on an airfoil. *AIAA Journal*, 49(8).
- Mian, A., & Daobo, W. (2008). Nonlinear flight control strategy for an underactuated quadrotor aerial robot. In *ICNSC 2008. IEEE International Conference on Networking, Sensing and Control, 2008* (p. 938-942).
- Mnif, F., & Ghommem, J. (2002). Stabilization for a class of underactuated mechanical systems. *IEEE International Conference on Systems, Man and Cybernetics*, vol.6, 4.
- Mondschein, S. T., Tao, G., & Burkholder, J. O. (2011, June-July). Adaptive actuator nonlinearity compensation and disturbance rejection with an aircraft application. In *American Control Conference* (pp. 2951–2956).
- Morse, A. S. (1993, July). A gain matrix decomposition and some of its properties. *Systems and Control Letters*, 21(1), 1–10.
- Morse, A. S. (1998). Control Using Logic-Based Switching. In *Trends in Control: A European Perspective* (pp. 69–113). Springer-Verlag.
- Mudgett, D., & Morse, a. (1984). Adaptive stabilization of linear systems with unknown high-frequency gains. *The 23rd IEEE Conference on Decision and Control*(2), 666–668.
- Muse, J. A., Tchieu, A. A., Kutay, A. T., Chandramohan, R., Calise, A. J., & Leonard, A. (2009). Vortex Model Based Adaptive Flight Control Using Synthetic Jets. In *AIAA Paper 2009-5761*.
- Nelson, R. (1998). *Flight Stability and Automatic Control* (2nd Edition ed.). McGraw-Hill.
- Nordkvist, N., & Bullo, F. (2008). Control Algorithms Along Relative Equilibria

- of Underactuated Lagrangian Systems on Lie Groups. *IEEE Transactions on Automatic Control*, 53(11), 2651-2658.
- Nussbaum, R. D. (1983). Some Remarks on a Conjecture in Parameter Adaptive Control. *System and Control Letters*, 243-246.
- Ogata, K. (2002). *Modern control engineering* (4th Edition ed.). Upper Saddle River, NJ: Prentice Hall.
- Olfati-Saber, R. (2000). Cascade normal forms for underactuated mechanical systems. *Proceedings of the 39th IEEE Conference on Decision and Control*, 3, 2162–2167.
- Orlov, Y., Aguilar, L., & Aho, L. (2005). Model orbit robust stabilization (mors) of pendubot with application to swing up control. In *CDC-ECC '05. 44th IEEE Conference on Decision and Control, 2005 and 2005 European Control Conference* (p. 6164-6169).
- Ozawa, T., Lesbros, S., & Hong, G. (2010). LES of synthetic jets in boundary layer with laminar separation caused by adverse pressure gradient. *Computers and Fluids*, 39(5), 845–858.
- Ozawa, T., Lesbros, S., & Hong, G. (2012). Forcing a low Reynolds number channel flow to generate synthetic turbulent-like structures. *Computers and Fluids*, 55, 101–108.
- Patre, P. M., MacKunis, W., Makkar, C., & Dixon, W. E. (2008, Mar.). Asymptotic tracking for systems with structured and unstructured uncertainties. *IEEE Transactions on Control Systems Technology*, 16(2), 373–379.
- Pettersen, K., & Egeland, O. (1996). Exponential stabilization of an underactuated surface vessel. In *Proceedings of the 35th IEEE Conference on Decision and*

- Control, 1996* (Vol. 1, p. 967-972 vol.1).
- Price, D. B., Ton, C., MacKunis, W., & Drakunov, S. V. (2013, July). Self-reconfigurable control for dual-quaternion/dual-vector systems. In *European control conference*. Zurich, Switzerland.
- Qian, D., & Yi, J. (2010). Fuzzy aggregated hierarchical sliding mode control for underactuated systems. In *2010 International Conference on Mechatronics and Automation (ICMA)* (p. 196-201).
- Qian, D., Yi, J., & Zhao, D. (2007). Robust control using sliding mode for a class of under-actuated systems with mismatched uncertainties. In *2007 IEEE International Conference on Robotics and Automation* (p. 1449-1454).
- Qu, Z. (1998). *Robust control of nonlinear uncertain systems*. New York: Wiley Inc.
- Reyhanoglu, M., Schaft, A. van der, McClamroch, N., & Kolmanovsky, I. (1999). Dynamics and control of a class of underactuated mechanical systems. *IEEE Transactions on Automatic Control*, 44(9), 1663-1671.
- Rosas-Flores, J., Alvarez-Gallegos, J., & Castro-Linares, R. (2000). Stabilization of a class of underactuated systems. In *2000. Proceedings of the 39th IEEE Conference on Decision and Control* (Vol. 3, p. 2168-2173 vol.3).
- Salih, A. L., Moghavvemi, M., Mohamed, H. a. F., & Gaeid, K. S. (2010, May). Modelling and PID controller design for a quadrotor unmanned air vehicle. *2010 IEEE International Conference on Automation, Quality and Testing, Robotics (AQTR)*, 1-5.
- Shageer, H. M., Tao, G., & Burkholder, J. O. (2008, Dec.). Adaptive spline function based compensation of synthetic jet actuators for aircraft flight control. In *Conf. on Decision and Control* (pp. 1397-1342).

- Shiriaev, A., & Kolesnichenko, O. (2000). On passivity based control for partial stabilization of underactuated systems. In *2000. Proceedings of the 39th IEEE Conference on Decision and Control* (Vol. 3, p. 2174-2179 vol.3).
- Singhal, C., Tao, G., & Burkholder, J. O. (2009). Neural network-based compensation of synthetic jet actuator nonlinearities for aircraft flight control. In *AIAA Guidance, Navigation, and Control Conf.* Chicago, IL. (AIAA 2009-6177)
- Tamburello, D. A., & Amitay, M. (2008). Active control of a free jet using a synthetic jet. *International Journal of Heat and Fluid Flow*, 29(4), 967 - 984.
- Tao, G. (1996). *Adaptive control of systems with actuator and sensor nonlinearities*. John Wiley and Sons.
- Tao, G. (2003). *Adaptive control design and analysis* (S. Haykin, Ed.). Wiley-Interscience.
- Tayebi, A., & McGilvray, S. (2006). Attitude stabilization of a vtol quadrotor aircraft. *IEEE Transactions on Control Systems Technology*, 14(3), 562-571.
- Tchieu, A. A., Kutay, A. T., Muse, J. A., Calise, A. J., & Leonard, A. (2008). Validation of a low-order model for closed-loop flow control enable flight. In *AIAA Paper 2008-3863*.
- Ton, C., & Mackunis, W. (2012, dec). Robust attitude tracking control of a quadrotor helicopter in the presence of uncertainty. In *IEEE Conference on Decision and Control (CDC)* (p. 937-942). Maui, Hawaii.
- Travnicek, Z., Nemcova, L., Kordik, J., Tesar, V., & Kopecky, V. (2012). Axisymmetric impinging jet excited by a synthetic jet system. *International Journal of Heat and Mass Transfer*, 55(4), 1279 - 1290.
- Tseng, L.-Y., Yang, A.-S., & Lin, J.-C. (2011, Dec.). Study of a crossflow over a

- zero-net-mass-flux synthetic jet driven by a vibrating diaphragm. *Journal of Mechanics*, 27(4), 503–510.
- Utkin, V. (1977). Variable Structure Systems with Sliding Modes. *IEEE Transactions on Automatic Control*, 22, 212-222.
- Utkin, V., Drakunov, S., Izosimov, D. B., Lukjanovand, A. G., & Utkin, V. A. (1984). Hierarchical principle of the control system decomposition based on motion separation. In *Proceedings of the 9th World IFAC Congress* (p. 101-108).
- Utkin, V. I. (1992). *Sliding modes in control and optimization*. Berlin: Springer-Verlag.
- Vries, E. d., & Subbarao, K. (2010, December). Backstepping based nested multi-loop control laws for a quadrotor. *2010 11th International Conference on Control Automation Robotics & Vision*(3), 1911–1916.
- Vukasinovic, B., Glezer, A., Gordeyev, S., Jumper, E., & Kibens, V. (2009). Fluidic control of a turret wake, Part I: Aerodynamic effects. In *AIAA Aerospace Sciences Meeting and Exhibit*. (AIAA 2009-816)
- Wang, J., Bierling, T., Achtelik, M., Holzapfel, F., Zhao, W., Go, T. H., et al. (2011). Attitude Free Position Control of a Quadcopter using Dynamic Inversion. *AIAA Infotech@Aerospace, 2011*(March). (AIAA 2011-1583)
- Wang, W., Yi, J., Zhao, D., & Liu, D. (2004). Design of a stable sliding-mode controller for a class of second-order underactuated systems. *IEE Proceedings - Control Theory and Applications*, 151(6), 683-690.
- Waslander, S. L., & Wang, C. (2009, April). Wind Disturbance Estimation and Rejection for Quadrotor Position Control. *AIAA Infotech@Aerospace, 2009*. (AIAA 2009-1983)

- Wie, B. (2008). *Space vehicle dynamics and control* (2nd Edition ed.). American Institute of Aeronautics and Astronautics, Inc.
- Xian, B., Dawson, D. M., Queiroz, M. S. de, & Chen, J. (2004, July). A continuous asymptotic tracking control strategy for uncertain nonlinear systems. *IEEE Transactions on Automatic Control*, 49(7), 1206–1211.
- Xin, X. (2009). On the energy based control for underactuated mechanical systems. In *ICCAS-SICE, 2009* (p. 1465-1470).
- Xin, X., & Kaneda, M. (2002). The swing up control for the acrobot based on energy control approach. In *Proceedings of the 41st IEEE Conference on Decision and Control, 2002* (Vol. 3, p. 3261-3266 vol.3).
- Xu, J.-X., Guo, Z.-Q., & Lee, T. H. (2010, November). An integral sliding mode control design for a class of underactuated motion systems. *IECON 2010 - 36th Annual Conference on IEEE Industrial Electronics Society*, 2385–2390.
- Xu, J.-X., Guo, Z.-Q., & Lee, T. H. (2012, January). Sliding mode controller design for underactuated systems. *2012 12th International Workshop on Variable Structure Systems*, 385–390.
- Xudong, Y., & Jingping, J. (1998). Adaptive nonlinear design without a priori knowledge of control directions. *IEEE Transactions on Automatic Control*, 43(11), 1617–1621.
- Yan, L., Hsu, L., Costa, R. R., & Lizarralde, F. (2008, April). A variable structure model reference robust control without a prior knowledge of high frequency gain sign. *Automatica*, 44(4), 1036–1044.
- Yan, L., & Xu, J. (2004). A model reference robust control with unknown high frequency gain sign. In *American Control Conference, 2004. Proceedings of the*

- 2004 (Vol. 4, p. 3291-3296 vol.4).
- Yang, Z., Yam, S., Li, L., & Wang, Y. (2009, June). Robust control for uncertain nonlinear systems with unknown and changing control direction. *2009 17th Mediterranean Conference on Control and Automation*, 235–239.
- Yi, J., Wang, W., Zhao, D., & Liu, X. (2005). Cascade sliding-mode controller for large-scale underactuated systems. In *2005 IEEE/RSJ International Conference on Intelligent Robots and Systems, 2005. (IROS 2005)* (p. 301-306).
- Zhang, X., & Zhang, Y. (2010, August). Fault Tolerant Control for Quad-rotor UAV by Employing Lyapunov-based Adaptive Control Approach. *AIAA Guidance, Navigation, and Control Conference*. (AIAA 2010-8052)
- Zhu, B., & Huo, W. (2010). Trajectory linearization control for a quadrotor helicopter. In *2010 8th IEEE International Conference on Control and Automation (ICCA)* (p. 34-39).